

TOWSON UNIVERSITY
OFFICE OF GRADUATE STUDIES

GROUP DIFFERENCES AND INDIVIDUAL VARIABILITY IN THE FREQUENCY-
FOLLOWING RESPONSE TO DYNAMIC TONAL GLIDES AS A FUNCTION OF
AGE, HEARING IMPAIRMENT, AND SWEEP COUNT

by

Jane Grabowski

A Thesis

Presented to the faculty of

Towson University

in partial fulfillment

of the requirements for the degree

Doctor of Audiology

Department of Audiology, Speech Language Pathology, and Deaf Studies

Towson University
Towson, Maryland 21252

May 2016

**TOWSON UNIVERSITY
OFFICE OF GRADUATE STUDIES**

THESIS APPROVAL PAGE

This is to certify that the thesis prepared by Jane Grabowski entitled Group Differences and Individual Variability in the Frequency-Following Response to Dynamic Tonal Glides as a Function of Age, Hearing Status, and Sweep Count has been approved by the thesis committee as satisfactorily completing the thesis requirements for the degree Doctor of Audiology.




Chairperson, Thesis Committee Signature Saradha Ananthakrishnan

4-28-2016
Date



Committee Member Signature Peggy Korczak

4-28-16
Date



Committee Member Signature Curtis Billings

4-28-16
Date



Committee Member Signature Michelle Molis

4-28-16
Date



Dean of Graduate Studies

4-29-16
Date

ACKNOWLEDGEMENTS

Although only my name appears on the cover of this thesis, many people have contributed to its production. While many wonderful people have contributed to this project, the errors in this document are likely all mine, especially as they relate to the statistics. I am truly grateful to my fantastic thesis committee, whose valuable insights and guidance have made the completion of this project possible.

Dr. Saradha Ananthakrishnan, who chaired my thesis committee, first sparked my interest in the frequency-following response. Without her guidance, criticism, and encouragement, a far inferior product would have resulted. I consider myself incredibly fortunate to have had the opportunity to work with Dr. Ananthakrishnan and to her I give my deepest gratitude.

Dr. Peggy Korczak has been a wonderful mentor the past few years and I feel grateful to have had the opportunity to learn about all aspects of electrophysiology from her. She has been a source of encouragement throughout this whole thesis writing process. It has been an absolute privilege working with Dr. Korczak.

I am incredibly grateful to Dr. Michelle Molis and Dr. Curtis Billings for agreeing to take me into their lab as an NIH T-35 research trainee and to the VA RR&D National Center for Rehabilitative Auditory Research for providing me with an academic home for the summer of 2015. The intellectual climate that Michelle and Curtis were able to create for those three months was simply incredible. I can't thank Michelle enough for sitting in the lab with me for hours coaching me through the more challenging aspects of the project and through various thought experiments. Curtis was always the voice of reason when these thought experiments got out of hand and taught me the value of improving

the wheel, rather than re-inventing it. He also patiently taught me how to burn my first CD (for the transfer of .DAT files between computers).

I also wish to thank my amazing cohort for helping me get through the difficult times, providing me with almost-pee-in-your-pants laughter, and making three years seem like a breeze. They are by far some of the most level-headed, down-to-earth, kind, generous and thoughtful individuals I have ever met; I can't wait to see how they will shape the face of audiology.

My husband deserves special recognition for insisting on getting a 32" extended desktop computer display and for dutifully making late-night runs to the grocery store for essentials like cave-ripened washed-rind cheeses, artisanal bread, and assortments of red wine blends.

Last but not least, I would like to extend my sincerest gratitude to Dr. Diana Emanuel and the Towson University Department of Audiology for taking a chance on me many moons ago (when interactions with other programs were most discouraging) and supporting my wild ideas (even if they didn't always work out). Thank you for letting me dream!

TABLE OF CONTENTS

LIST OF TABLES	vii
LIST OF FIGURES	viii
ABSTRACT.....	xii
CHAPTER 1: INTRODUCTION	1
CHAPTER 2: LITERATURE REVIEW	3
Classification System of AEPs.....	4
Basic Acoustics	7
<i>Periodicity</i>	8
<i>Complexity</i>	10
<i>Acoustics of speech</i>	11
Auditory Neural Encoding	13
History of the FFR.....	17
What is the FFR?.....	18
Neural Generators of the FFR	20
FFR Technical Parameters.....	22
<i>FFR Stimulus Parameters</i>	23
<i>Stimulus Type</i>	23
<i>Stimulus Intensity</i>	26
<i>Stimulus Frequency</i>	29
<i>Stimulus Presentation Rate</i>	30
<i>Stimulus Polarity</i>	32
<i>Recording Parameters</i>	34
<i>Electrode Montage</i>	34
<i>Sampling Rate</i>	37
<i>Response Filter Settings</i>	39
<i>Number of Sweeps</i>	40
<i>Averaging Window</i>	43
<i>Artifact</i>	43
<i>Subject Parameters</i>	45
<i>Subject State</i>	46
<i>Effect of Aging</i>	46
<i>Effect of Hearing Impairment</i>	49
What information does the FFR provide us?	52
Goals of the Current Study.....	52
CHAPTER 3: METHODOLOGY	54
Participants	54
Audiometry.....	54
Stimuli	55
FFR Data Acquisition.....	57
FFR Data Analyses.....	59
<i>Qualitative Data Analyses</i>	60
<i>Quantitative Analyses</i>	60
<i>Statistical Analyses</i>	60

CHAPTER 4: RESULTS	61
Effect of Hearing Status and Age on FFR	61
<i>Qualitative Grand-Averaged FFR Temporal Waveform Analysis</i>	61
<i>Qualitative Grand-Averaged FFR Spectrogram Analysis</i>	63
<i>Descriptive Statistical Analysis of Age and Hearing Status Effects on FFR</i>	64
<i>Inferential Statistical Analysis of Age and Hearing Status Effects on FFR</i>	65
Within and Across Group Variability of FFR	68
<i>Qualitative Individual FFR Temporal Waveform Analysis</i>	68
<i>Qualitative Individual FFR Spectrogram Analysis</i>	69
<i>Analysis of Variability Across and Within Groups</i>	70
Effect of Sweep Count on FFR	75
<i>Qualitative Individual FFR Temporal Waveform Analysis as a Function of Sweep Count</i>	75
<i>Qualitative Individual FFR Spectrogram Analysis as a Function of Sweep Count</i>	77
<i>Quantitative Analysis of the Effect of Sweep Count on FFR_{TFS}</i>	79
Summary of Results	84
CHAPTER 5: DISCUSSION	86
On the Effect of Age on the FFR	86
On the Effect of Hearing Loss on the FFR	90
On Within and Across Group Variability of the FFR	95
On the Effect of Sweep Count on the FFR	100
Clinical Implications	104
Study Limitations	105
Future Directions	107
REFERENCES	108
CURRICULUM VITA	124

LIST OF TABLES

<i>Table 1.</i> Classification of Auditory Evoked Potentials.....	6
<i>Table 2.</i> Average Response Nomenclature.....	33
<i>Table 3.</i> Start and Stop Frequencies (in Hz) of Test Stimuli by Direction of Change and Extent of Change.....	56
<i>Table 4.</i> Mean, Standard Deviation, Minimum, Maximum, and Range of Cross- Correlation. Coefficients Attained by Each Group at 2600 Sweeps.....	72
<i>Table 5.</i> Comparison Between Individual EEG and Max Cross-Correlation Coefficient.....	74
<i>Table 6.</i> Mean Cross-Correlation Coefficients by Group and Sweep Count.....	81

LIST OF FIGURES

<i>Figure 1.</i> Representation of waveform as variation in air pressure as a function of time...	8
<i>Figure 2.</i> Periodic waveform and spectrum of 100 Hz sine wave.....	8
<i>Figure 3.</i> Aperiodic waveform and spectrum.....	9
<i>Figure 4.</i> Two waveforms with equal amplitude, with the top waveform completing one cycle per one-hundredth of a second and the bottom waveform completing three cycles per one-hundredth of a second.....	10
<i>Figure 5.</i> Flowchart showing the differences between simple and complex waveforms and their various subtypes.....	11
<i>Figure 6.</i> Three simple sine waves (100 Hz, 200 Hz, and 300 Hz) forming a complex waveform.....	12
<i>Figure 7.</i> Source-filter model of speech production.....	13
<i>Figure 8.</i> Schematic of cochlear filtering, temporal fine structure, and temporal-envelope modulation.....	15
<i>Figure 9.</i> Waveforms at the outputs of simulated normal auditory filters centered at 369, 1,499, and 4,803 Hz in response to the sound “en” in “sense”. The thick lines show the Hilbert envelopes of the waveforms.....	16
<i>Figure 10.</i> Hierarchy of acoustic stimuli.....	24
<i>Figure 11.</i> Steady-state and time-varying complex stimuli.....	25
<i>Figure 12.</i> FFR waveforms to 500 Hz tone as a function of stimulus intensity.....	27
<i>Figure 13.</i> FFR frequency-amplitude curves at three intensities (60, 70, and 80 dB).....	28

<i>Figure 14.</i> FFR evoked at the frequencies indicated from B through F at 70 dB SL illustrating that the response is difficult to recognize at higher frequencies (≥ 1.5 kHz) relative to lower frequencies (≤ 1.0 kHz).....	29
<i>Figure 15.</i> Amplitude modulated sinewave stimuli with ISIs.....	31
<i>Figure 16.</i> Contrast between condensation (left) and rarefaction (right) waveforms.....	32
<i>Figure 17.</i> Electrode locations in the 10-20 system.....	35
<i>Figure 18.</i> Example of a one-channel (left), two-channel (middle), and three-channel (right) electrode montage.....	36
<i>Figure 19.</i> Superimposed individual FFR waveforms (left) and corresponding group averages (right) to 200 Hz pure-tone stimulus recorded from horizontal and vertical electrode montage.....	37
<i>Figure 20.</i> A wave sampled at a high sampling frequency (top) yields a more faithful representation than a wave sampled at a low sampling frequency (bottom).....	38
<i>Figure 21.</i> Relation of signal-to-noise ratio to number of sweeps.....	40
<i>Figure 22.</i> ABR recordings as a function of the number of sweeps included in the averaged waveform ranging from 100 sweeps (bottom tracing) to 3200 sweeps (top tracing).....	41
<i>Figure 23.</i> Group average puretone thresholds and standard deviations as a function of frequency for younger normal-hearing, older normal-hearing, and older hearing-impaired study participants.....	55
<i>Figure 24.</i> Schematic illustrating extent (1.00 vs. 0.67 vs. 0.33 octaves) and direction of change (rising vs. falling) of tonal glide stimuli.....	56

<i>Figure 25.</i> Four-channel electrode recording montage with the non-inverting (active) electrodes placed at C _z , C ₇ , A ₁ , and F _z , the inverting (reference) electrode positioned at A ₂ , and the common ground electrode located at Fp _z	58
<i>Figure 26.</i> Comparison between stimulus waveform (top) and response waveforms for grand-averaged recordings obtained from YNH, ONH, and OHI individuals.....	61
<i>Figure 27.</i> Grand-averaged spectrograms for FFR _{TFS} obtained from YNH, ONH, and OHI subjects post-stimulus onset (at 0 ms).....	63
<i>Figure 28.</i> Histogram of standardized residuals suggesting that data contain normally distributed errors.....	66
<i>Figure 29.</i> Normal P-P plot of standardized residuals suggesting that data contain normally distributed errors but deviate from a normal distribution.....	66
<i>Figure 30.</i> Scatterplot of standardized predicted values suggesting that the data are heteroscedastic.....	67
<i>Figure 31.</i> Comparison between stimulus waveform (top) and response waveforms for the best and poorest individual recordings obtained from different participants in the YNH, ONH, and OHI groups.....	68
<i>Figure 32.</i> Spectrograms for best (top) and poorest (bottom) FFR _{TFS} obtained from different individual responses from YNH, ONH, and OHI subjects post-stimulus onset (at 0 s).....	69
<i>Figure 33.</i> Box-plot distributions of data showing cross-correlation coefficients at 100, 1000, 2000, and 2600 sweeps (the maximum number of sweeps achieved by all groups) by group (YNH vs. ONH vs. OHI).....	71

<i>Figure 34.</i> Individual cross-correlation coefficients as a function of sweep count for all participants displayed by group membership (YNH vs. ONH vs. OHI).....	72
<i>Figure 35.</i> FFR recordings as a function of the number of sweeps included in the averaged waveform ranging from 100 sweeps (top tracing) to 2920 sweeps (bottom tracing) for two YNH participants to showcase good (left) and poor (right) FFR representation.....	76
<i>Figure 36.</i> Spectrograms of FFR recordings as a function of the number of sweeps included in the averaged waveform ranging from 100 sweeps (top) to 2920 sweeps (bottom) for two YNH participants to showcase good (left column) and poor (right column) FFR representation.....	78
<i>Figure 37.</i> Mean stimulus to frequency-following response cross-correlation coefficients as a function of sweep count by group (YNH vs. ONH vs. OHI) for a dynamic tonal stimulus 120 ms in duration rising over the extent of two-thirds of an octave.....	80
<i>Figure 38.</i> Mean cross-correlation coefficients by group (YNH vs. ONH vs. OHI) and order of epochs (averaged every 100 sweeps as they were collected vs. averaged every 100 sweeps in random epochs without replacement) as a function of sweep count.....	84

ABSTRACT

Synchronous neural firing and accurate phase-locking support the encoding of time-varying acoustic features of speech critical for speech discrimination. Evidence suggests that phase-locking is disrupted in older and hearing-impaired adults, which may help account for the frequently-reported perceptual deficits in those populations not otherwise accounted for by peripheral hearing sensitivity. The frequency-following response (FFR) has previously been utilized to index subcortical encoding in various populations. However, normative data for the FFR has not been formally established to date, in part because the response may be elicited by a variety of stimuli, such as pure tones, tonal sweeps, and speech stimuli in a number of populations, such as in older individuals and individuals with hearing loss. As such, the aims of this study are two-fold. First, the study examined group differences in FFR quality between three listener groups: younger normal hearing (YNH) ($N = 10$, $M = 28.1$ years, range = 24-33), older normal hearing (ONH) ($N = 10$, $M = 61.1$ years, range = 51-66), and older hearing-impaired (OHI) ($N = 10$, $M = 66.8$ years, range = 54-78) adults as a function of sweep count. Second, individual response variability within each group was evaluated qualitatively by analyzing averaged time waveforms and corresponding spectrograms to begin documenting the range of responses which might be obtained in homogenous groups in which degree of hearing loss and age are controlled. Three-thousand sweeps were collected in alternating polarity to rising tonal stimuli 120 ms in length spanning one-third, two-thirds, and one whole octave centered around 500 Hz. FFR waveforms were averaged in increasing increments of 100 consecutive sweeps and were quantitatively analyzed via cross-correlation analysis. Results reveal that ONH and OHI

adults require significantly more sweeps than YNH adults to achieve FFRs of similar quality, suggesting that older adults are more prone to desynchronization in temporal information encoding than younger individuals, independent of hearing status. However, further analysis of individual responses reveals that independent of hearing loss and age, each group included individuals who robustly encoded the stimuli, as well as individuals for which the FFR was indistinguishable from baseline biologic electroencephalographic activity.

CHAPTER 1: INTRODUCTION

Older individuals with and without hearing loss frequently report difficulty understanding speech, particularly in adverse listening environments. The difficulties these individuals report are often not otherwise accounted for by peripheral hearing sensitivity or degree of hearing loss. An essential function of the auditory system is to neurally encode acoustic features of speech. Speech is an inherently complex auditory signal and is composed of numerous acoustic features which influence how a particular stimulus is neurally encoded in the auditory system (Liederman, Frye, Fisher, Greenwood, & Alexander, 2005). Acoustic features of speech include the fundamental frequency, harmonics, formants, formant transitions, acoustic onsets, periodicity and the speech envelope (Abrams & Kraus, 2009). Formants and formant transitions are time-varying features of speech critical for speech sound identification, with the lowest three formants capable of conveying enough information for successful vowel and consonant identification.

In order to decode complex acoustic stimuli such as speech, the auditory system has to be able to faithfully represent rapid spectrotemporal changes (Skoe & Kraus, 2010). Faithful neural encoding of the acoustic features of speech is instrumental for decoding this information into meaningful linguistic information. The encoding of these dynamic features relies on neural synchrony within the auditory system. The synchronous neural firing which supports the encoding of spectrotemporal resolution has been demonstrated to be disrupted in older (Anderson, Parbery-Clark, White-Schwoch, & Kraus, 2012; Clinard & Cotter, 2015; Clinard & Tremblay, 2013; Clinard, Tremblay, &

Krishnan, 2010; Presacco, Jenkins, Lieberman, & Anderson, 2015) and hearing-impaired adults (Ananthakrishnan, Krishnan, & Bartlett, 2016; Plyler & Ananthanarayan, 2001).

It has been established that the frequency-following response (FFR) or complex auditory brainstem response (cABR) is capable of providing an objective assessment of neural encoding at the level of the rostral brainstem to both simple and complex steady-state and time-varying stimuli, thereby indexing the degree of synchronous neural firing (Skoe & Kraus, 2010). The FFR is a scalp-recorded auditory evoked potential capable of phase-locking to sustained auditory stimuli, thereby representing various acoustic stimuli, such as those required for speech discrimination (Krishnan, 2007; Skoe & Kraus, 2010). The FFR is capable of encoding these time-varying and harmonically complex sounds and faithfully represents acoustic properties of speech in part because it is sensitive to small changes in stimulus frequency (Batra, Kuwada, & Maher, 1986; Skoe & Kraus, 2010), such as those inherent to formant transitions.

The current study will focus on the FFR to dynamic tonal stimuli approximating various formant transitions in English in younger normal-hearing (YNH), older normal-hearing (ONH), and older hearing-impaired (OHI) participants. Specifically, the aim is to determine in what ways aging and hearing impairment might affect the quality of the FFR recording. A better understanding how acoustic information is encoded could help illuminate why perceptual difficulties of speech exist for different populations, such as those reported in older individuals and those with hearing impairment.

CHAPTER 2: LITERATURE REVIEW

Evoked potentials are neuro-electric responses to sensory stimuli which can be recorded using various signal averaging techniques (Walsh, Kane, & Butler, 2005). Evoked potentials can be elicited in response to a number of stimuli across various sensory modalities. Specifically, they can be recorded in the visual, auditory and somatosensory domains, providing objective modality-specific information about how a particular sensory pathway of the central nervous system (CNS) functions. Evoked potentials are distinct from spontaneous potentials, which represent the underlying neural energy present at any given point in time.

Over the years, evoked potentials have found a clinical home as complements to other diagnostic testing. They may be used to demonstrate abnormal sensory system conduction, contribute site of lesion information, provide insight into disease processes, and be used to monitor neurological status (Chiappa, 1997; Walsh et al., 2005). Advantages of using evoked potentials clinically include that they allow for physiological assessment and are sensitive to neurological disease processes. Furthermore, they can be recorded in anaesthetized or comatose patients (Walsh et al., 2005).

Auditory-evoked potentials (AEPs) are changes in electrical energy that occur in the neural structures associated with the auditory system in response to an auditory stimulus. AEPs might be recorded from the cochlea, cranial nerve (CN) VIII, neural generators in the brainstem, and from various sub-cortical and cortical regions. In most clinical settings, they are recorded by surface electrodes positioned on the scalp, filtered, amplified, and averaged over numerous trials. AEPs are frequently used clinically because they may be used to reliably estimate behavioral threshold sensitivity in difficult

to test populations, determine otoneurologic status and site of lesion information, and provide information about how the auditory system encodes more complex stimuli and speech information (Hall, 2007; Picton, 2011).

Classification System of AEPs

Auditory evoked potentials (AEPs) can be classified in four different ways, namely by the temporal relationship of the response to the onset of the stimulus, in relation to the stimulus itself, in relation to the neural generators responsible for the response, and as either exogenous or endogenous (Picton, 2011).

Temporal classification relates to the latency at which a response occurs following stimulus onset. Applying this classification scheme to AEPs, five major categories may be identified; first, fast, middle, slow, and late potentials. First responses occur 0-5 ms post-stimulus onset and include the compound action potential (CAP), the cochlear microphonic (CM), the summing potential (SP), and waves I and II of the auditory brainstem response (ABR). Fast auditory potentials occur 2-20 ms post-stimulus onset and capture waves I-V of the ABR, the frequency-following response (FFR), and the fast auditory steady-state response (ASSR). Middle auditory potentials occur 10-100 ms post-stimulus onset and include waves Na, Pa, and Nb of the middle-latency response (MLR) and the 40-Hz potential. At latencies between 30-500 ms slow responses are expected. Slow auditory evoked potentials include waves P1, N1, P2, N2 of the vertex or slow cortical potentials, the slow ASSR, and the cortical sustained potential. Lastly, late potentials occur 200-1000 ms post-stimulus onset and include the mismatch negativity (MMN), processing negativity, acoustic change complex (ACC), and late positive waves, such as the P300 (Hall, 2007; Picton, 2011).

AEPs may also be classified in relation to the stimulus type in response to which they are evoked. Transient potentials are evoked by a single stimulus. Transient potentials include the auditory brainstem response (ABR), middle-latency response (MLR), vertex potential, mismatch negativity (MMN), and late cortical potentials. Sustained potentials are evoked by repeated or continuous stimulus. Examples of sustained potentials include the SP, cortical sustained potential (CNV) and cortical sustained potential. Steady-state potentials are evoked by rapidly repeating stimuli ($\geq 40/s$) such that response from one stimulus presentation overlaps with the response of a subsequent stimulus presentation. Steady-state potentials include the CM, ASSR, and 40-Hz potential.

A neural generator-based classification scheme is based on the probable source(s) responsible for generating a given response. Not surprisingly, there is a relationship between the anatomical sources of a given response and the latencies at which those responses occur, such that potentials which are generated in the cochlea or brainstem occur at shorter latencies, while cortical potentials occur much later. Cochlear potentials, such as the CAP, correspond to first AEPs. Potentials generated in CN VIII and lower portions of the brainstem might also be classified as fast AEPs. Higher portions of the brainstem and sub-cortical generators correspond to potentials which occur at approximately the same latencies as the middle AEPs. Lastly, slow and late potentials correspond to neural generators in the primary auditory cortex and neocortex (Hall, 2007; Picton, 2011).

Another way of classifying AEPs relates to the obligatory nature of the response. AEPs are either exogenous or endogenous. Exogenous potentials are also known as sensory potentials. They are obligatory responses that occur in response to a stimulus.

Most AEPs, such as the ABR, FFR, and MLR are exogenous potentials. On the other hand, endogenous or processing-contingent potentials require interpretation of incoming sensory information beyond the obligatory response. These might include the MMN and P300 response (Picton, 2011). Classically, endogenous potentials are recorded in response to occasional changes in stimulus condition within a sequence of repeating stimuli, known as an oddball paradigm. Table 1 presents a summary of the various classification schemes used for AEPs.

Table 1

Classification of Auditory Evoked Potentials

Latency	Transient	Steady-State	Sustained
First (0-5 ms)	Cochlear Nerve Compound Action Potential	Cochlear Microphonic	Summating Potential
Fast (1-15 ms)	Auditory Brainstem Response	Frequency Following Response; Fast (>70 Hz) Auditory Steady-State Response	Pedestal of Frequency-Following Response
Middle (10-50 ms)	Middle-Latency Response	40-Hz Potential	
Slow (30-500 ms)	Vertex Potential	Slow (<30 Hz) Auditory Steady-State Response	Cortical Sustained Potential
Late (200-1000 ms)	Mismatch Negativity; Processing Negativity; Late Positive Waves		Contingent Negative Variation

Note. Adapted from “Human Auditory Evoked Potentials,” by T. W. Picton, p. 5. Copyright 2011 by Plural Publishing, Inc.

Following these classification schemes, the FFR, which is the focus of the current study, is considered an exogenous, fast, steady-state potential generated by neural sources in the brainstem. A unique feature of the FFR is that it phase-locks to the cycle of a given stimulus up to 1500 Hz, meaning that it fires at a rate that is equivalent to the period of a given stimulus. As an example, assume that a 1000 Hz tone, which has a period of 1 ms, is used to evoke the FFR. In response to a 1000 Hz tone, an FFR recording in the temporal domain would then have peaks every 1 ms. A 250 Hz tone has a period of 4 ms. As such, the FFR would phase-lock to the stimulus every 4 ms. Given this unique characteristic, the FFR might be used to further explore the role of phase-locking in the encoding of complex stimuli, such as speech sounds and other time-variant stimuli (Krishnan, 2007).

Basic Acoustics

Much of the interest surrounding the FFR relates to its capacity for neurally encoding certain features of acoustic stimuli relating to pitch through neural phase-locking. A basic foundation in acoustics will facilitate a better understanding of the neural mechanisms attributed to the FFR and its implications for speech perception. Specifically, the FFR is capable of encoding both simple and complex acoustic stimuli. Acoustic signals are made up of sound waves, which are variations in air pressure over time. These variations in air pressure can be plotted as pressure at a given point in time, termed an oscillogram or waveform, as seen in Figure 1 below.

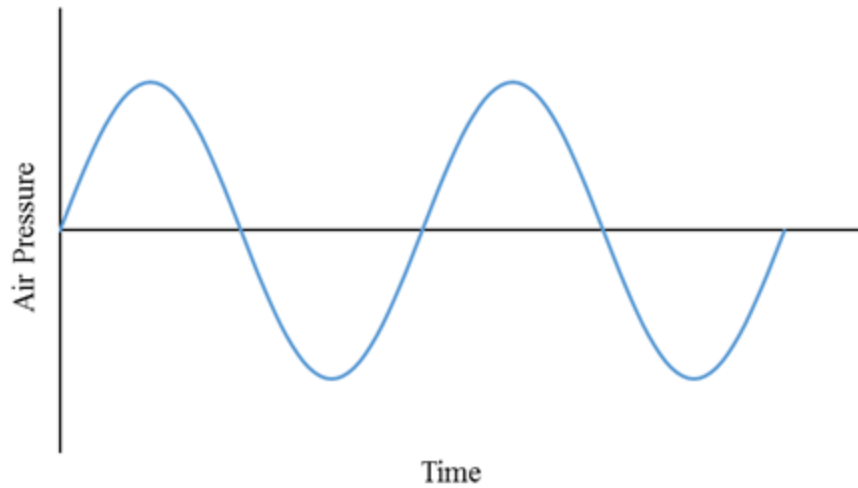


Figure 1. Representation of waveform as variation in air pressure as a function of time.

Periodicity

Waveforms can be periodic (Figure 2), meaning that the pressure variations are repeated over time, or aperiodic (Figure 3), in which there is no discernable discrete pattern to its air pressure changes as a function of time.

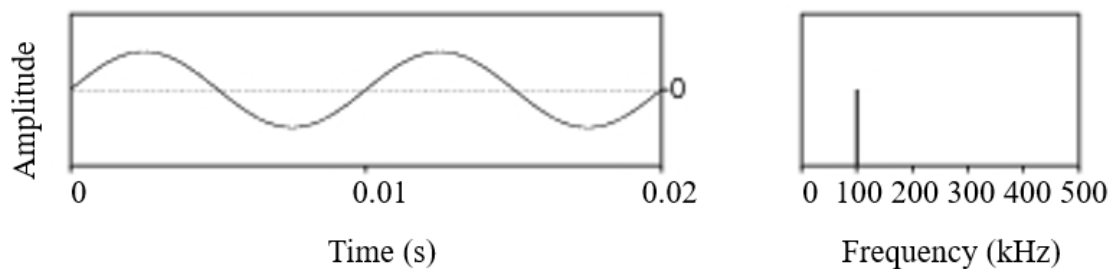


Figure 2. Periodic waveform and spectrum of 100 Hz sine wave. Adapted from http://www.hum.uu.nl/uilots/lab/courseware/phonetics/basics_of_acoustics_2/spectra_periodic_signals.html.

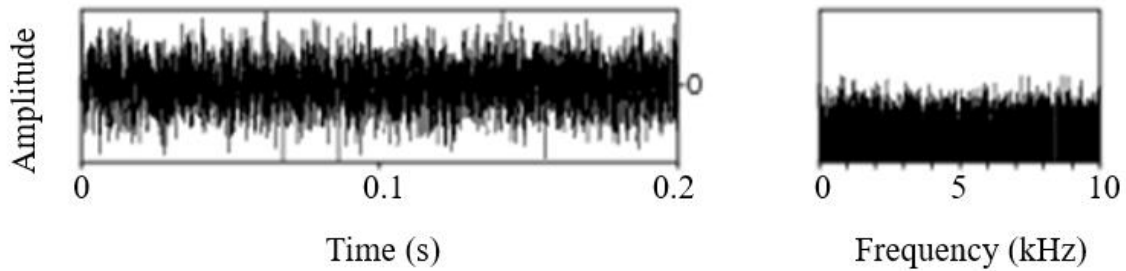


Figure 3. Aperiodic waveform and spectrum. Adapted from http://www.hum.uu.nl/uilots/lab/courseware/phonetics/basics_of_acoustics_2/spectra_aperiodic_signals.html

Perfectly periodic waveforms are theoretical ideals (due to interference from other sound waves and friction), with real world sounds ranging from more periodic to less periodic. Periodicity in general is a concept which straddles a continuum, such that a perfectly periodic waveform is akin to a sine wave and is perceived as a pure tone, and an entirely aperiodic waveform composed of completely random variations in sound pressure is termed white noise.

Each repetition of a periodic waveform is called a cycle. The number of times a cycle of a sound repeats given a unit time (s) determines its frequency, which is measured in Hertz (Hz), such that

$$\text{Hertz (Hz)} = \frac{\text{cycles}}{\text{second}}$$

Frequency is the physical correlate of the perceptual pitch. The higher the frequency (i.e., the more cycles per unit time), the higher in pitch the perceived tone. Considering the two sine waves in Figure 4 below, the waveform on the left completes one cycle per 0.01 seconds, whereas the waveform on the right completes three cycles per 0.01 seconds. The frequencies of the waveforms are 100 Hz and 300 Hz respectively, meaning that the waveform on the left would be perceived as having a lower pitch than the waveform on the right.

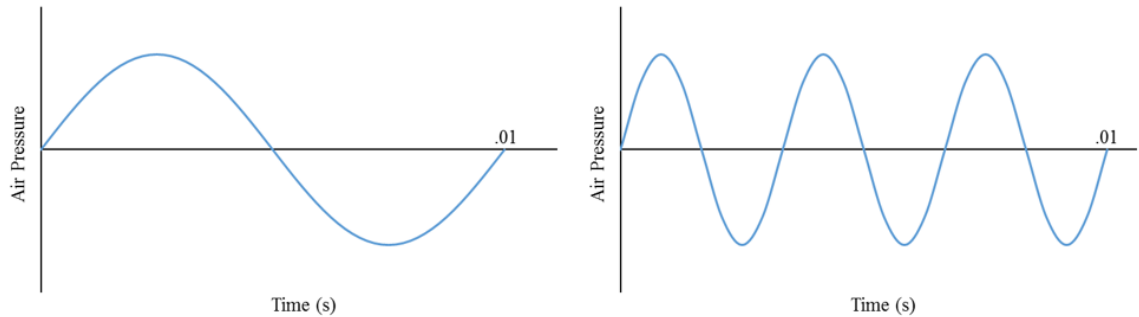


Figure 4. Two waveforms with equal amplitude, with the top waveform completing one cycle per one-hundredth of a second and the bottom waveform completing three cycles per one-hundredth of a second.

Complexity

In addition to periodicity, waveforms can be described in terms of complexity.

Periodic waveforms can be both simple and complex, with sinusoidal waveforms considered to be simple and non-sinusoidal waveforms considered to be complex.

Aperiodic waveforms can further be classified by their relative duration as either continuous, such as is the case for noise, or transient, such as is the case for brief tone clicks or pulses. Figure 5 provides a summary of the taxonomy of the complexity of waveforms. By the nature of the environment with which they interact and the sources which generate them, all waveforms encountered in a natural environment are complex.

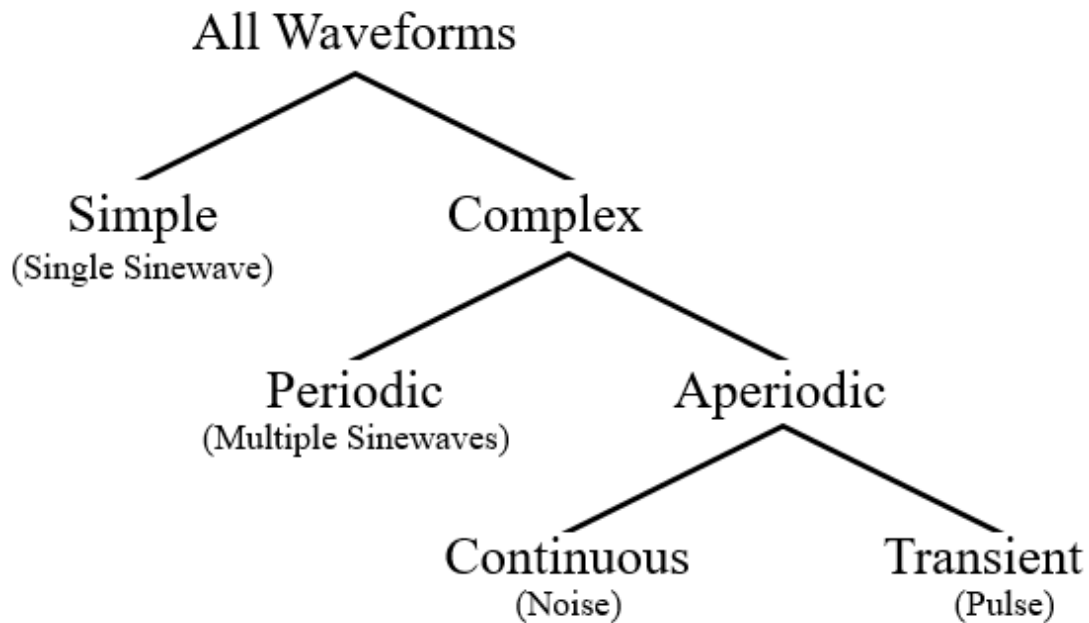


Figure 5. Flowchart showing the differences between simple and complex waveforms and their various subtypes.

Acoustics of speech

Speech is an inherently complex auditory signal and is composed of numerous acoustic features which influence how a particular stimulus is neurally encoded in the auditory system. Non-linguistic acoustic features of speech include the fundamental frequency, harmonics, formants, formant transitions, acoustic onsets, periodicity and the speech envelope (Abrams & Kraus, 2009).

The fundamental frequency may be defined in one of two ways. Firstly, the fundamental frequency is the frequency of repetition of the lowest frequency component of a given complex waveform (Ladefoged, 1996). If we were to construct a complex waveform containing 100 Hz, 200 Hz, and 300 Hz, we would see that the pattern of the newly-formed waveform would repeat at a frequency of 100 Hz or every .01 seconds, as illustrated in Figure 6 below.

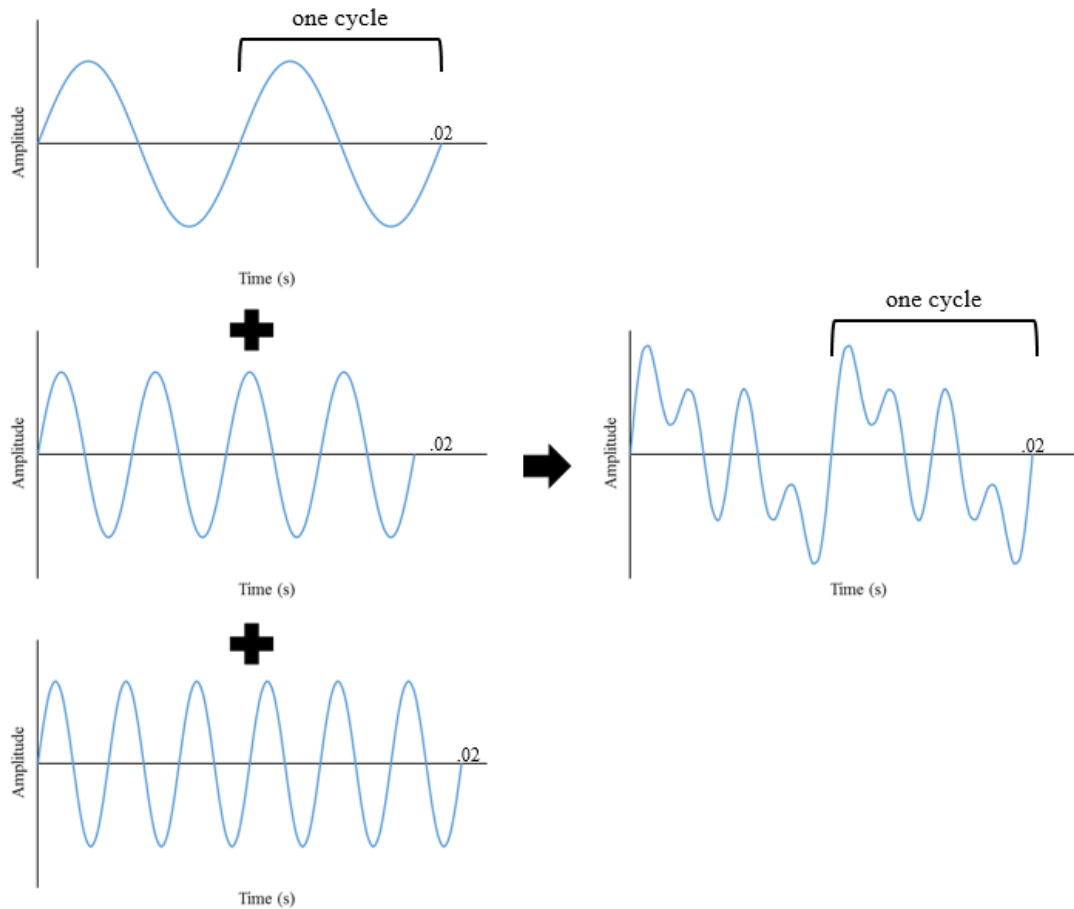


Figure 6. Three simple sine waves (100 Hz, 200 Hz, and 300 Hz) forming a complex waveform.

In the field of acoustic phonetics, the fundamental frequency is designated as F_0 and is determined by rate of vocal fold vibration. That is to say, if the vocal folds are opening and shutting 100 times per second, F_0 is 100 Hz. Harmonics are whole-number integer multiples of the fundamental frequency. If the fundamental frequency, or first harmonic (F_1), of a given stimulus is 100 Hz, for example, we would expect harmonics at 200 Hz, 300 Hz, 400 Hz, and so on, termed the second (F_2), third (F_3), and fourth harmonic (F_4), respectively.

The complex vibration of the vocal folds in turn produces a complex periodic wave containing harmonics of the fundamental frequency. The source of the sound is

vocal fold vibration, which is then filtered by the vocal tract. The vocal tract has its own characteristic resonant frequencies which are contingent on its length and shape. As the sounds which are produced by the vocal folds are passed through the vocal tract filter, certain frequencies in the source signal will be enhanced. These enhanced resonant frequencies are termed formants and represent an increase in acoustic energy (Abrams & Kraus, 2009; Ladefoged, 1996). Formants and formant transitions are critical for speech sound identification, with the lowest three formants capable of conveying enough information for successful vowel and consonant identification.

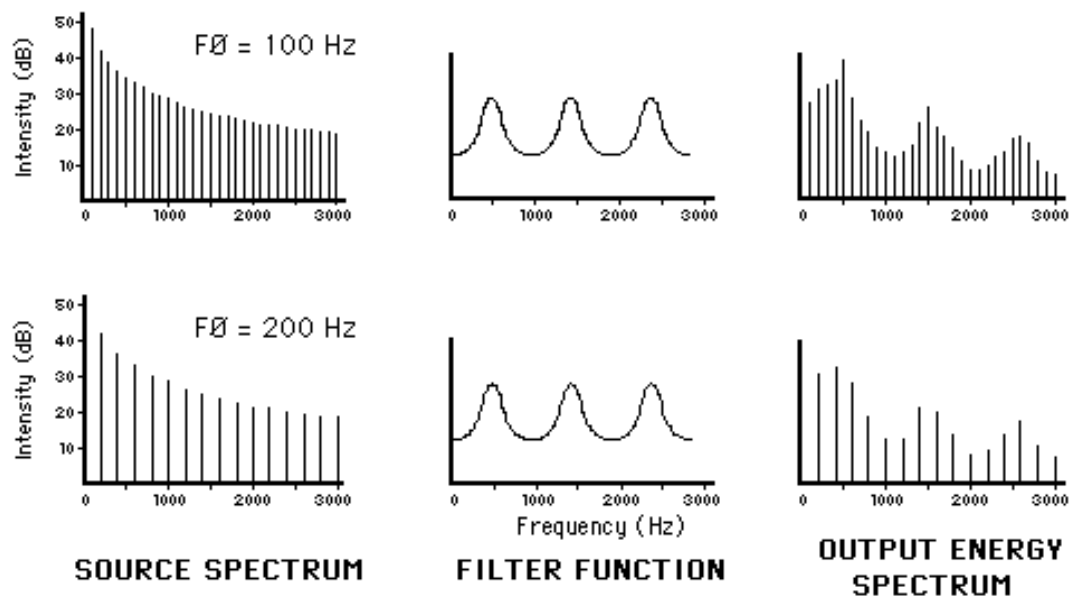


Figure 7. Source-filter model of speech production. Adapted from “The Acoustic Theory of Speech Production: The Source-Filter Model,” retrieved from <http://www.haskins.yale.edu/featured/heads/mmssp/acoustic.html>.

Auditory Neural Encoding

In order to decode complex acoustic stimuli such as speech, the auditory system has to be able to faithfully represent rapid spectrotemporal changes (Skoe & Kraus, 2010). These spectrotemporal changes can be represented through place and time coding. The place theory of pitch perception suggests that auditory stimuli are encoded based on

their relative frequency components, which stimulate a particular area of the basilar membrane sensitive to those particular frequencies. In contrast, time-coding schemes conceptualize neural firing rates as the driver behind auditory perception of pitch (Gelfand, 2004). Neither theory alone is sufficiently explanatory; rather, both place and time coding are thought to contribute to auditory neural encoding, with the place mechanism critical for high-frequency representations and phase-locking important for low-frequency stimuli.

Speaking more to place coding, the basilar membrane has been conceptualized as a series of tonotopically organized bandpass filters, with low frequencies represented at the apex and high frequencies represented at the base. Cochlear filters centered on high characteristic frequencies (CF) are more sharply tuned than those which occur at low CFs. The CF is the frequency at which a particular neuron is optimally responsive (Gelfand, 2004). These cochlear filters are logarithmically spaced, but the spacing of the harmonics of complex stimuli is linear. This results in lower harmonics each passing through individual cochlear filters, thereby being *resolved*, while multiple higher harmonics may pass through a single cochlear filter in the high-frequency region and are considered to be *unresolved* (Sayles & Winter, 2008). Complex stimuli are thus separated into envelope (in red) and temporal fine structure (in blue) components, as seen in Figure 8. Generally, resolved harmonics result in temporal fine structure (TFS) information, while unresolved harmonics form a complex waveform at the output of the cochlear filter. This complex waveform consists of an envelope, or the slowly varying feature of the waveform, superimposed on the TFS, the more rapidly oscillating feature of the waveform.

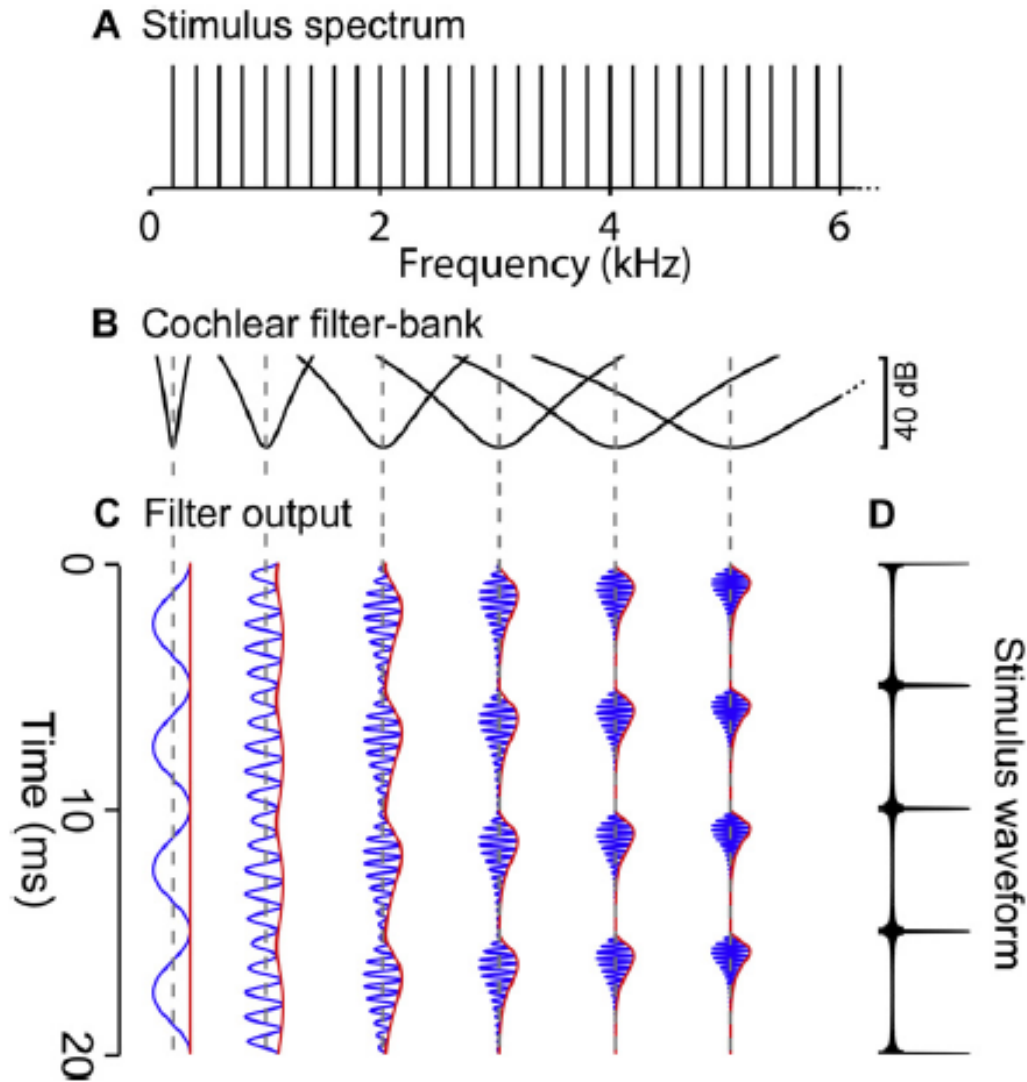


Figure 8. Schematic of cochlear filtering, temporal fine structure, and temporal-envelope modulation. Adapted from “Reverberation Challenges the Temporal Representation of the Pitch of Complex Sounds,” by M. Sayles and I. M. Winter, 2008, *Neuron*, 58, p.790. Copyright 2008 by Elsevier Inc.

Envelope structure refers to slow amplitude variations over the course of an auditory stimulus, while TFS is generated by rapid amplitude variations or oscillations of the stimulus, with the oscillations occurring at a rate that is close to the CF of the cochlear filter (Moore, 2008; Sayles & Winter, 2008). Figure 9 shows the output of three cochlear filters with CFs at 4803 Hz, 1499 Hz, and 369 Hz. The thick line super-imposed

on the waveform is the envelope, and the rapid oscillations contained within the envelope are the temporal fine structure. As described, these vary at a rate that approximated the CF of the cochlear filter, with more rapid oscillations noted for the filter with a CF of 4803 Hz than for the one with a CF of 369 Hz.

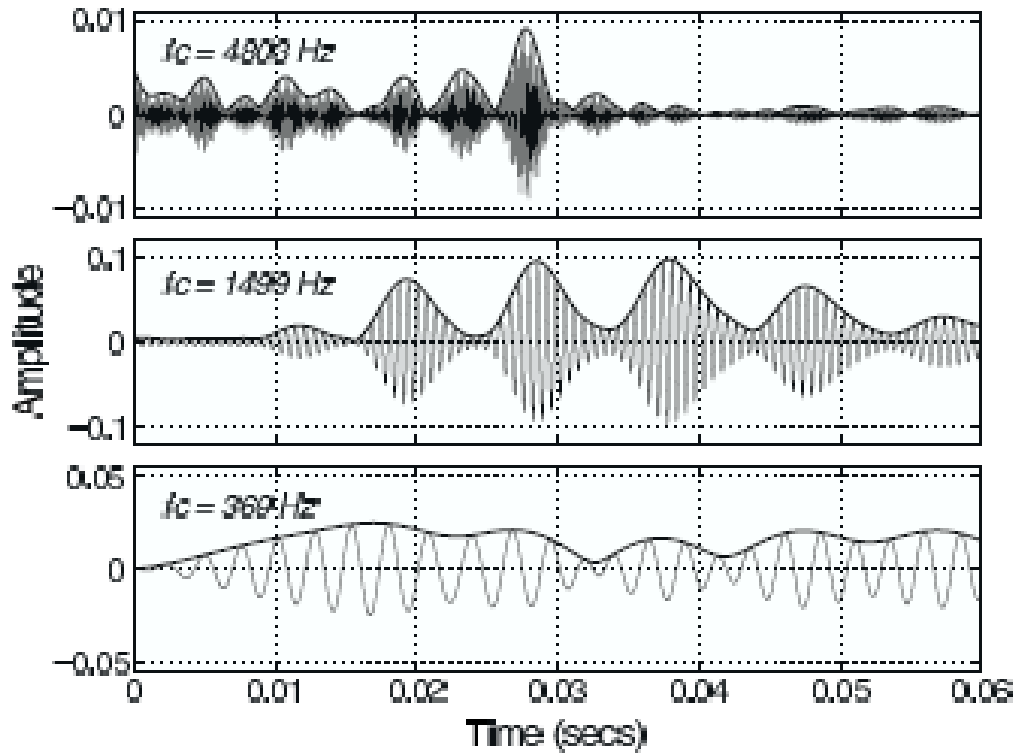


Figure 9. Waveforms at the outputs of simulated normal auditory filters centered at 369, 1,499, and 4,803 Hz in response to the sound “en” in “sense”. The thick lines show the Hilbert envelopes of the waveforms. Adapted from “The Role of Temporal Fine Structure Processing in Pitch Perception, Masking, and Speech Perception for Normal-Hearing and Hearing-Impaired people,” by B. C. Moore, 2008, *Journal of the Association for Research in Otolaryngology*, 9(4), p. 400. Copyright 2008 by Springer.

Envelope and TFS can both be represented using a time coding scheme, in which neural phase-locking to individual cycles of the stimulus mimics the frequency content of the waveform being encoded (Moore, 2008). Since the FFR reflects sustained neural activity integrated over a population of neural elements that is phase-locked to the individual cycles of the stimulus waveform, namely the TFS, as well as the envelope of

the periodic stimulus (Krishnan, 2007), it provides a unique window into characterizing temporal aspects of pitch perception.

History of the FFR

Wever and Bray (1930) first talked about the CM response, which “reproduces” the frequency information inherent in the signal. Worden and Marsh (1968) were first to describe the FFR and suggested the name *frequency-following response* to differentiate it as a neural response from the CM. Initially, the response was thought to be of non-neural origin, such as cross talk in the recording system, remote pickup of the CM, or other artifact (Marsh, Worden, & Smith, 1970).

In order to formally describe the FFR, Worden and Marsh (1968) collected near-field recording in 17 cats to tone pulses from the afferent portion of the auditory nerve. They determined that the FFR could only be reliably recorded in the afferent portion of the auditory pathway up to the inferior colliculus, suggesting that phase-locking is a special characteristic of the brainstem.

To establish that the FFR is of neural origin and to differentiate it from the CM, Marsh et al. (1970) conducted a mini meta-analysis and further experiments which involved severing CN VIII and cooling various auditory brainstem nuclei in cats. Through their research, they concluded that the FFR can be recorded at latencies of 3-6 ms which correspond to its neural generator. In contrast, the CM occurs at latencies (1-2 ms post-stimulus onset) unlikely to be of neural origin (Krishnan, 2007). In addition, the FFR could only be recorded from afferent neurons in the auditory system up to the inferior colliculus, but disappeared when the electrodes were placed in close proximity

(within 1 mm) of non-auditory neurons. Marsh et al. (1970) also determined that the FFR has an abrupt onset which corresponds to the onset of the stimulus.

Perhaps the most compelling evidence differentiating the FFR from the CM came from experiments in which the FFR disappeared under anoxia, but the CM remained. Marsh et al. (1970) showed that severing CN VIII disrupted the FFR and other evoked potentials. Similarly, cooling the cochlear nucleus abolished the FFR with FFR function recovering when the temperature of the cochlear nucleus returned to normal. In contrast, the CM remained unaffected in response to the cooling of the cochlear nucleus or severing of CN VIII. Furthermore, FFR function was only inhibited when the ear ipsilateral to the side of cooling was stimulated, but remained recordable from the superior olivary complex with contralateral stimulation.

In light of this evidence uncovered by initial research, the FFR has been established as a neural response. Recent efforts relating to FFR research are no longer looking to differentiate the FFR from the CM. Instead, current FFR research is looking to evaluate the FFR as a marker of subcortical neural plasticity and in establishing its clinical and research utility.

What is the FFR?

The FFR is a subcortical auditory-evoked response characterized by sustained neural phase-locking at the level of the rostral brainstem (Glaser, Suter, Dasheiff, & Goldberg, 1976; Smith, Marsh, & Brown, 1975). Through its phase-locking ability to sustained auditory stimuli, the FFR provides an objective assessment of neural encoding of spectral information to various acoustic stimuli, such as single-frequency tonebursts and tonal stimuli (Batra et al., 1986; Gardi, Merzenich, & McKean, 1979; Moushegian,

Rupert, & Stillman, 1973; Smith et al., 1975; Worden & Marsh, 1968), two-frequency tone complexes (Bidelman & Krishnan, 2009), inharmonic tones, missing fundamentals (Galbraith, 1994), tonal sweeps (Carcagno & Plack, 2010; Clinard & Cotter, 2015; Krishnan & Parkinson, 2000), iterated rippled noise (IRN) (Krishnan, Bidelman, & Gandour, 2010; Krishnan, Gandour, & Bidelman, 2012; Swaminathan, Krishnan, & Gandour, 2008), and musical intervals (Lee, Skoe, Kraus, & Ashley, 2009). The FFR has furthermore been successfully recorded in response to stimuli approximating acoustic features of speech, such as two-tone steady-state approximations of formants (Greenberg, Marsh, Brown, & Smith, 1987; Krishnan, 1999), formant transitions (Plyler & Ananthanarayan, 2001), Mandarin tones (Krishnan, Gandour, & Cariani, 2004), approximations of Mandarin tone contour patterns (Swaminathan et al., 2008; Wong, Skoe, Russo, Dees, & Kraus, 2007), and natural and synthesized consonant-vowel stimuli (Banai et al., 2009; Cunningham, Nicol, Zecker, Bradlow, & Kraus, 2001; King, Warrier, Hayes, & Kraus, 2002; Musacchia, Sams, Skoe, & Kraus, 2007; Russo, Nicol, Musacchia, & Kraus, 2004; Wible, Nicol, & Kraus, 2004). The FFR has been successfully recorded in a number of different populations, such as adults with and without hearing impairment (Ananthakrishnan et al., 2016; Anderson et al., 2012; Plyler & Ananthanarayan, 2001), musicians (Kraus et al., 2009; Musacchia, Strait, & Kraus, 2008; Parbery-Clark, Skoe, & Kraus, 2009), bilinguals (Krishnan, Gandour, & Cariani, 2005; Xu et al., 2006), as well as children with dyslexia (Banai et al., 2009; Chandrasekaran, Hornickel, Skoe, Nicol, & Kraus, 2009), specific language impairment (Cunningham et al., 2001), and autism spectrum disorder (Russo et al., 2008; Russo, Nicol, Trommer, Zecker, & Kraus, 2009).

Neural Generators of the FFR

Multiple neural generators of the FFR have been proposed. Worden and Marsh (1968) first determined that the FFR can be recorded from the afferent portion of the auditory pathway up to the level of the inferior colliculus in cats and that it is not generated in non-auditory parts of brain. It was further established that the FFR disappears under anoxia, as previously reviewed (Marsh et al., 1970).

In an attempt to establish specific neural generators of the FFR, Smith et al. (1975) conducted near-field FFRs in cats at the level of the cochlear nucleus (CN), superior olivary complex (SOC), and inferior colliculus (IC) and compared the onset latencies of the response with far-field recordings obtained from cats and humans. They determined that near-field recordings at the level of the IC occurred at latencies (5.4 ms) that best approximated the latencies of the far-field recordings in cats (5.8 ms) and humans (6.5 ms).

To corroborate their findings, Smith et al. (1975) attempted to isolate the specific neural generator by evaluating the effects of a reversible cryogenic blockage on the FFR obtained from cats. Cryoprobes were used to cool the lateral medial superior olive (LMSO), left inferior colliculus (LIC), and right inferior colliculus (RIC) and near- and far-field recordings were obtained pre-, during, and post-cooling. Notably, near-field recordings obtained from the RIC and LIC were sensitive to cooling effects. Furthermore, with RIC and LIC cooling, far-field vertex recordings were significantly lower in amplitude or absent. With recovery following cooling, the FFR returned to pre-treatment baseline in both the near-field and far-field conditions. Results from the Smith et al. (1975) experiments suggest that the FFR is generated at the level of the IC.

In contrast to Smith et al. (1975), Gardi et al. (1979) suggested that the IC provides minimal contribution to the scalp-recorded FFR in cats. Instead, they determined that the CN is the greatest contributor, accounting for 50% of the amplitude, followed by cochlear contributions on the order of 25%, and the SOC, specifically the lateral lemniscus (LL), providing 20% of the response amplitude. Gardi et al. (1979) suggest that the differential distribution of sources contributing to the FFR contributes to documented differences in amplitude as a function of stimulus frequency.

Stillman, Crow, and Moushegian (1978) also suspected that the FFR is comprised of multiple neural sources because phase-locking had previously been established to occur in different portions of the brainstem (Marsh, Brown, & Smith, 1974; Starr & Hellerstein, 1971; Worden & Marsh, 1968). They explored potential relative contributions to the FFR by utilizing two different scalp-recorded electrode montages in humans, a horizontal recording montage to capture responses generated by peripheral structures, such as the auditory nerve, and a vertical recording montage to capture more centrally-occurring energy.

Comparing recordings from the horizontal and vertical recording montages, Stillman et al. (1978) found that two main distinct waveforms contributed to the FFR. One of the waveforms was prominent in both recording montages, while the other could only be obtained in the vertical configuration. They suggest that the waveform obtained in the vertical recording montage was generated by central neural generators, such as the IC, while the waveform generated in both recording montages is generated more peripherally. This evidence led Stillman et al. (1978) to conclude that the FFR is comprised of multiple waveform contributions generated by different neural sources

which can be distinguished by comparing simultaneous recordings from the vertical and horizontal recording montages.

Galbraith (1994) further established that different FFR patterns are evoked as a function of dipole orientation to puretone and missing fundamental (MF) stimuli, further suggesting that the FFR is comprised of multiple neural generators. In response to a low-frequency puretone stimulus, the FFR is robustly recordable in both the horizontal and vertical recording montages. In contrast, to MF stimulation, the FFR is only recordable in the vertical recording montage and missing or poorly defined in the horizontal montage. Furthermore, the FFR is phase-delayed relative to the phase of the puretone stimulus in the horizontal montage as expected, and further phase-delayed in the vertical montage, suggesting successive levels of processing. Galbraith (1994) suggests that the horizontal recording configuration assesses distal portions of the auditory nerve and vertical montages assess neurons of the contralateral (to auditory stimulation) LL and IC.

Taken together, these studies have demonstrated that the FFR is first and foremost (a) a neural response (b) generated by multiple subcortical neurons in the brainstem, (c) specifically reflecting sources at the level of the LL, CN, and IC.

FFR Technical Parameters

Not unlike the ABR, the FFR is small in amplitude and can be recorded using similar data acquisition procedures (Krishnan, 2007; Skoe & Kraus, 2010). In order to obtain optimal FFR recordings, various technical parameters relating to stimulus, recording, and subject variables need to be considered. Stimulus parameters include stimulus type, intensity, frequency, rate, and polarity. Recording parameters include electrode montage, averaging window length, filter settings, sweep count, and artifact

rejection protocols. Subject variables are biological characteristics unique to individual participants and might include maturation effects, age, peripheral hearing sensitivity, attention or subject state, and musical background.

FFR Stimulus Parameters

There are a number of stimulus parameters that can affect the response properties of the scalp-recorded FFR, such as stimulus type, stimulus intensity, stimulus frequency, stimulus rate, and stimulus polarity. These stimulus parameters will be discussed in more detail in the sections below.

Stimulus Type

The FFR can be reliably recorded in response to both simple and complex sustained acoustic stimuli (Krishnan, 2007; Skoe & Kraus, 2010). Sustained acoustic stimuli contain continuous acoustic features which can elicit a sustained brainstem response reflecting neural phase-locking (Skoe & Kraus, 2010). As previously described, acoustic waveforms can be described in terms of periodicity (periodic vs. aperiodic) and complexity (simple and complex). Alternatively, the acoustic stimuli used to evoke the FFR may be described by their spectrotemporal characteristics or by their linguistic relevance, as illustrated in Figure 10.

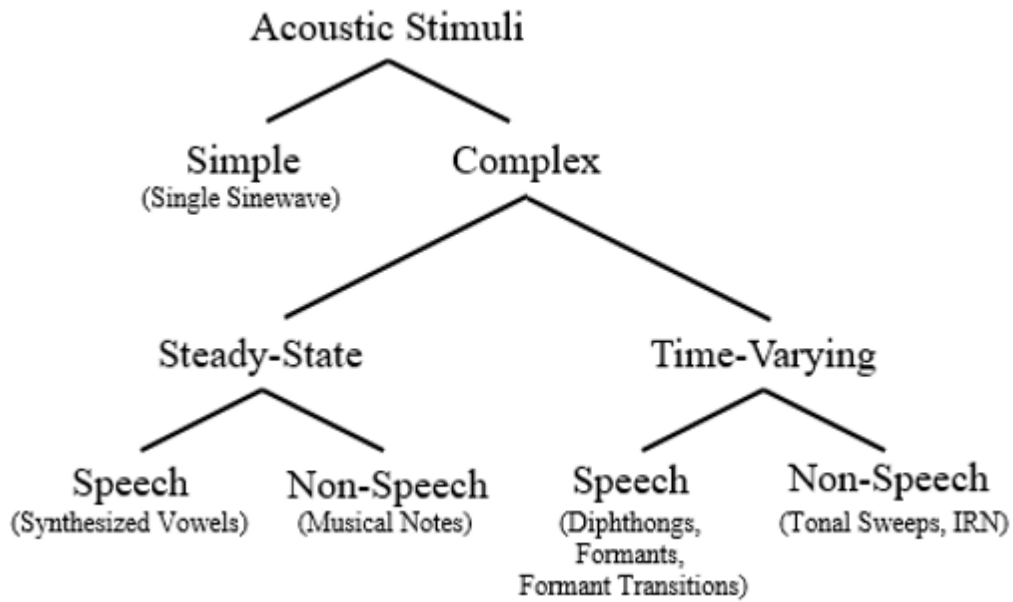


Figure 10. Hierarchy of acoustic stimuli.

As previously discussed, simple waveforms consist of a single sine wave, an example of which is a puretone. Complex waveforms are comprised of multiple simple waveforms and can be further classified by their spectrotemporal characteristics as steady-state or time-varying. Steady-state stimuli remain constant as a function of time, while time-varying stimuli contain frequency and amplitude components which may vary as a function of time, as seen in Figure 11. Both steady-state and time-varying stimuli can further be characterized by their linguistic relevance, as speech or non-speech entities.

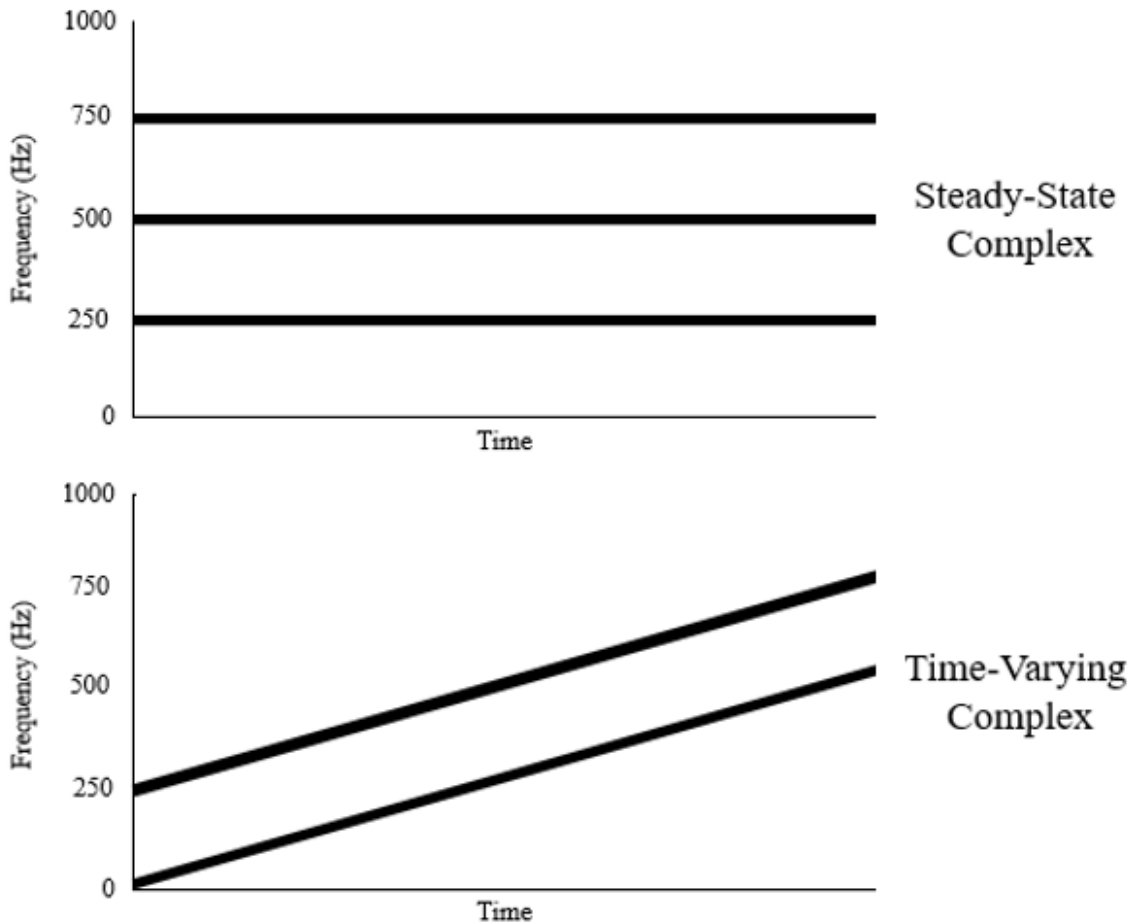


Figure 11. Steady-state and time-varying complex stimuli.

An example of a complex steady-state non-speech stimulus might be a two- or multi-tone complex comprised of multiple pure-tones or musical notes. In contrast, a linguistically relevant counterpart to a complex steady-state stimulus is a synthesized vowel consisting of several formants or a natural vowel that has been resynthesized so that its formants are flattened to a specific frequency. Complex time-varying, non-speech stimuli include IRN and tonal sweeps. Examples of linguistically relevant time-varying stimuli are plentiful because speech is inherently dynamic; these include formants, formant transitions, vowels, diphthongs, CV syllables, and speech in general.

Through its phase-locking ability to sustained auditory stimuli, the FFR provides an objective assessment of neural encoding of spectral information to various acoustic

stimuli and has been successfully recorded in response to a number of different stimuli, previously discussed in more detail. Of particular interest is that the FFR is capable of encoding time-varying and harmonically complex sounds and faithfully represents acoustic properties of speech in part because it is sensitive to small changes in stimulus frequency (Batra et al., 1986; Skoe & Kraus, 2010). For stimuli that change in frequency, a change in neural firing rate may be observed relative to the change in periodicity of the stimulus. In addition, FFR amplitude has been demonstrated to be inversely proportional with frequency within a time-domain waveform, meaning that FFR amplitude decreases as the frequency of the stimulus rises (Clinard & Cotter, 2015). FFRs to rising and falling stimuli both have amplitude increases near response onset (Clinard & Cotter, 2015), however, greater pitch strength has been documented for stimuli increasing in frequency than for stimuli decreasing in frequency (Clinard & Cotter, 2015; Krishnan & Parkinson, 2000; Krishnan et al., 2004).

Stimulus Intensity

Like other auditory-evoked potentials, the FFR is intensity dependent, meaning that the response amplitude and latency varies as a function of stimulus intensity. Specifically, the FFR increases in amplitude as a function of increasing intensity (Davis & Hirsh, 1976; Moushegian et al., 1973; Smith et al., 1975; Stillman et al., 1978; Worden & Marsh, 1968), as illustrated in Figure 12. Notably, the amplitude of the FFR is greatest at stimulus onset and gradually declines even while stimulus intensity remains constant (Worden & Marsh, 1968). This marked increase of FFR amplitude with increasing stimulus intensity is independent of stimulus type; it has been reported for simple pure-

tones or tonebursts (Worden & Marsh, 1968) and complex speech and non-speech stimuli (Krishnan, 2002).

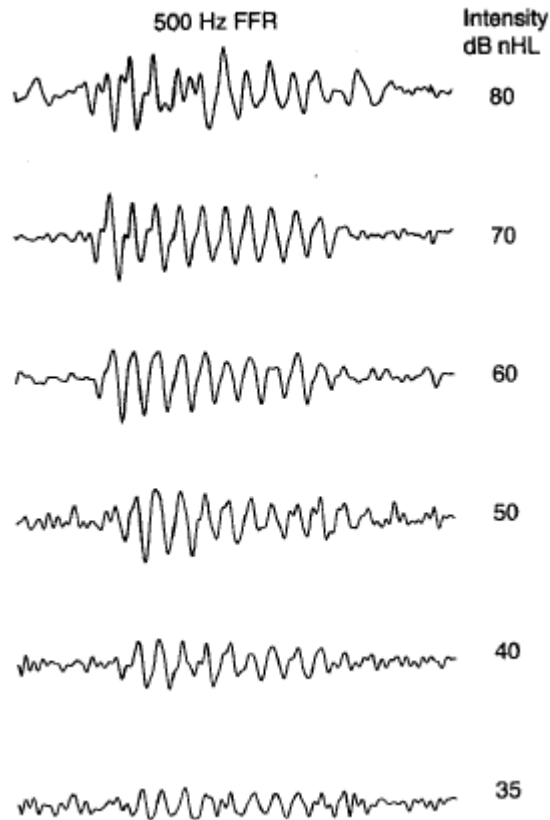


Figure 12. FFR waveforms to 500 Hz tone as a function of stimulus intensity (35, 40, 50, 60, 70, and 80 dB nHL). Note the systematic decrease in amplitude with decreasing stimulus level with little or no change in latency. Adapted from “Frequency-Following Response,” by A. Krishnan, 2007, in Ed. Eggermont, *Auditory evoked potentials: Basic principles and clinical applications*, p. 315. Copyright 2007 by Lippincott Williams & Wil.

An increase in FFR amplitude is largely frequency independent, meaning that the response increases in amplitude as a function of stimulus intensity across frequencies the FFR is capable of encoding (Worden & Marsh, 1968). While an increase in stimulus frequency will elicit greater FFR amplitudes across various frequencies, this effect is more marked for simple low-frequency stimuli and low-frequency components of complex stimuli.

At higher intensities, the neurons which contribute to the FFR are capable of responding to a broader frequency range (Worden & Marsh, 1968), as depicted in Figure 13. The concept of higher intensities eliciting a broader frequency response is attributed to the tuning-curve characteristics of the neurons in the afferent auditory pathway (Gelfand, 2004; Worden & Marsh, 1968).

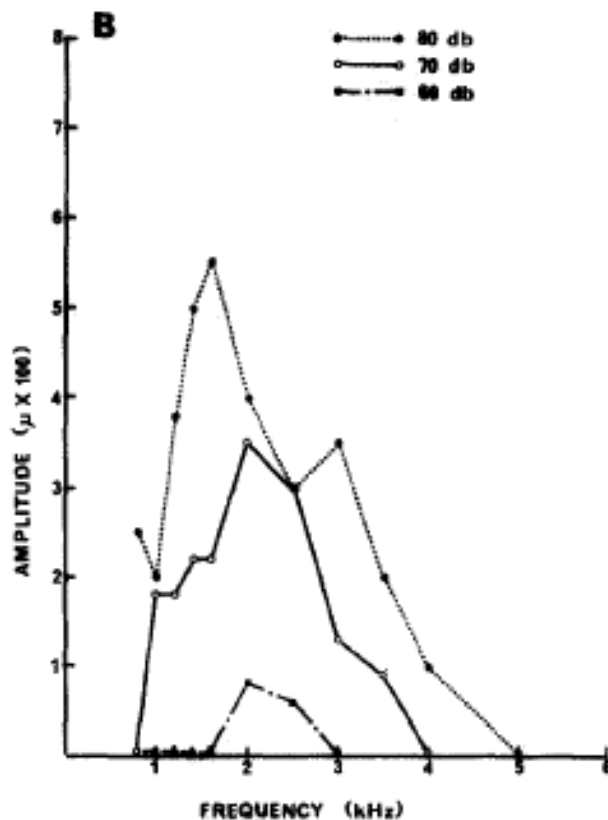


Figure 13. FFR frequency-amplitude curves at three intensities (60, 70, and 80 dB). Adapted from “Frequency-Following (Microphonic-Like) Neural Responses Evoked by Sound,” by F. G. Worden and J. T. Marsh, 1968, *Electroencephalography and Clinical Neurophysiology*, 25, p. 46. Copyright 1968 by Elsevier Inc.

The FFR is identifiable near behavioral threshold (within 10-20 dB SL), but a higher sensation level (SL) (on the order of 35-60 dB SL) is required to elicit temporally precise FFRs (Akhoun et al., 2008; Davis & Hirsh, 1976; Moushegian et al., 1973; Stillman et al., 1978). Supra-threshold stimulus intensity levels on the order of 60-85 dB

SPL are recommended for recording the FFR, as they result in greater response amplitudes and temporal precision (Skoie & Kraus, 2010).

Stimulus Frequency

Another important consideration for stimulus selection is that the FFR is essentially a low-pass response, meaning that it occurs at frequencies below 1500-2000 Hz (Batra et al., 1986; Moushegian et al., 1973; Krishnan, 2007) and is best recorded at frequencies <500 Hz (Greenberg et al., 1987; Harrison & Evans, 1979). At frequencies above 1500 Hz, the response is difficult to recognize, as seen in Figure 14 (Moushegian et al., 1973).

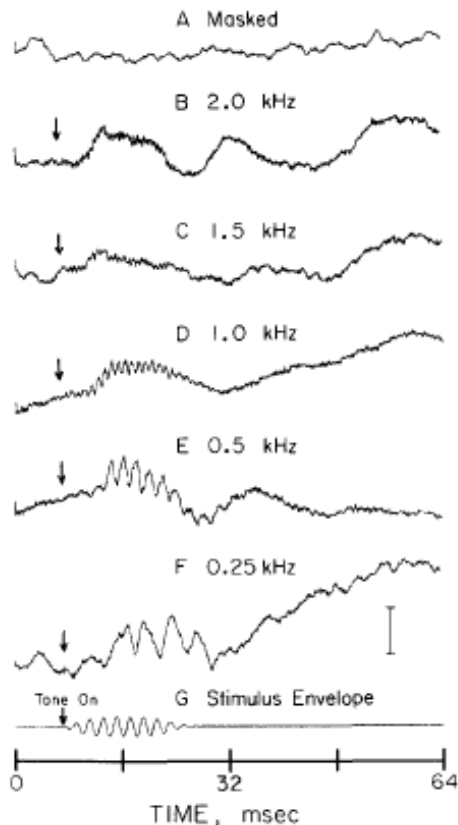


Figure 14. FFR evoked at the frequencies indicated from B through F at 70 dB SL illustrating that the response is difficult to recognize at higher frequencies (≥ 1.5 kHz) relative to lower frequencies (≤ 1.0 kHz). Adapted from “Scalp-Recorded Early Responses in Man to Frequencies in the Speech Range,” by G. Moushegian et al, 1973, *Electroencephalography and Clinical Neurophysiology*, 35, p. 666. Copyright 1968 by Elsevier Inc.

The upper frequency limit of the FFR is contingent on the phase-locking limitations of single neuronal units. Multiple neurons firing together contribute to the FFR, which extends the frequency limit to which the FFR can be recorded to 1500 Hz because neurons take turns firing every few cycles (Batra et al., 1986).

Despite being recordable to stimuli of frequencies up to 1500-2000 Hz, there is a marked increase in variability as a function of increasing frequency (Worden & Marsh, 1968) and a decrease in amplitude as a function of increasing frequency for tonebursts and continuous tones (Glaser et al., 1976; Moushegian et al., 1973; Worden & Marsh, 1968), two-tone stimuli (Krishnan, 1999), and two-tone synthetic vowels (Krishnan, 2002). Furthermore, at higher stimulus frequencies, the response occurs 1-2 ms post-stimulus onset and is likely the CM (Batra et al., 1986). In light of the stimulus frequency limitations of the FFR, Krishnan (2007) recommends that for tonal stimuli, frequencies below 1000 Hz be used. Skoe and Kraus (2010) suggest that for complex stimuli, such as speech, the stimulus should contain a fundamental frequency between 80-300 Hz.

Stimulus Presentation Rate

The stimulus rate refers to the frequency at which a given stimulus is presented. Stimulus rate is typically represented as the number of times a stimulus is presented per second. The rate at which a stimulus is presented is contingent on the length of the stimulus and the requisite inter-stimulus interval (ISI). The ISI is the period of silence between two stimuli, illustrated in Figure 15.

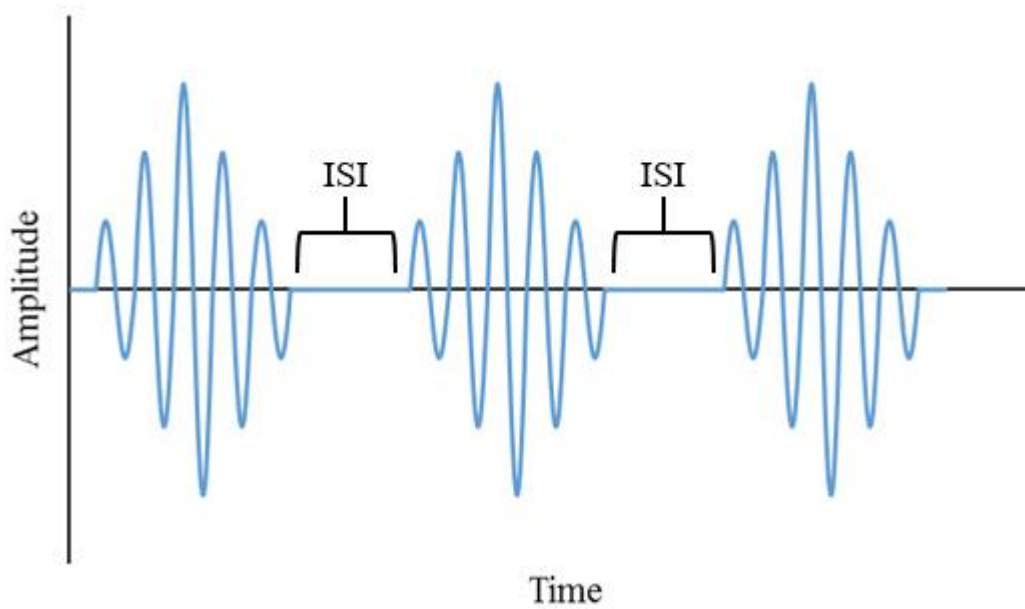


Figure 15. Amplitude modulated sinewave stimuli with ISIs.

Faster stimulus presentation rates (with shorter ISIs) allow for greater number of sweeps to be collected in a given amount of time, which contributes to more rapid SNR increase of the response waveform. Many AEPs, however, are prone to rate-related decreases in response amplitude. These rate effects are directly related to the ISI, which allows the auditory nerve to recover following an excitatory state. During this period of recovery, known as the refractory period, the neuron is unable to fire optimally. If the ISI is shorter than the refractory period, then the onset of the next stimulus occurs during the refractory period, yielding a less robust response of lower amplitude and delayed latency (Picton, 2011). As such, the presentation rate should allow for the response to return to baseline.

Skoe & Kraus (2010) recommend that an ISI 30% of the stimulus duration is used based on a non-descript literature review they conducted. Based on this, a stimulus 120 ms (0.12 s) in length would require an ISI of 36 ms (0.036s). Adding the stimulus length

and the ISI together would yield the total requisite stimulus interval of 156 ms (0.156 s).

To calculate the stimulus rate, the following equation may be used.

$$\text{stimulus rate} = \frac{(1 \text{ second})}{(\text{stimulus length} + \text{ISI})}$$

Following the equation above, a stimulus and ISI with a total duration of 156 ms could then be presented at a rate of 6.41/s.

Krishnan (2007) recommends a presentation rate of 3.1-7.1/s, but notes that the rate should be slower for stimuli of longer duration.

Stimulus Polarity

The FFR can be recorded using condensation, rarefaction, and alternating polarity stimuli (Xu & Ye, 2014). It has been previously established that acoustic waveforms are variations in air pressure (Ladefoged, 1996), alternating in regions of compression and decompression (Skoe & Kraus, 2010). When plotting these variations in pressure as a function of amplitude in the time domain, periods of compression are seen as upward deflections and periods of decompression are seen as negative deflections from baseline, as seen in Figure 16 below.

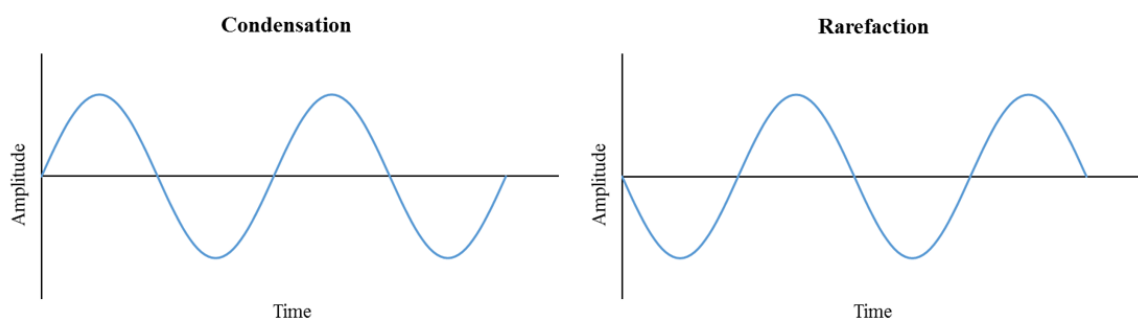


Figure 16. Contrast between condensation (left) and rarefaction (right) waveforms.

Stimuli used to elicit the FFR which begin with a positive deflection or period of compression are said to be condensation stimuli. Conversely, stimuli which begin with a

negative deflection or period of decompression are rarefaction stimuli. The FFR can be elicited in response to both condensation and rarefaction stimuli. It can be recorded to a stimulus of a single polarity or to both polarities (Skoe & Kraus, 2010). Collecting the FFR to both condensation and rarefaction stimuli allows the response to be further manipulated by adding or subtracting responses obtained in one polarity from those of another. Specifically, adding the responses of the two polarity conditions accentuates the lower-frequency components, such as the FFR envelope. In contrast, subtracting responses obtained in one polarity from the other highlights higher-frequency components, such as the spectral FFR. The subtraction manipulation, however, further introduces stimulus artifact and includes contributions from the CM (Aiken & Picton, 2008). Table 2 summarizes the possible response manipulations to stimuli of differing polarities and the components those manipulations separate out.

Table 2

Average Response Nomenclature

Response	Derivation	Components
++	Average together all responses to original stimulus	Envelope FFR Spectral FFR Cochlear microphonic Stimulus artifact
+-	Average together an equal number of responses to the original stimulus and responses to the inverted stimulus	Envelope FFR
--	Subtract responses to the inverted stimulus from an equal number of responses to the original stimulus and divide by the total number of responses	Spectral FFR Cochlear microphonic Stimulus artifact

Note. Adapted from “Envelope and Spectral Frequency-Following Responses to Vowel Sounds,” by S. J. Aiken and T. W. Picton, 2008, *Hearing Research*, 245(1), p. 36. Copyright 2008 by Elsevier Inc.

Recording Parameters

Numerous recording parameters, such as electrode montage, sampling rate, length of averaging window, number of trials, filter settings, and artifact rejection, contribute to a successful FFR recording. These recording parameters will be discussed in more detail in the sections below.

Electrode Montage

The FFR can be obtained in single-channel, two-channel, and three-channel, vertical or horizontal recording montages. In a three-electrode, single-channel recording, the electrodes are termed non-inverting, inverting, and common or ground (Hall, 2007). The International 10-20 system, pictured in Figure 17, is commonly used for correlating external scalp electrode placement with underlying neural generators (American Clinical Neurophysiology Society [ACNS], 2006). It is based on the identification of anatomical landmarks, such as the nasion, inion, and midline, with incremental designations for electrode placement in 10% or 20% steps (ACNS, 2006; Sharbrough, 1991). The 10-20 system allows for reliable positioning of electrodes near a desired neural generator independent of head size (Sharbrough, 1991; Picton, 2011).

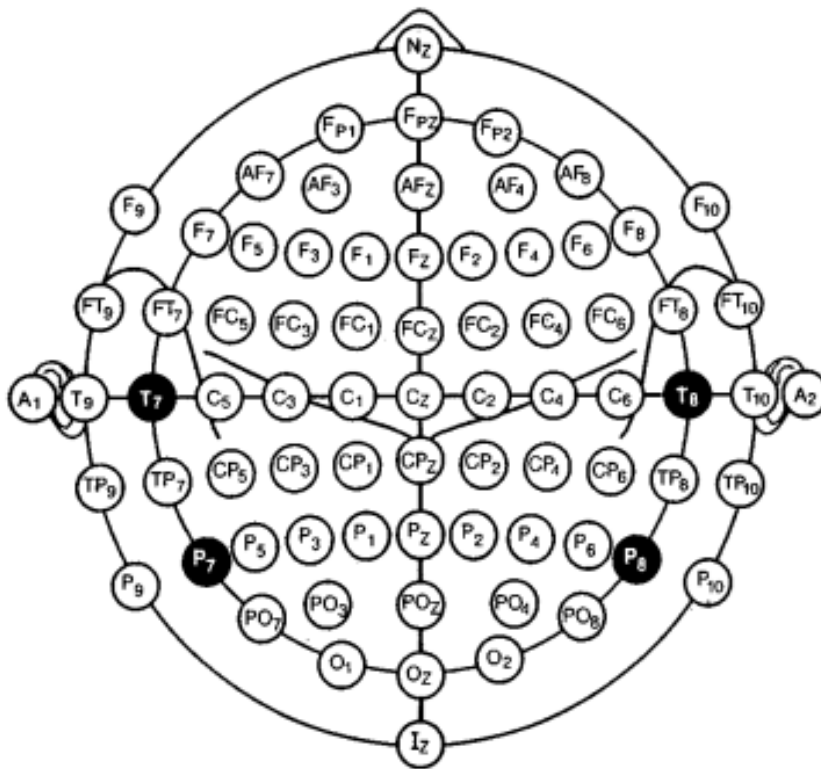


Figure 17. Electrode locations in the 10-20 system, where A = auricle, AF=, C=central, CP=centroparietal, F=frontal, FC=frontocentral, Fp=frontal polar, FT=frontotemporal, I=inion, M=mastoid (not pictured), N=nasion, O=occipital, P=parietal, PO=parieto-occipital, T=temporal. Odd-numbered subscripts are used to refer to positions on the left side and even-numbered subscripts are used for positions on the right. Locations named with a subscript “z” denote the midline. Adapted from “American Electroencephalographic Society Guidelines for Standard Electrode Position Nomenclature,” by F. Sharbrough et al., 1991, *Journal of Clinical Neurophysiology*, 8(2), p. 201. Copyright 1991 by American Electroencephalographic Society.

Following the International 10-20 schematic, a single-channel montage conventionally used for brainstem AEPs would feature a reference or inverting electrode on the mastoid (M₁ or M₂) or the auricle (A₁ or A₂), an active or non-inverting electrode at the vertex (C_z), and a ground electrode, typically placed near the nasion or forehead (Fp_z). A two-channel electrode montage would be the same as the one-channel montage described above, with the addition of another active electrode. A three-channel montage would feature three active electrodes, and so forth. An example of a one-channel, two-

channel, and three-channel electrode montage is provided in Figure 18. Choice of additional active electrodes for two-channel, three-channel, etc. electrode configurations depends on which features or underlying neural generators are desired to be captured as contributing to the evoked response.

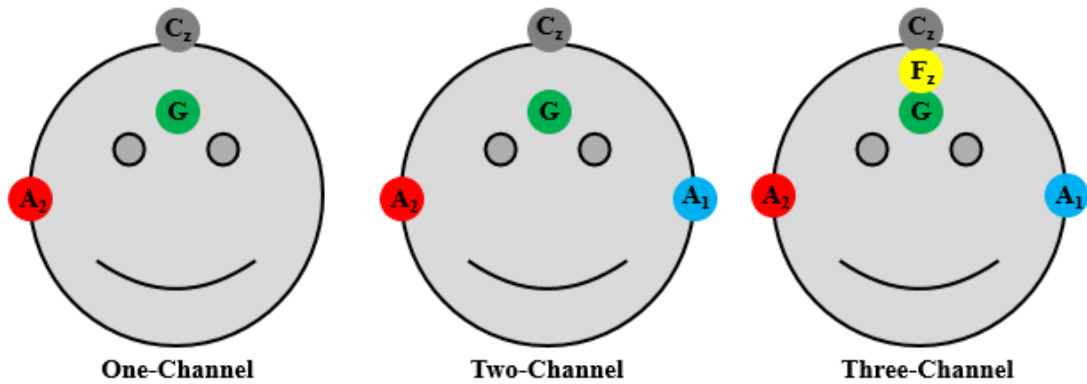


Figure 18. Example of a one-channel (left), two-channel (middle), and three-channel (right) electrode montage, in which G is ground (at Fp_z), A_2 is the reference (inverting) electrode, and C_z , A_1 , and F_z are designated as the active (non-inverting) electrodes.

While both vertical and horizontal electrode montages may be employed to record the FFR, it has previously been established that there are multiple neural generators which are suspected contributors to the FFR (Davis & Hirsh, 1976; Gerken, Moushegian, Stillman, & Rupert, 1975; Glaser et al., 1976; Marsh et al., 1975; Moushegian et al., 1973; Stillman et al., 1976). Approximate relative contributions of these neural generators can be distinguished from one another by comparing the latency and spectral characteristics of the FFR obtained in the horizontal and vertical electrode montage, with FFRs obtained in the horizontal configuration exhibiting shorter latencies than those obtained in the vertical montage, as seen in Figure 19.

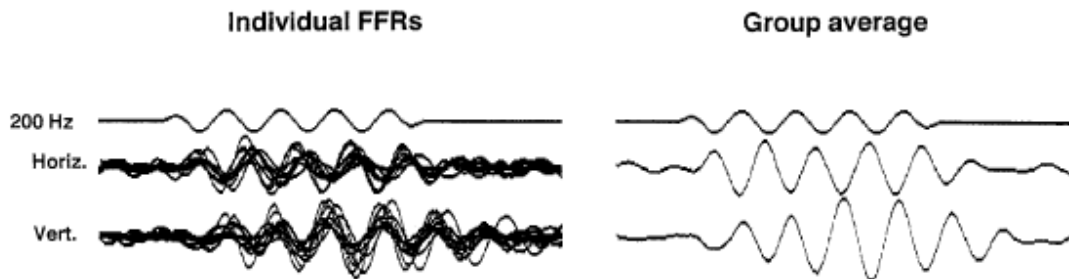


Figure 19. Superimposed individual FFR waveforms (left) and corresponding group averages (right) to 200 Hz pure-tone stimulus recorded from horizontal and vertical electrode montage. Adapted from “Two-Channel Brain-Stem Frequency-Following Responses to Pure Tone and Missing Fundamental Stimuli,” by G. C. Galbraith, 1994, *Electroencephalography and Clinical Neurophysiology*, 92, p. 324. Copyright 1994 by Elsevier Inc.

Given the latency differences between the two electrode configurations, it stands to reason that shorter latencies correspond to contributions from peripheral neural generators while longer latencies reflect contributions from neural generators further up the auditory pathway. Consequently, horizontal montage captures energy from more peripheral structures, such as the auditory nerve, while a vertical montage is more likely to capture more central contributions from the rostral brainstem (Galbraith, 1994; Stillman et al., 1976). Selection of an electrode recording montage is therefore contingent on the neural generators of interest, with a vertical montage recommended unless an attempt is made to capture contributions from more peripherally occurring neurons as well (Galbraith, 1994; Skoe & Kraus, 2010).

Sampling Rate

The sampling rate refers to the frequency at which a particular signal is analyzed and subsequently digitized. Sampling allows for a continuous signal varying in amplitude, such as a sound wave, to be represented by a set of discrete numbers (or samples). The accuracy with which a continuous signal can be represented depends on the number of samples taken per second, with higher sampling rates yielding more

felicitous waveform representations, as shown in the bottom waveform of Figure 20. If a wave is sampled at a rate that is too slow, variations which occur at rapid rates cannot be faithfully represented, as depicted in the top waveform of Figure 20.

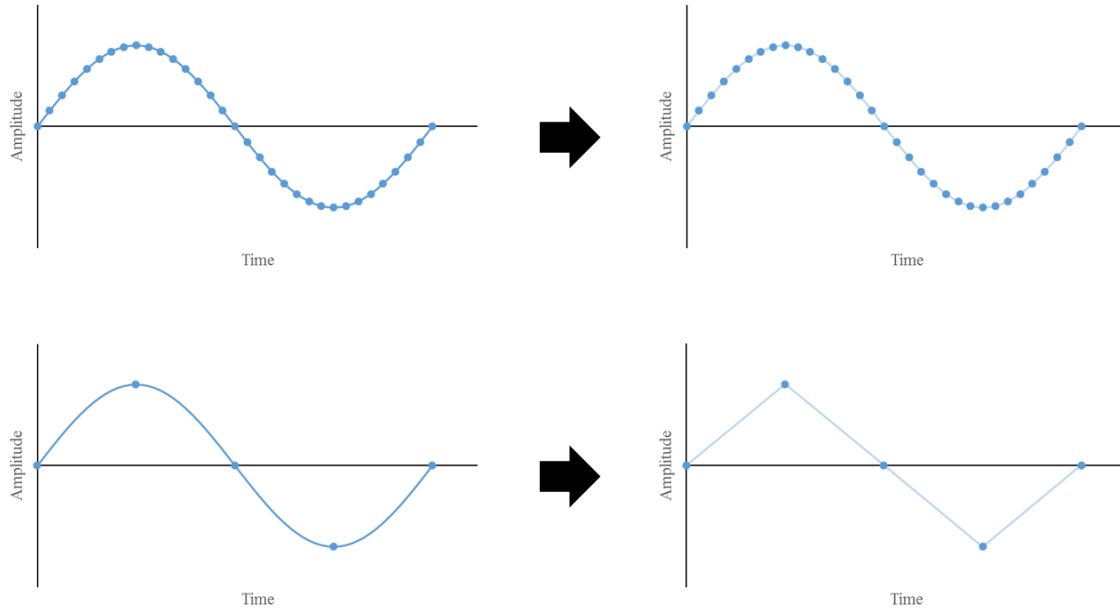


Figure 20. A wave sampled at a high sampling frequency (top) yields a more faithful representation than a wave sampled at a low sampling frequency (bottom).

To avoid aliasing, which is an incorrect representation of a signal of a given frequency resulting from under-sampling, the sampling rate should be at least twice the frequency of the highest frequency component present in a given signal. This is known as the Nyquist frequency and corresponds to the lowest rate at which a signal can be sampled without introducing errors (Ladefoged, 1996).

To avoid sampling errors, over-sampling is generally recommended when obtaining FFR recordings (Akhoun et al., 2008; Banai et al., 2009; Krishnan et al., 2005). Given that the FFR is a low-frequency response optimally recorded below 500 Hz, a sampling frequency of 1000-2000 Hz would be sufficient in most cases. Skoe and Kraus

(2010) recommend a sampling rate between 6,000-20,000 Hz, citing better temporal precision as their rationale.

Since the frequency of the stimulus predicts the frequency components present in the FFR, a sampling rate twice the frequency of the highest frequency component of the stimulus should be sufficient to faithfully represent the FFR. The highest stimulus frequency in the current study is 707 Hz, indicating a sampling frequency of 1414 Hz to be sufficient. To avoid misrepresenting higher frequency components which may be present in the FFR recording, however, a sampling rate of 22,000 Hz will be utilized.

Response Filter Settings

Not unlike the sampling rate, response filter settings are contingent on the frequency components predicted to be present in the FFR. Filters should be set so as to reduce unwanted noise in the recording but allow the desired response to be captured. Filtering the FFR recording isolates cortical from subcortical activity and increases the SNR of the response (Skoe & Kraus, 2010).

Skoe and Kraus (2010) recommend bandpass filtering from 100-3000 Hz because this frequency range has been shown to maximize the response and is capable of capturing higher frequency components elicited by the onset response. Krishnan (2007) suggests digitally filtering the response post-averaging from 30-3000 Hz. Lowering the high-pass filter cut-off frequency permits the capture of the response to lower frequency stimuli typically used to elicit the FFR.

Number of Sweeps

Early AEPs, such as the ABR and FFR, are low-amplitude responses. In order to distinguish these relative low-amplitude responses from the surrounding undesirable higher-amplitude background EEG activity, responses to a large number of sweeps are averaged together and submitted to signal processing magic. Sweeps or trials refer to the number of times a stimulus is presented during a particular recording run. Conversely, epochs are the stimulus waveforms which meet the response collection criteria which differentiate the desired FFR from artifact.

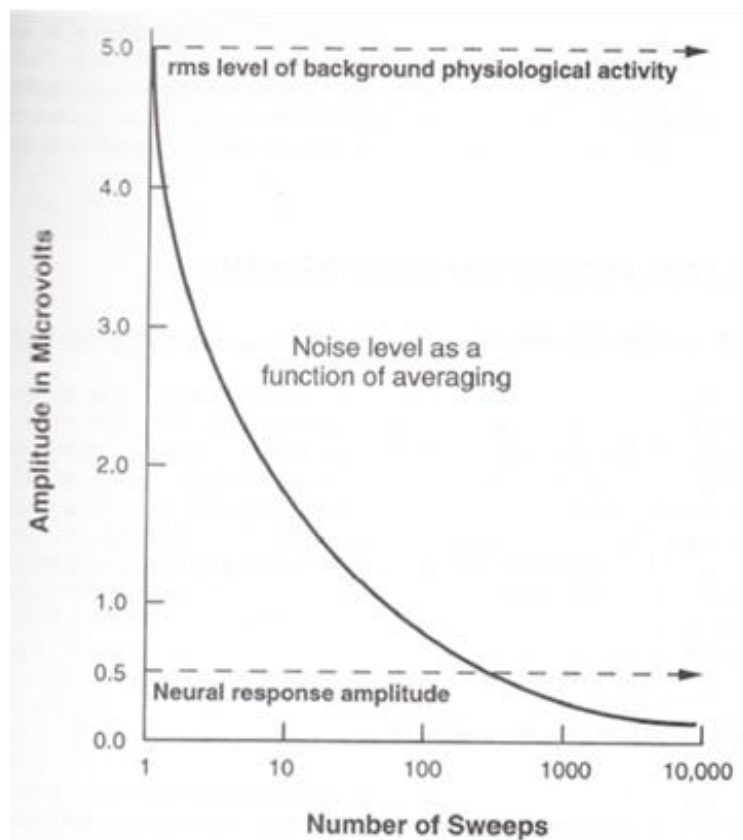


Figure 21. Relation of signal-to-noise ratio to number of sweeps. In this figure, the neural (e.g., ABR) amplitude is 0.5 μV and the level of the background physiological noise is 5.0 μV . The bold line shows the decreasing amplitude of physiological activity as a function of increasing the number of sweeps from 1 to 10,000. rms = root mean square. Adapted from “Clinical Applications of the Auditory Brainstem Response,” by L. J. Hood, 1998, p. 33. Copyright 1998 by Cengage Learning.

Recordings with higher sweep counts generate AEPs at a more favorable signal-to-noise ratio (SNR), following the principle that the SNR is proportional to the square root of the number of sweeps, as seen in Figure 21 (Hall, 2007; Hood, 1998; Özdamar & Delgado, 1996). The effect that sweep count has on the quality of the ABR waveform is illustrated in Figure 22, which shows a series of responses averaged at various increasing sweep interval. Below 800 sweeps, for example, the ABR is difficult to distinguish and lacks the desired replicability. Above 800 sweeps, the waveform is clearly identifiable, exhibiting excellent replicability and morphology.

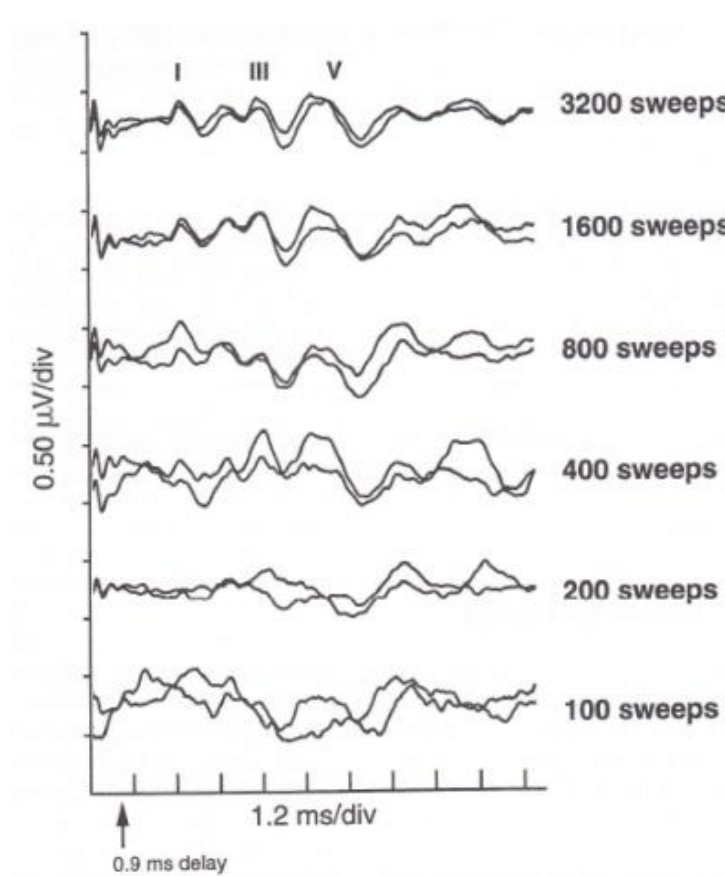


Figure 22. ABR recordings as a function of the number of sweeps included in the averaged waveform ranging from 100 sweeps (bottom tracing) to 3200 sweeps (top tracing). As the number of sweeps increases, the background noise decreases, making the ABR more visible. Adapted from “Clinical Applications of the Auditory Brainstem Response,” by L. J. Hood, 1998, p. 32. Copyright 1998 by Cengage Learning.

To my knowledge, the effect of sweep count on the quality of the FFR has not been formally established. Krishnan (2007) recommends that 1000-2000 sweeps are sufficient for high-intensity stimuli, but notes that the sweep count is contingent on the complexity of the stimulus and the underlying noise inherent to the recording. Skoe and Kraus (2010) suggest a wider range of 1000-6000 sweeps for FFR data collection, noting that a more conservative approach with higher sweep numbers allows for sub-averaging to track how the response develops over time and allows for more subtle group differences to emerge which might not be inherent to the response at lower sweep counts. While there is no inherent drawback to collecting the FFR to sweeps in excess, this may considerably and unnecessarily prolong testing time and patient discomfort. In the event that the FFR is utilized clinically in the future, testing time would become especially relevant. Responses that are analyzed in the frequency domain may require fewer sweeps if response detection is the goal (Aiken & Picton, 2006; Aiken & Picton, 2008; Dajani et al., 2005). Complex, time-varying stimuli requiring more complex analyses may require additional stimulus presentations.

Skoe and Kraus (2010) contend that an optimal number of sweeps may be difficult to establish for the FFR due to variations in the populations tested and the stimuli utilized to elicit the response. They suggest that the optimal range may be estimated by collecting pilot data with an excessive number of sweeps and sub-averaging at discrete intervals to characterize the relationship between sweep count and FFR quality for a given population and stimulus.

Averaging Window

The length of the averaging window in ms allows for the desired neural signal to be collected and averaged. It should be long enough to include the pre-stimulus baseline period, the response period, and the post-stimulus period (Skoe & Kraus, 2010). The pre-stimulus window consists of baseline EEG activity. Establishing baseline EEG activity is critical for the interpretation of the FFR as it allows the response to be distinguished from the underlying EEG activity and aids in its interpretation. Skoe and Kraus (2010) recommend a pre-stimulus window length that includes one full analysis window. A pre-stimulus period of 40 ms was used for this study.

The length of the response period is contingent on the length of the stimulus. For the present study, a tonal sweep 120 ms in length was utilized. The post-stimulus window should be long enough to account for stimulus transmission delay and neural conduction time (Skoe & Kraus, 2010). While Skoe and Kraus (2010) suggested a post-stimulus window of 10-50 ms to be sufficient, a post-stimulus window of 240 ms was used for the present study. The total length of the averaging window was 280 ms, which included the 40 ms of pre-stimulus and 240 of post-stimulus window lengths. It should be noted, however, that the figures in the present document representing the response waveform have been shortened for aesthetic reasons with respect to the pre- and post-stimulus windows as appropriate.

Artifact

There are different types of artifact which may contaminate an FFR recording. They can be classified as either biological artifact or external artifact. Biological artifacts arise from the subject and include myogenic contamination and the CM. External

artifacts are generated by non-biologic sources, such as the recording equipment, transducers, and electricity; this includes electrical line noise and stimulus artifact.

Myogenic, or muscular, artifact is generally a large amplitude contamination of the response in response to subject movement. Since the FFR is relatively small in amplitude, myogenic artifact obscures the desired neural response. In order to exclude myogenic responses from the final average, amplitude rejection filters between $\pm 20 \mu\text{V}$ to $\pm 75 \mu\text{V}$ are recommended (Skoe & Kraus, 2010). To avoid excessive sweeps from lowering the number of sweeps contributing to the final average, however, it is best to avoid myogenic artifact when possible. This can be accomplished by stabilizing participants' head and neck, instructing participants to close their eyes and remain still and relaxed, and encouraging participants to fall asleep.

The CM is also considered a biologic artifact generated as an electrical potential within the cochlea and can mimic temporal aspects of stimulus waveform, complicating the interpretation of the FFR. Generally, the CM can be differentiated from the desired neural response with respect to the latency at which it occurs, with the CM occurring 1-2 ms post-stimulus onset, while the FFR occurs between 6-10 ms. In addition, the FFR can be distinguished from the CM in that the FFR is privy to rate and intensity effects like other neural responses (Skoe & Kraus, 2010).

External artifacts, such as electrical noise, are typically generated by line noise, which is a fluctuation of the electrical impulses carried in standard AC current. Line noise occurs between 50-60 Hz and can be reduced or eliminated by applying line filters and by minimizing electrical interference by unplugging and turning off excessive equipment and conducting the testing in an electrically shielded room or booth.

Stimulus artifact is another example of external artifact and arises from stimulus transducers not adequately shielded. If the transducer is not well-shielded, the electrical signal generating the stimulus can leak and be picked up by the recording electrodes. Since the FFR is capable of faithfully representing certain stimuli waveforms, adequate electromagnetic shielding of the transducers is crucial to avoid potential contamination of the response (Skoe & Kraus, 2010). In addition to adequately shielding the transducers, potential contributions from stimulus artifact can be reduced by extending the transducer tubing, thereby positioning the transducers further from the electrodes. Care should be taken to account for any response latency delays due to additional tubing length.

Lastly, to ensure that efforts to minimize stimulus artifact were successful, a clamped run can be conducted. In a clamped run, the stimulus is generated at the desired sound pressure level (SPL) and routed through the transducer, but the tubing leading to the participants' ear is obstructed by a clamp to ensure that no stimulus is heard. If a response is obtained in the clamped condition, it is likely that stimulus artifact has contaminated the recording session and results should therefore be interpreted with caution.

Subject Parameters

Subject parameters are inherent to the individuals being studied and relate to anatomical or physiological differences. These might include things such as subject state, maturation, and hearing status. Subject state, which relates to attention, maturation, which deals with aging, and hearing status have all been documented to have variable effects on the quality of FFR recordings. The effects of subject parameters on the FFR are difficult

to compare since great variability exists in the populations studied and the stimuli used to elicit the response.

Subject State

A clear consensus on the effects of attention and sleep on the FFR have not been definitely established. The FFR has been documented to be recordable in both sleeping and awake conditions and is allegedly minimally affected by sleep and sedation (Skoe & Kraus, 2010). While some researchers encourage their subjects to remain awake and relaxed throughout the recording session to avoid introducing variables related to attention (Skoe & Kraus, 2010), others encourage their subjects to sleep to reduce myogenic artifact (Aiken & Picton, 2006).

The FFR has also been recorded in active conditions to both tonal and speech stimuli in which subjects were asked to selectively attend to one stimulus over another (Galbraith & Arroyo, 1993; Galbraith et al., 1998; Galbraith & Kane, 1993; Galbraith & Doan, 1995; Galbraith, Olfman, & Huffman, 2003; Hoormann, Falkenstein, & Hohnsbein, 1994) with conflicting results. While some studies suggest that there might be some attention-related modulation effects occurring at the level of the brainstem (Galbraith & Arroyo, 1993; Galbraith et al., 1998; Galbraith & Doan, 1995; Galbraith et al., 2003; Hoormann et al., 1994), others fail to corroborate those findings for sub-cortically generated response, such as the FFR (Galbraith & Kane, 1993).

Effect of Aging

Speech discrimination is contingent on accurate temporal processing and is often compromised in older adults, potentially accounting for the increase in communicative difficulties reported by that population not otherwise accounted for by peripheral hearing

sensitivity. Age-related perceptual changes in temporal resolution have been explored in humans using voice-onset time discrimination (Tremblay, Piskocz, & Souza, 2003), gap-detection threshold estimation (Lister & Roberts, 2005; Lister & Tarver, 2004), duration discrimination (Fitzgibbons & Gordon-Salant, 1995), masking level difference estimations, and interaural timing differences (Strouse, Ashmead, Ohde, & Grantham, 1998).

Previous studies have also demonstrated that aging negatively impacts neural phase-locking as indexed by the FFR, affecting the amplitude and peak timing of the response (Anderson et al., 2012; Clinard & Cotter, 2015; Clinard & Tremblay, 2013; Clinard et al., 2010; Marmel et al., 2013; Presacco et al., 2015).

Clinard et al. (2010) obtained frequency discrimination difference limens (FDLs) to 500 Hz and 1000 Hz tonebursts and FFRs to tonebursts of 6 different frequencies (463, 498, 500, 925, 998, and 1000 Hz) in 32 normal hearing adults ranging in age from 22-77 years, with approximately 5 subjects representing each age decade. They established that frequency discrimination as determined by FDLs was significantly negatively correlated with increasing age. While FFR data showed a similar trend with respect to amplitude and phase-coherence (PC) at test frequencies ≥ 925 Hz, no difference in the FFR as a function of age was established at test frequencies ≤ 500 Hz. They concluded that neural representation of frequency was degraded as a function of increasing age but was also frequency dependent, with higher frequencies represented less robustly than lower frequencies.

Clinard and Tremblay (2013) further explored the effects of age on the neural representation of speech with complex consonant-vowel (CV) stimulus /da/. They

evaluated both transient onset and offset responses and found age-related latency delays for both parameters not otherwise accounted for by hearing sensitivity. Sustained response components also exhibited age-related degradation, specifically poorer onset-of-periodicity encoding. As expected, reduced amplitudes and increased latencies as a function of increasing age contributed to poorer phase-coherence.

To evaluate the effects of age on subcortical temporal neural precision, Anderson et al. (2012) recorded complex auditory brainstem responses (cABRs) in response to speech syllable /da/ in normal-hearing younger adults (18-30 years old) and older adults (60-67 years old). They found that younger adults' responses had earlier peak latencies corresponding to the onset of the stimulus, as well as better neural phase-locking to both the formant transition and steady-state portion of the stimulus. Response amplitudes were also significantly greater in young adults than in older adults corresponding to the entire stimulus, with older adults exhibiting higher pre-stimulus EEG amplitudes. Anderson et al. (2012) also evaluated response consistency, with younger adults exhibiting less noisy responses than the older adults. They conclude that there is a marked decrease in neural precision in older adults independent of peripheral hearing thresholds, leading to temporal processing deficits in that population.

Clinard and Cotter (2015) further evaluated aging effects on the FFR in normal hearing younger adults (21-24 years old) and older adults (51-67 years old) in response to falling and rising dynamic tonal stimuli. Three rates of frequency change (1333, 3999, and 6667 Hz/sec) were selected to approximate formant transitions found in the English language. They found that younger adults' FFR waveforms had larger amplitudes than the older adults across all stimulus conditions. Furthermore, stimulus-to-response

correlations and time-frequency analyses of discrete portions of the response indicated age-related degradation for older adults, suggesting that older adults encode dynamic stimuli, such as formant transitions, less effectively than their younger adult counterparts.

Ananthakrishnan et al. (2016) explored the effects of aging on subcortical neural representation of envelope and TFS by eliciting FFRs to a 265 ms in length, synthesized, steady-state, four-formant vowel /u/ at 80 dB SPL in 25 individuals with normal hearing (age $M = 27.72$ years, $SD = 9.33$) and 19 individuals with SNHL (age $M = 54.26$ years, $SD = 19.40$). They concluded that degree of hearing loss, but not age, significantly predicted F_0 encoding. Similarly, an effect of hearing loss, but not age, was documented when F_1 of the FFR was analyzed.

Effect of Hearing Impairment

Sensorineural hearing loss (SNHL) has been demonstrated to have detrimental effects on both speech perception (Abel, Krever, & Alberti, 1990; Lorenzi, Gilbert, Carn, Garnier, & Moore, 2006) and neural encoding of auditory information (Ananthakrishnan et al., 2016; Anderson et al., 2013; Marmel et al., 2013; Plyler & Ananthanarayan, 2001). Specifically, neural encoding of both envelope and TFS cues has been demonstrated to be degraded in individuals with hearing impairment (Ananthakrishnan et al., 2016). The degradation of neural encoding attributed to SNHL may be accounted for by both reduced audibility of the stimulus and distortion of the signal (Ananthakrishnan et al., 2016; Plyler & Ananthanarayan, 2001).

To evaluate the effects of hearing loss on phase-locking, Plyler and Ananthanarayan (2001) recorded FFRs in response to a 100 ms four-formant, 15-step /ba/, /da/, /ga/ synthesized continuum in 32 adults (20-67 years old) equally split into

normal-hearing and hearing-impaired groups. The age distribution for each of the two groups is not available. Of particular interest to the study was the encoding of F_2 , which was varied in onset frequency from 900 to 2300 Hz in 100 dB steps before transitioning to its steady-state portion at 1250 Hz. The researchers evaluated the degree to which the FFR could represent the time-varying frequency content of the F_2 transition and found that hearing-impaired participants produced FFRs with less or no spectral shift than FFRs obtained from the participants with normal hearing. They concluded that hearing loss might result in reduced phase-locking due to wider critical bands and loss of cochlear frequency tuning, which would contribute to a lack of spectral shift in the FFR recorded from hearing-impaired participants. Of particular interest, however, is that while the hearing-impaired group demonstrated a systematic degradation of phase-locked activity, an undisclosed number of participants with hearing loss had FFRs which did demonstrate phase-locking to the transition of F_2 .

Anderson et al. (2013) evaluated the effects of hearing loss on envelope and TFS encoding in 30 adult participants using the FFR in response to a synthesized 40-ms /da/ syllable in quiet and in noise. Of the 30 participants, 15 had mild to moderately-severe SNHL; the 15 normal-hearing participants were matched in age and gender. To correct for audibility in the hearing impaired group, participants with hearing loss were submitted to an additional two stimulus conditions which were amplified to each participant's hearing loss configuration using the National Acoustics Laboratory-Revised algorithm. Results from the study suggest that hearing loss does not impact TFS encoding, but that the representation of the stimulus envelope is enhanced in individuals

with peripheral hearing deficits, thereby disrupting the relative balance between TFS and envelope encoding.

Marmel et al. (2013) investigated the relationship between phase-locking and frequency discrimination as a function of age and hearing loss. Frequency difference limens (FDLs) and FFRs were obtained from participants ($N = 27$, age = 22-77) with normal hearing and hearing loss to 660 Hz tones. FFRs were furthermore obtained to 620, 640, 664, 680, and 720 Hz stimuli 200 ms in length. Marmel et al. (2013) determined that FFR stimulus-to-response cross-correlation synchronization strength was significantly positively correlated with behaviorally obtained FDLs independent of age and hearing loss, meaning that the greater the correlation between the stimulus and the response for the FFR, the more precise the frequency discrimination of the participants. In contrast to the findings from Plyler and Ananthanarayan (2001) and Anderson et al. (2013), Marmel et al. (2013) found that thresholds did not predict FFR signal-to-response fidelity, but age did, such that poorer audiometric thresholds did not result in poorer phase-locking but older age did.

Most recently, Ananthakrishnan et al. (2016) explored the effects of hearing loss on the subcortical neural representation of envelope and TFS by eliciting FFRs to a 265 ms in length, synthesized, steady-state, four-formant vowel /u/. Ten individuals with normal hearing (age $M = 24.55$ years, $SD = 3.35$) and nine listeners with mild to moderate SNHL (age $M = 50.66$, $SD = 17.80$) participated in the experiment. Stimuli were presented monaurally at multiple SPLs (60-85 dB SPL in the normal-hearing participants and 70-95 dB SPL in the hearing-impaired participants) to (a) evaluate the effect of stimulus intensity on the FFR and (b) to make comparisons between groups at

equal SL. Predictably, as the intensity of the stimulus increased, so did the amplitude of the FFR response for both the normal hearing and hearing impaired individuals.

Individuals with SNHL, however, exhibited waveforms with smaller amplitudes and spectrograms of the response with less clear response bands and more spectral smearing for both FFR_E and FFR_{TFS}. When compared at equal SL (50, 55, and 60 dB SL), however, a statistically significant effect of hearing loss was documented between participants with normal hearing and SNHL for the FFR_{TFS} only. Unfortunately, restoring audibility for a signal does not mitigate the effects of hearing impairment on subcortical neural encoding (Ananthakrishnan et al., 2016).

What information does the FFR provide us?

The FFR provides an objective and non-invasive measure of how sustained acoustic stimuli are encoded at the level of the brainstem across a wide range of populations (Skoe & Kraus, 2010). Because precise neural encoding of various stimuli is indicative of a normal auditory system, the FFR could further our understanding of the neural correlates which might account for a functional and a deficient auditory system and shed light on communicative difficulties reported by individuals which are not otherwise accounted for by peripheral hearing sensitivity (Batra et al., 1986).

Goals of the Current Study

Speech is an inherently dynamic signal. Formants are essential time-varying features of speech critical for speech discrimination. Neural synchrony of the auditory system is important for encoding sustained, dynamic features of speech, such as formants and formant transitions. The synchronous neural firing which supports the encoding of time-varying features of auditory signals has been demonstrated to be disrupted in older

and hearing-impaired adults. It has been established that the FFR is capable of providing an objective assessment of neural encoding at the level of the rostral brainstem to both simple and complex steady-state and time-varying stimuli, thereby indexing the degree of synchronous neural firing.

In light of this, the goal of this thesis is to utilize the FFR to characterize the degree of neural synchrony to synthesized dynamic tonal stimuli approximating formant transitions in three groups, YNH, ONH, OHI individuals. Specifically, the aim is

- to establish the effect age and hearing status on FFR recordings,
- to explore individual FFR differences within and across the three groups (YNH, ONH, OHI) that were tested, and
- to determine how sweep count affects FFR fidelity.

CHAPTER 3: METHODOLOGY

Participants

Thirty adult subjects participated in this study. They were divided into three groups, young normal-hearing (YNH) ($N = 10$, mean age = 28.1 years, $SD = 3.6$, age range = 24-33 years), older normal-hearing (ONH) ($N = 10$, mean age = 61.1 years, $SD = 4.8$, age range = 51-66 years) and older hearing-impaired (OHI) ($N = 10$, mean age = 66.8 years, $SD = 7.8$, age range = 54-78 years). All subjects were remunerated for their participation and provided informed consent in accord with the Institutional Review Board at the National Center for Rehabilitative Auditory Research (NCRAR). Demographic information was collected and subjects were screened for sleep and mood-altering medications prior to FFR collection.

Audiometry

Otoscopy and pure-tone audiometry were conducted to establish if subjects met experiment inclusion criteria. Air conduction thresholds were established from 250-8000 Hz at octave and inter-octave frequencies, with the exception of 750 Hz. Normal hearing was defined as thresholds better than 20 dB HL from 250-4000 Hz in the test ear. All HI participants had mild to moderately-severe hearing loss from 250-4000 Hz. Mean frequency-specific pure-tone thresholds are summarized in Figure 23 by group membership.

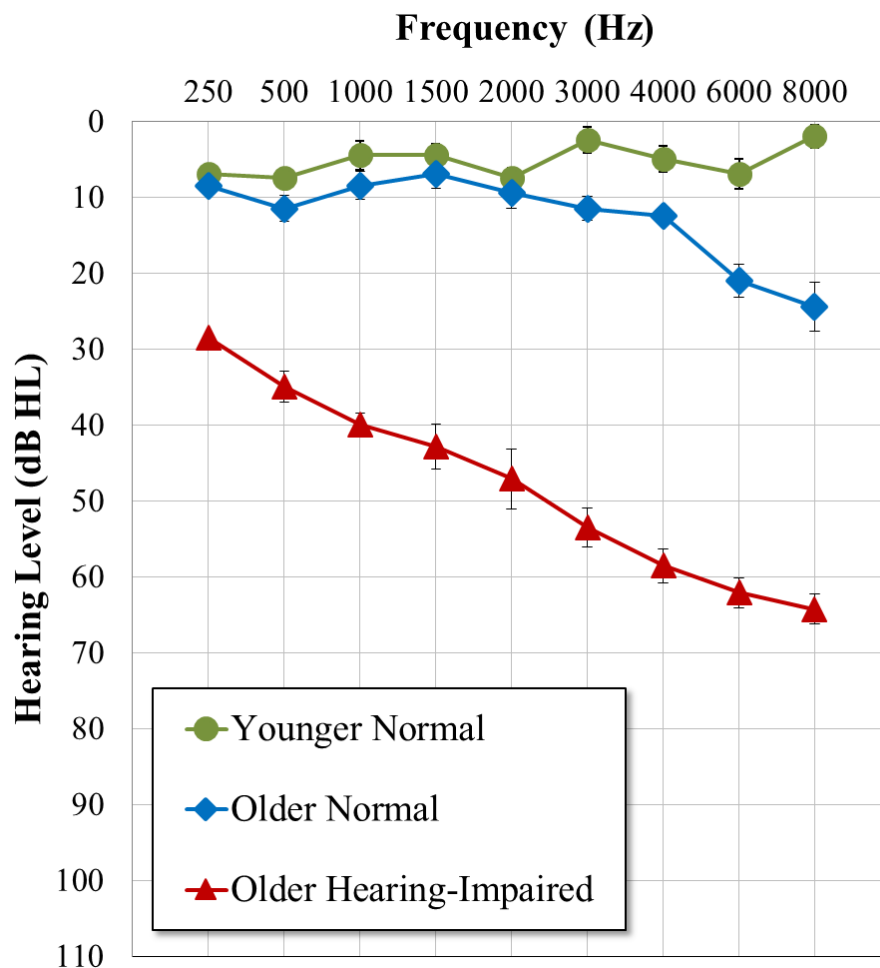


Figure 23. Group average puretone thresholds and standard deviations as a function of frequency for younger normal-hearing, older normal-hearing, and older hearing-impaired study participants.

Stimuli

Stimulus conditions consisted of 6 time-varying tonal glides 120 ms in duration.

Stimuli were either rising or falling in frequency and centered around 500 Hz, spanning 1.00, 0.67, or 0.33 octave intervals, as illustrated in Figure 24, with start and stop frequencies of the stimuli summarized in Table 3.

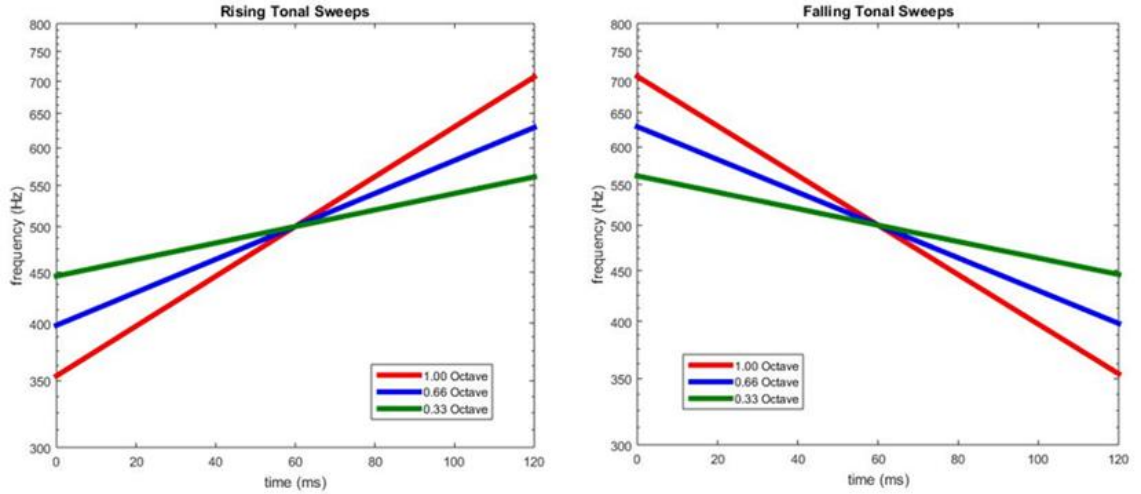


Figure 24. Schematic illustrating extent (1.00 vs. 0.67 vs. 0.33 octaves) and direction of change (rising vs. falling) of tonal glide stimuli.

Table 3

Start and Stop Frequencies (in Hz) of Test Stimuli by Direction of Change and Extent of Change

	Rising		Falling	
	Start Frequency	End Frequency	Start Frequency	End Frequency
Extent of Change				
0.33 Octave	446 Hz	561 Hz	561 Hz	446 Hz
0.67 Octave	398 HZ	629 Hz	629 Hz	398 Hz
1.00 Octave	354 Hz	707 Hz	707 Hz	354 Hz

While FFRs were collected to a number of different stimulus conditions, data analysis will be restricted to the 0.67 octave rising stimulus condition to narrow the scope of this thesis. This stimulus condition was chosen for further analysis because no response differences were observed between the 0.67 octave rising stimulus and the 0.33 and 1.00 octave rising stimuli and the 0.67 octave rising condition presented a middle ground. Some differences in the response were observed between the rising and the falling stimuli; analysis of what might contribute to these differences will be reserved for a future study.

FFR Data Acquisition

Subjects were comfortably situated in a recliner with neck supports in place in a semi-recumbent position in an acoustically and electrically shielded booth. They were instructed to refrain from excessive movement and instructed to relax. Sleeping was encouraged to further reduce myogenic contributions of artifact. Subjects were informed that there would be a total of nine stimulus conditions of approximately 10 minutes each. The presentation order of the stimuli was randomized across participants. Requests for breaks in the event that they were needed were encouraged between stimulus conditions, which were marked with a period of silence approximately two minutes in length.

To ensure that the response originated from the brainstem and is not due to electrical artifact, responses were recorded to a control stimulus which was routed through the insert transducer but not coupled to the participant's ear. To further insure the stimulus was inaudible, the participant's ears were occluded with Sound Guard Two Color Disposable Ear Plugs made from polyvinyl chloride foam. The insert earphone transducer remained attached to the participant in the same location as when it was coupled to the ear. The distance between the transducer and the participant's ear was measured and recorded. The artifact control condition was always the last condition of the test session despite randomization of the other stimuli. Recording significant responses in this condition would suggest that desired FFR recordings made with the insert normally coupled to a subject's ears might be contaminated with stimulus or CM artifact.

FFRs were recorded using the Neuroscan SynampsRT (Scan) acquisition system at a sampling rate of 20 kHz and online filtered from 100-3000 Hz. Artifact rejection was

set at $\pm 60 \mu\text{V}$ for each trial. FFRs were recorded with Ambu snap electrodes in a four-channel electrode recording montage with the non-inverting (active) electrodes placed at C_z , C_7 , A_1 , and F_z , the inverting (reference) electrode positioned at A_2 , and the common ground electrode located at Fp_z , as illustrated in Figure 25. While responses were recorded differentially between the non-inverting electrodes at C_z , C_7 , A_1 , and F_z and the inverting electrode A_2 , responses obtained between C_z and A_2 will be analyzed for the present study. Impedances across all electrodes were verified and maintained below $5 \text{ k}\Omega$ between stimulus conditions as needed. Gauze was wrapped around the subject's head to hold the C_z electrode in place over the duration of the testing session.

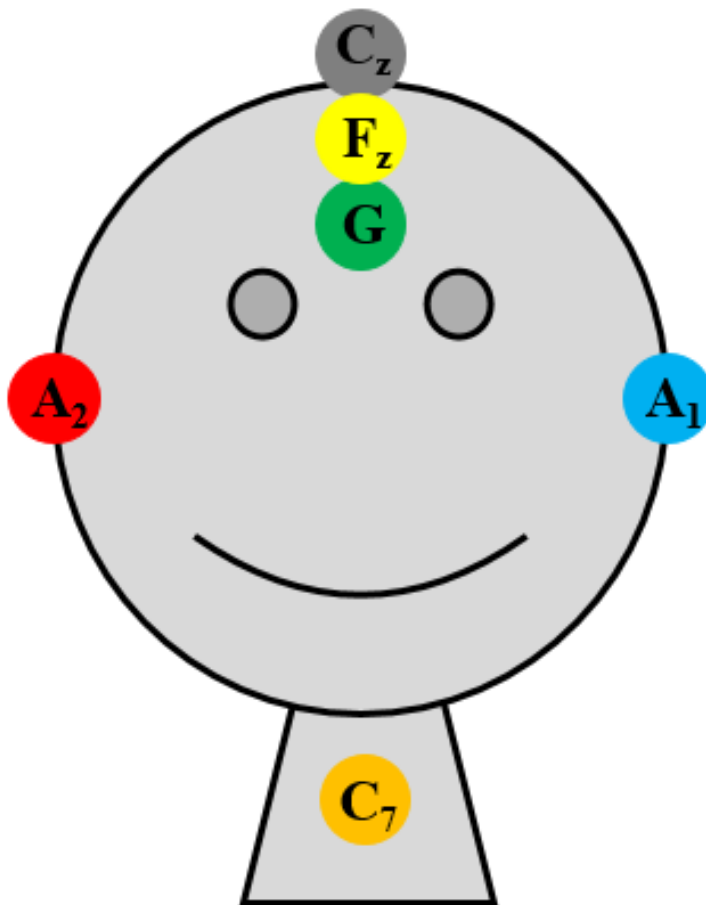


Figure 25. Four-channel electrode recording montage with the non-inverting (active) electrodes placed at C_z , C_7 , A_1 , and F_z , the inverting (reference) electrode positioned at A_2 , and the common ground electrode located at Fp_z .

Responses were obtained to monaural stimulation at 85 dB SPL at a stimulus repetition rate of 3.1/s, with stimuli routed through Mu-metal magnetically-shielded Etymotic ER-3A insert earphones with double-length tubing. Stimuli were always presented to the left ear when hearing was symmetrical and within normal limits. When hearing was asymmetrical, the better ear was stimulated. FFRs were recorded to both condensation and rarefaction stimuli, whose inter-stimulus intervals were jittered (onset to offset) at 146, 163, or 180 ms, in alternating polarity for a total of 3000 sweeps per stimulus condition (1500 rarefaction, 1500 condensation). Recording sessions took approximately 3 hours, with 30 minutes devoted to protocol set-up.

FFR Data Analyses

FFR post-acquisition processing included baseline correcting each sweep with respect to its pre-stimulus condition. Adding FFRs obtained to both stimulus polarities theoretically yields responses phase-locked to the envelope of the stimulus (FFR_E). Performing this computation yielded no analyzable response for the tonal stimuli used in this experiment, suggesting that dynamic tonal stimuli such as those used for this experimental protocol contain fine structure information only. FFRs obtained to condensation stimuli were subtracted from those obtained to rarefaction stimuli, yielding FFRs phase-locked to the fine structure of the stimulus (FFR_{TFS}) and used for further analysis, including both qualitative and quantitative metrics. Responses were then averaged in 100-sweep intervals (50 rarefaction, 50 condensation) from 100-3000 sweeps.

Qualitative Data Analyses

Qualitative analyses included visually inspecting grand-averaged FFR_{TFS} and individual waveforms obtained across groups in terms of periodicity and amplitude. Grand-averaged waveforms were then used to generate spectrograms, which were compared across groups in terms of frequency resolution.

Quantitative Analyses

The FFR_{TFS} was submitted to further analysis to explore neural encoding as a function of sweep count and to establish any differences in neural encoding between YNH, ONH, and OHI; this involved obtaining stimulus-to-response correlation coefficients. Maximal cross-correlation coefficients were calculated by systematically sliding the entire stimulus waveform over the entire FFR_{TFS} waveform (Clinard & Cotter, 2015; Krishnan et al., 2010) using MATLAB version 8.5.0.197613 (R2015a). Cross-correlation coefficient values ranged from 0 to 1, with a higher cross-correlation coefficient (near 1) indicative of a more faithful FFR_{TFS} representation of the stimulus. Due to the post-acquisition processing utilized prior to submitting the FFR for further analysis (subtracting rarefaction waveforms from condensation waveforms), sweep count is doubled.

Statistical Analyses

Both descriptive and inferential statistical analyses contribute to data analysis. First, the Kolmogorov-Smirnov (S-V) test of normality was conducted to determine if data are normally distributed. In addition, Levene's test established if equality of variances between groups is met. Since assumptions for parametric testing were not met, data were analyzed using a multiple linear regression analysis.

CHAPTER 4: RESULTS

The results section will be divided into three main sections devoted to exploring the effects of age and hearing status on the FFR_{TFS} , within and across group variability inherent to the FFR_{TFS} , and the effect of sweep count on the FFR_{TFS} .

Effect of Hearing Status and Age on FFR

Qualitative Grand-Averaged FFR Temporal Waveform Analysis

Grand-averaged waveforms representing FFR_{TFS} for the YNH, ONH, OHI groups are shown in relation to the eliciting stimulus in Figure 26. Inspection of the grand-averaged temporal waveforms reveals a number of trends with respect to waveform morphology and mean amplitude of the response across the YNH, ONH, and OHI groups.

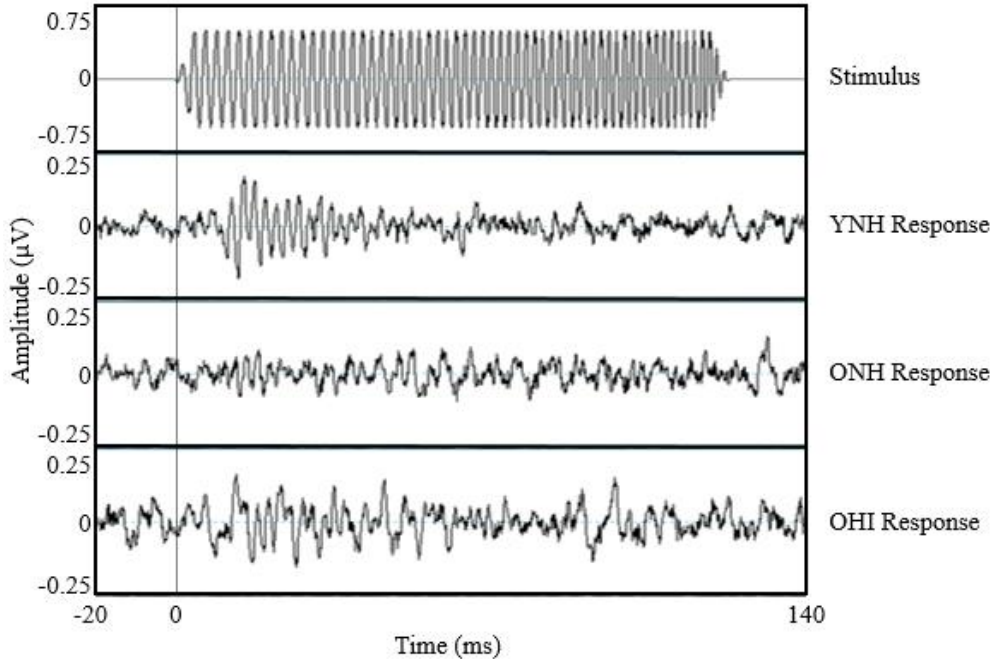


Figure 26. Comparison between stimulus waveform (top) and response waveforms for grand-averaged recordings obtained from YNH, ONH, and OHI individuals. Note that amplitude scaling for the stimulus is -0.75 to 0.75 μV and amplitude scaling for the FFR_{TFS} responses is -0.25 to 0.25 μV to aid in visualization.

First, phase-locking can be seen approximately 10 ms post-stimulus onset in all three groups, characterized by the portion of the response waveform which mimics the waveform of the stimulus. This is most robustly seen for the YNH group approximately between 10-50 ms post-stimulus onset. For the grand-averaged response waveforms obtained from the ONH and OHI individuals, any phase-locking is difficult to distinguish from the underlying EEG activity. As such, robust periodicity of the response, which suggests strong phase-locking to the stimulus, is only seen for the YNH group and difficult to distinguish in the ONH and OHI grand-averaged waveform. Second, the mean amplitude of the response is greatest at the response onset where the frequency of the stimulus is lowest (398 Hz) and decreases as a function of time and/or frequency in the YNH group. This relationship between response amplitude and time or frequency is not evident for the ONH and OHI grand-averaged waveforms, possibly because the response for those two groups is difficult to distinguish from the underlying EEG activity in the first place.

Qualitative Grand-Averaged FFR Spectrogram Analysis

Grand-averaged waveforms for the YNH, ONH, and OHI groups were converted from the temporal domain into the frequency domain as spectrograms using MATLAB, illustrated in Figure 27.

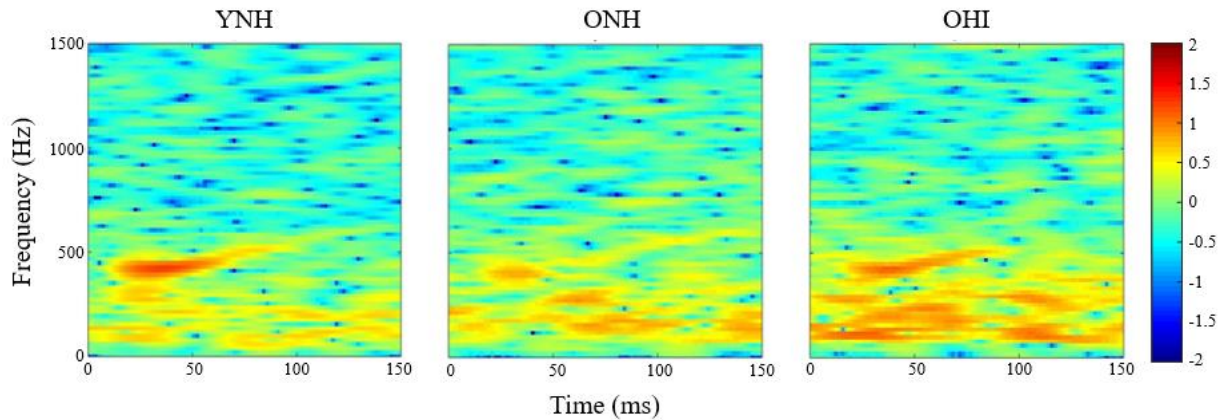


Figure 27. Grand-averaged spectrograms for FFR_{TFS} obtained from YNH, ONH, and OHI subjects post-stimulus onset (at 0 ms).

Inspection of the grand-averaged spectrograms reveals a clear response band corresponding to the frequency range of the stimulus (398-628 Hz) approximately 10 ms post-stimulus onset for the YNH group. Similar response bands are documented for the ONH and OHI grand-averaged spectrograms, however, the responses are markedly weaker for the ONH and OHI group. In addition, considerable spectral smearing can be seen below 400 Hz for all three grand-averaged group waveforms; however, spectral smearing is most noticeable for the ONH and OHI groups. Response bands are most salient at the lower end of the stimulus frequency range and become less robust as frequency and time increase for all three groups. The decline in response band robustness as a function of frequency or time is most clear in the YNH; this may potentially be accounted for in that the response band in the YNH group is most robust, and therefore a relative decline in response strength is most noticeable for that group.

Descriptive Statistical Analysis of Age and Hearing Status Effects on FFR

Individual responses were submitted to stimulus-to-response cross-correlation coefficient analysis in 100 sweep increments (50 condensation and 50 rarefaction) from 100 to 3000 sweeps and used for further quantitative analysis. As a reminder, maximal cross-correlation coefficients were calculated by systematically comparing the stimulus waveform with the FFR_{TFS} waveform using MATLAB. This generated a cross-correlation coefficient value which could theoretically range from 0 to 1, with a higher cross-correlation coefficient (near 1) indicative of a more faithful FFR representation of the stimulus.

On average, YNH participants had higher cross-correlation coefficients than both the ONH and OHI participants, independent of sweep count. The highest mean cross-correlation coefficients were achieved by the YNH individuals ($M = .3707$, $SD = .1802$) at 2900 sweeps, followed by the ONH group ($M = .2593$, $SD = 0.1595$) at 2900, and by the OHI group ($M = .2090$, $SD = .1875$) at 2600 sweeps. End-point sweep counts for the three groups vary because data points for mean cross-correlation coefficients were eliminated from analysis when 2 or more participants in a given group did not complete that number of sweeps to avoid biasing mean data. The OHI group saw a higher sweep rejection rate than the YNH and ONH groups. Comparing groups at 2600 sweeps, the maximum sweep count achieved by the OHI group on average, mean cross-correlation coefficients remained highest for the YNH group ($M = .3753$, $SD = .1696$), followed by the ONH ($M = .2380$, $SD = .1459$) and OHI ($M = .2090$, $SD = .1875$) groups.

Inferential Statistical Analysis of Age and Hearing Status Effects on FFR

A multiple linear regression analysis was conducted to determine whether age, hearing status and sweep count predict FFR fidelity as indexed by the cross-correlation coefficient. The data were screened for violation of assumptions prior to analysis with respect to outliers, multicollinearity, independence of errors, homoscedasticity, and non-zero variance. For the purpose of this metric, age and hearing status were interpreted as continuous variables, with hearing status represented using the three-frequency pure-tone average at 500 Hz, 1000 Hz, and 2000 Hz.

An analysis of standard residuals was carried out, which indicated that the data contains no outliers (Std. Residual Min = -2.185, Std. Residual Max = 2.425). Tests to determine if the data met the assumption of collinearity indicated that multicollinearity was not a concern (age, Tolerance = .546, VIF = 1.831; PTA, Tolerance = .546, VIF = 1.831; sweep count, Tolerance = .998, VIF = 1.002). The Durbin-Watson statistic was computed to evaluate independence of errors and was found to be 1.934, which suggests that the independence of errors assumption was met. An examination of the histogram of standardized residuals (Figure 28) and the normal P-P plot of standardized residuals (Figure 29) suggest that the data contain approximately normally distributed errors. The scatterplot of standardized residuals suggests that the data do not meet the assumption of homogeneity of variance and are heteroscedastic (Figure 30). Review of the partial scatterplot of the independent variables (age, hearing status, and sweep count) and the dependent variable (cross-correlation coefficient) indicates linearity is a reasonable assumption.

The predictor variables meet the assumption of non-zero variances (age, Variance = 316.614; PTA, Variance = 228.561; Sweep Count, Variance = 691,345.692).

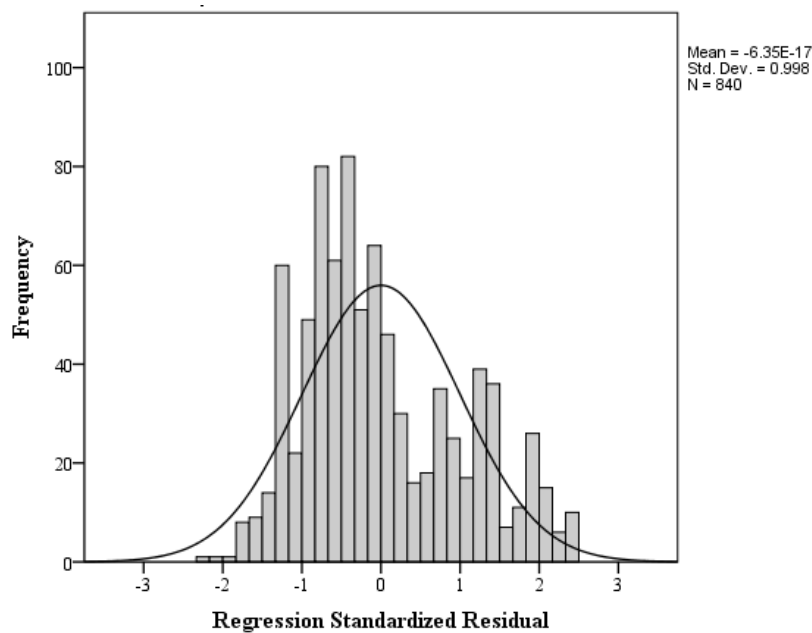


Figure 28. Histogram of standardized residuals suggesting that data contain normally distributed errors.

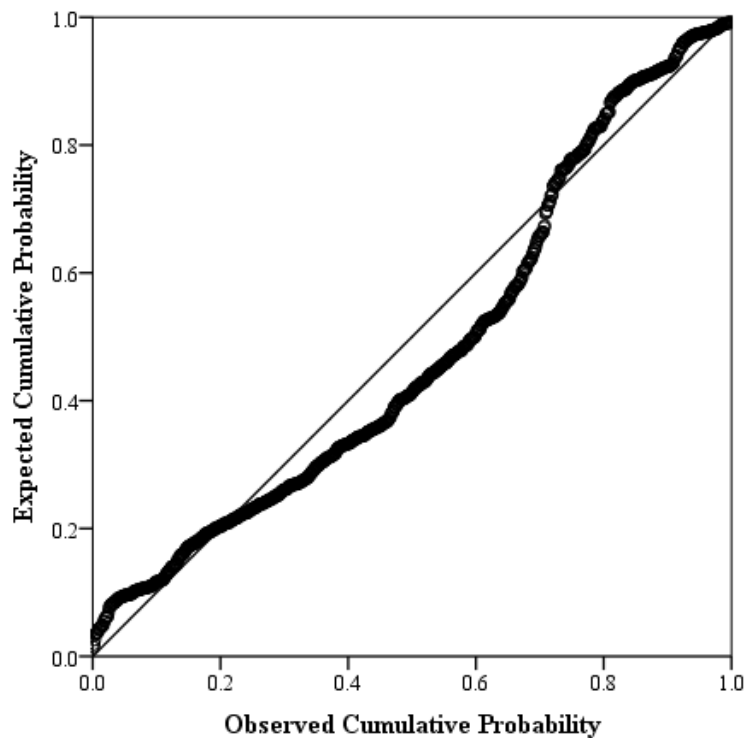


Figure 29. Normal P-P plot of standardized residuals suggesting that data contain normally distributed errors but deviate from a normal distribution.

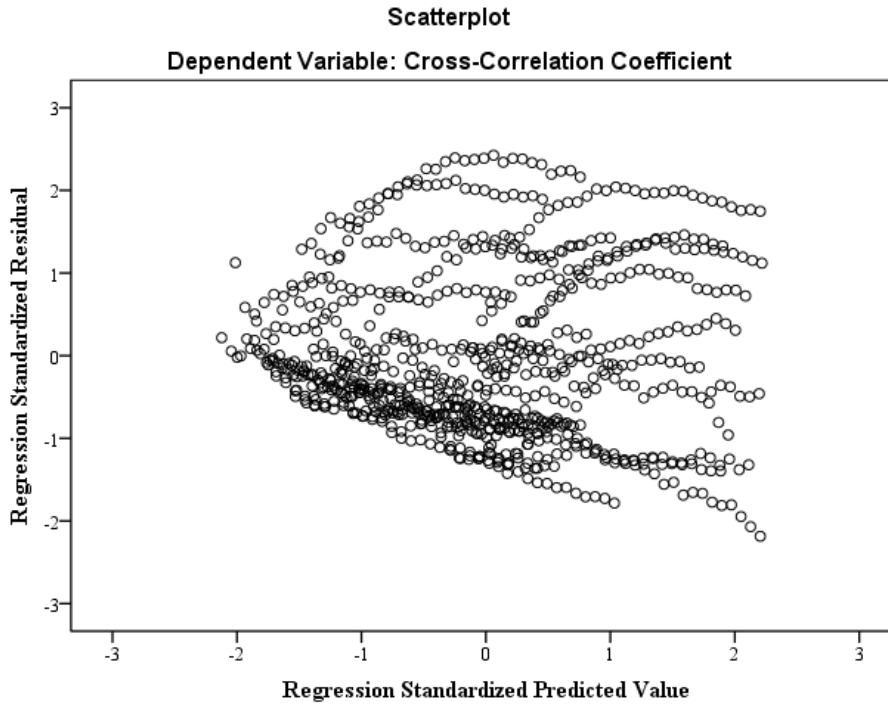


Figure 30. Scatterplot of standardized predicted values suggesting that the data are heteroscedastic.

Using the enter method, it was found that age, PTA, and sweep count explain a significant amount of the variance in FFR signal-to-response fidelity quantified by the cross-correlation coefficient, ($F(3, 836) = 102.727, p < .001, R^2 = .519, R^2_{Adjusted} = .267$). Further analysis suggests that PTA did not significantly predict FFR fidelity ($\beta = .027, t(833) = .681, p = .496$), but age ($\beta = -.401, t(833) = -10.019, p < .001$) and sweep count ($\beta = .334, t(833) = 11.277, p < .001$) did. This suggests that age and sweep count, but not degree of hearing loss, account for the observed group differences in cross-correlation coefficients.

Within and Across Group Variability of FFR

Qualitative Individual FFR Temporal Waveform Analysis

Select individual waveforms representing FFR_{TFS} for the YNH, ONH, OHI groups are shown in relation to the eliciting stimulus in Figure 31. One individual waveform from each group representing the best stimulus-to-response relationship and one individual waveform from each group representing the poorest stimulus-to-response relationship was chosen to illustrate the range of possibly responses elicited by individuals within each group. Inspection of the individual temporal waveforms reveals a number of trends with respect to waveform morphology and mean amplitude of the response across the YNH, ONH, and OHI groups.

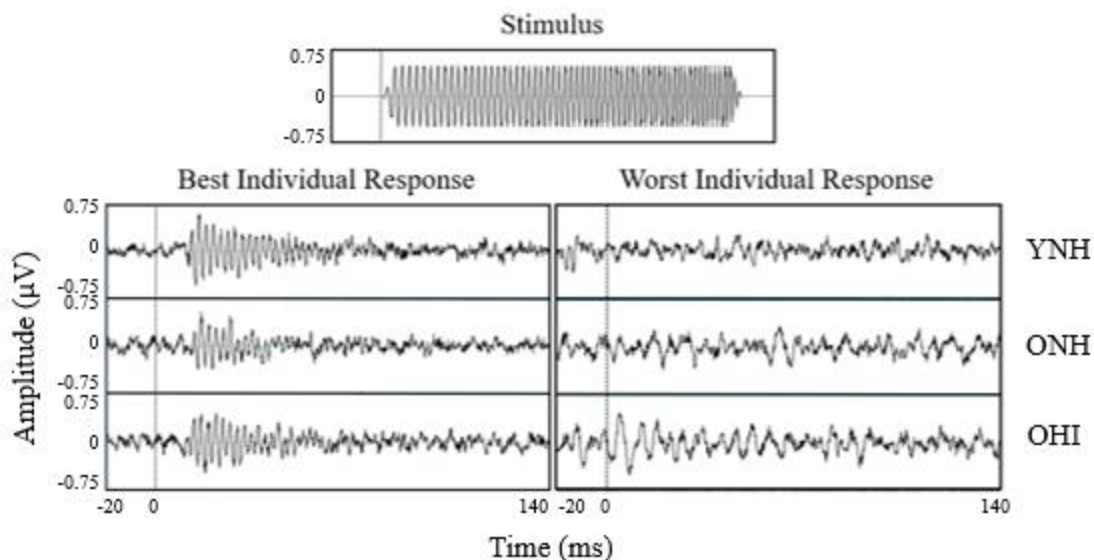


Figure 31. Comparison between stimulus waveform (top) and response waveforms for the best and poorest individual recordings obtained from different participants in the YNH, ONH, and OHI groups.

Most notably, tremendous inter-individual variability was found in the waveform morphology and amplitude of the FFR_{TFS} within each group, such that each group was comprised of individuals who produced FFR_{TFS} waveforms characterized by excellent phase-locking during the first half of the response (from approximately 10-60 ms post-

stimulus onset), as well as individuals whose FFR_{TFS} waveform was indistinguishable from the underlying EEG activity. Waveforms spanning the range from what is characteristic of the best and worst individual responses were furthermore found within each group. As previously discussed for the grand-averaged waveforms, mean amplitude of the individual responses is greatest at the response onset where the frequency of the stimulus is lowest (398 Hz) and decreases as a function of time or frequency for the responses in which phase-locking can be clearly distinguished.

Qualitative Individual FFR Spectrogram Analysis

Select individual waveforms for the YNH, ONH, and OHI groups were converted from the temporal domain into the frequency domain as spectrograms using MATLAB, illustrated in Figure 32.

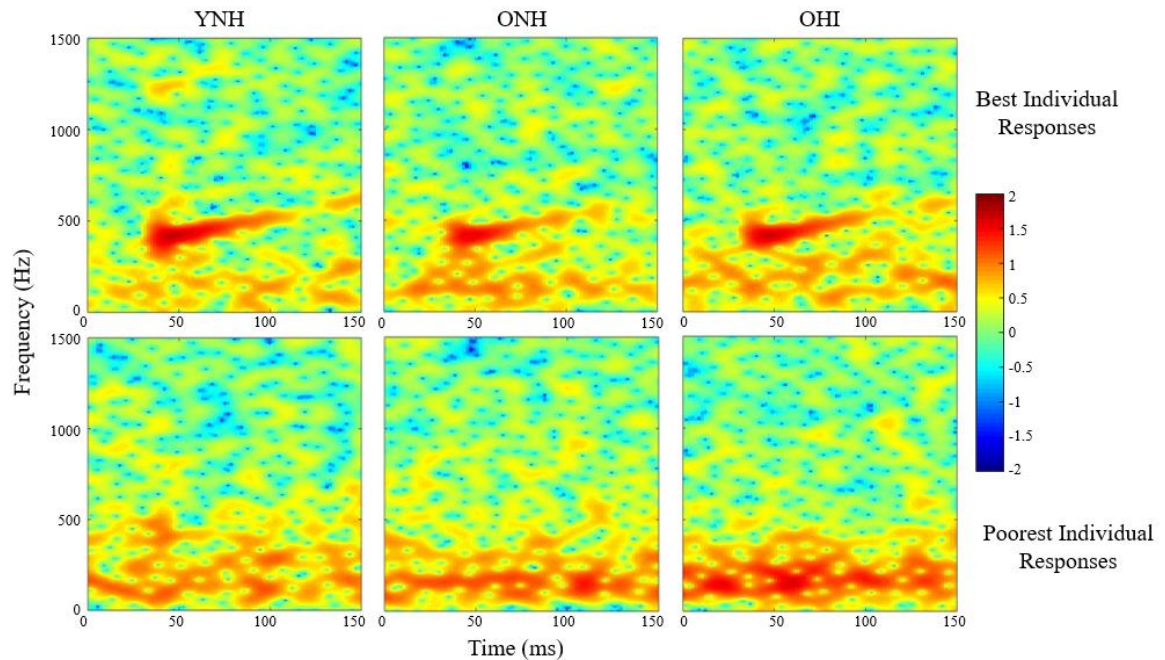


Figure 32. Spectrograms for best (top) and poorest (bottom) FFR_{TFS} obtained from different individual responses from YNH, ONH, and OHI subjects post-stimulus onset (at 0 ms).

Inspection of the spectrograms obtained from different individuals within each group reveals that the YNH, ONH, and OHI groups each were comprised of participants whose FFR_{TFS} is characterized by a clear response band corresponding to the frequency range of the stimulus (398-628 Hz) approximately 10 ms post-stimulus onset. Similarly, each group had individuals whose FFR_{TFS} produced a spectrogram without a clear response band and considerable spectral smearing below 400 Hz. For individuals who produced spectrograms with clear response bands, these again were more salient in response to the stimulus at a lower frequency and became less visible as the frequency or duration of the stimulus increased.

Analysis of Variability Across and Within Groups

The relationship between the three groups at 100, 1000, 2000, and 2600 sweeps is illustrated in Figure 33. Examination of the figure suggests that at early sweep counts, within group variability is relatively homogenous. At higher sweep counts, the responses begin to differentiate themselves such that the variability of the cross-correlation coefficients increases.

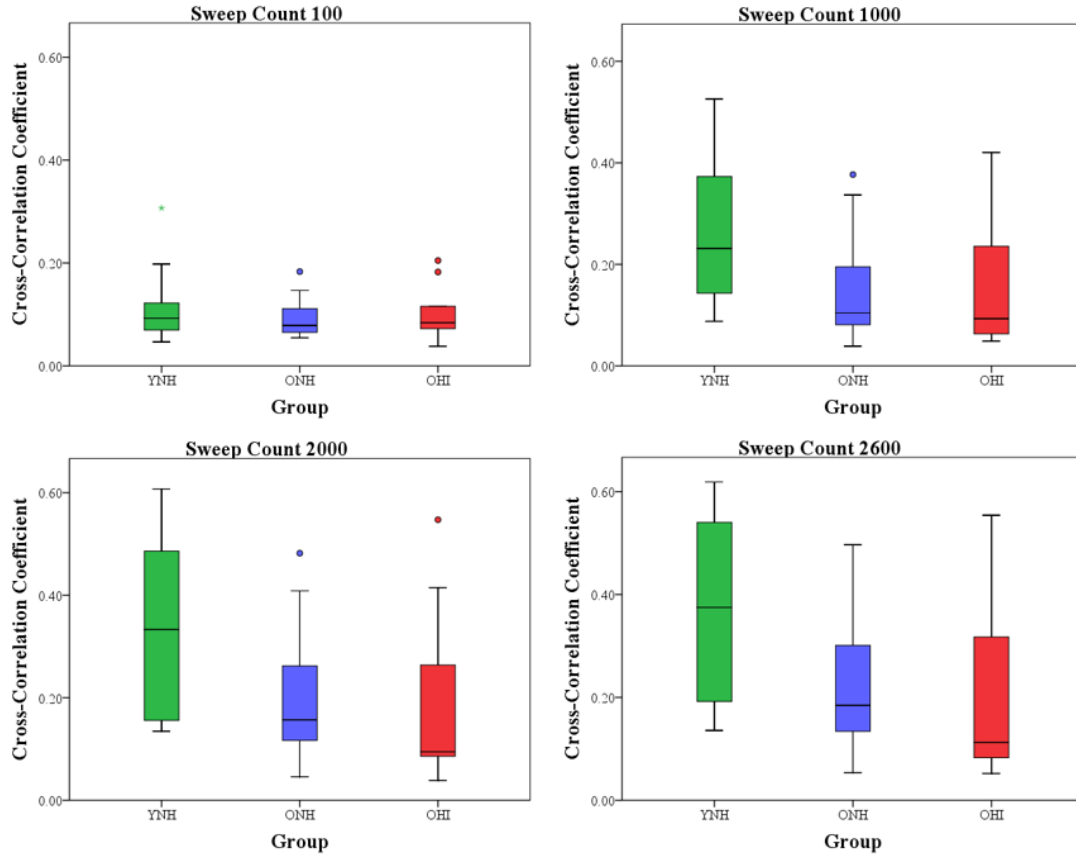


Figure 33. Box-plot distributions of data showing cross-correlation coefficients at 100, 1000, 2000, and 2600 sweeps (the maximum number of sweeps achieved by all groups) by group (YNH vs. ONH vs. OHI).

Table 4 displays the mean, standard deviation, minimum, maximum, and range of cross-correlation coefficients attained by each group at 2600 sweeps. As a reminder, this is the highest number of sweeps completed by all three groups in which at least 80 percent of the individuals within that group achieved that number of sweeps. In essence, these are the best individual responses obtained by each individual within each group that can be used to compare across groups without biasing the data. Notably, the YNH group achieved higher minimum and maximum cross-correlation coefficients than both the ONH and OHI, so while the range of responses between groups was comparable, the relative distribution varied.

Table 4

Mean, Standard Deviation, Minimum, Maximum, and Range of Cross-Correlation Coefficients Attained by Each Group at 2600 Sweeps

Group	N	Mean	SD	Minimum	Maximum	Range
YNH	10	0.3723	0.1696	0.1358	0.6187	0.4829
ONH	9	0.2381	0.1459	0.0537	0.4967	0.4430
OHI	9	0.2091	0.1875	0.0520	0.5541	0.5020

The spread of the data is best illustrated in Figure 34, in which individual data points for each individual participant are displayed as a function of sweep count categorized by group membership. An examination of the figure indicates that independent of group membership, each of three groups are comprised of individuals who exhibit FFRs with good stimulus-to-response fidelity as well as individuals whose responses exhibit poor stimulus-to-reponse encoding.

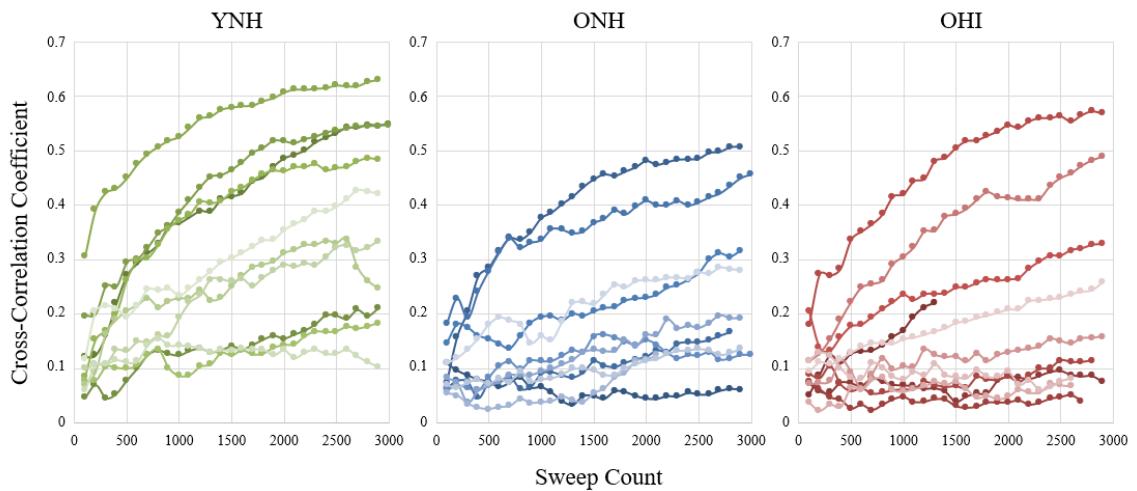


Figure 34. Individual cross-correlation coefficients as a function of sweep count for all participants displayed by group membership (YNH vs. ONH vs. OHI).

While each cohort is comprised of varying individual responses, the ONH and OHI groups contained more individuals whose FFR_{TFS} was indistinguishable from the underlying EEG activity as classified by the cross-correlation coefficient. To further explore the relationship between underlying EEG activity and cross-correlation coefficient,

cross-correlation coefficients for baseline EEG activity were calculated by sliding the stimulus waveform across the response obtained during a condition in which the stimulus transducer was clamped under the assumption that no acoustic leakage would result in no FFR. Mean cross-correlation coefficients obtained for the EEG condition were then compared to the cross-correlation coefficient obtained at the maximum number of sweeps for each individual. Results of this comparison are displayed in Table 5, which provides the mean cross-correlation coefficient and standard deviation obtained by each individual, the maximum cross-correlation coefficient achieved by each individual and at which number of sweeps, and the difference between the mean cross-correlation coefficient for each individual's EEG activity and their respective best cross-correlation coefficient.

Table 5

Comparison Between Individual EEG and Max Cross-Correlation Coefficient

Subject	<i>M</i> EEG	<i>SD</i> EEG	Max	Sweeps	Diff. Max – <i>M</i> EEG
YNH					
1	0.0753	0.0163	0.5778	3000	0.5024
2	0.0700	0.0177	0.3273	2900	0.2573
3	0.0429	0.0088	0.4916	3000	0.4487
4	0.0491	0.0153	0.5600	2900	0.5109
5	0.0317	0.0124	0.4999	2900	0.4681
6	0.0398	0.0091	0.1814	2900	0.1416
7	0.0406	0.0072	0.3025	3000	0.2618
8	0.0629	0.0127	0.3740	2900	0.3111
9	0.0526	0.0178	0.1262	2900	0.0736
10	0.0892	0.0151	0.2964	2900	0.2071
Group Mean	0.0554	0.0132	0.3737	2930	0.3183
ONH					
11	0.0682	0.0225	0.0339	2900	-0.0343
12	0.0711	0.0150	0.5496	2900	0.4785
13	0.0511	0.0138	0.2736	2900	0.2224
14	0.0569	0.0115	0.3606	2900	0.3037
15	0.0310	0.0201	0.3606	2900	0.3295
16	0.0777	0.0222	0.2051	2900	0.1274
17	0.0897	0.0187	0.1567	2900	0.0671
18	0.0689	0.0179	0.2092	2800	0.1403
19	0.0508	0.0191	0.1317	2900	0.0810
20	0.0808	0.0136	0.3070	2900	0.2263
Group Mean	0.0646	0.0174	0.2588	2890	0.1942
OHI					
21	0.0948	0.0358	0.2291	2400	0.1344
22	0.0577	0.0079	0.0230	2900	-0.0347
23	0.0512	0.0127	0.0445	2700	-0.0066
24	0.0749	0.0217	0.1371	1800	0.0621
25	0.1021	0.0165	0.5754	2900	0.4733
26	0.1178	0.0255	0.3045	2900	0.1867
27	0.0847	0.0143	0.5852	2900	0.5005
28	0.0620	0.0136	0.0594	2900	-0.0026
29	0.0381	0.0059	0.0513	2900	0.0132
30	0.0705	0.0219	0.0336	2700	-0.0369
Group Mean	0.0754	0.0176	0.2043	2700	0.1289

Further examination of the data displayed in Table 5 suggest that YNH subjects on average had lower EEG activity ($M = 0.0554$, $SD = 0.0132$) than ONH ($M = 0.646$, $SD = 0.0174$) and OHI ($M = 0.0754$, $SD = 0.0176$) individuals. At their best cross-correlation values, YNH individuals on average were also more likely to complete a greater number of sweeps ($M = 2930$) than ONH ($M = 2890$) and OHI ($M = 2700$) individuals. As discussed previously, YNH individuals were also more likely to achieve higher cross-correlation coefficients than their older counterparts.

When comparing each individual's best FFR to their mean underlying EEG activity suggests, the YNH group contains no individuals for whom their best recording is lower than their EEG activity. In contrast, the ONH group has one individual whose best response is lower than their underlying EEG, and the OHI group contains 4 individuals whose best FFR is indistinguishable from their underlying EEG activity. This suggests that OHI individuals are more likely to have noisier recordings, leading to greater artifact rejection during recording sessions. In addition, it is possible that OHI individuals are more likely to have degraded subcortical neural encoding of certain acoustic stimuli, such as dynamic tonal glides, resulting in an absent FFR and limited TFS encoding.

Effect of Sweep Count on FFR

Qualitative Individual FFR Temporal Waveform Analysis as a Function of Sweep Count

Select individual waveforms representing FFR_{TFS} for two different YNH participants are shown as a function of sweep count in Figure 35. One waveform series from a YNH participant representing the best stimulus-to-response relationship and one waveform series from a YNH participant representing the poorest stimulus-to-response

relationship was chosen to illustrate the range of possibly responses elicited by individuals within a given group and the effect of sweep count on the response. Inspection of the individual temporal waveforms reveals a number of trends with respect to waveform morphology and mean amplitude of the response as sweep count increases.

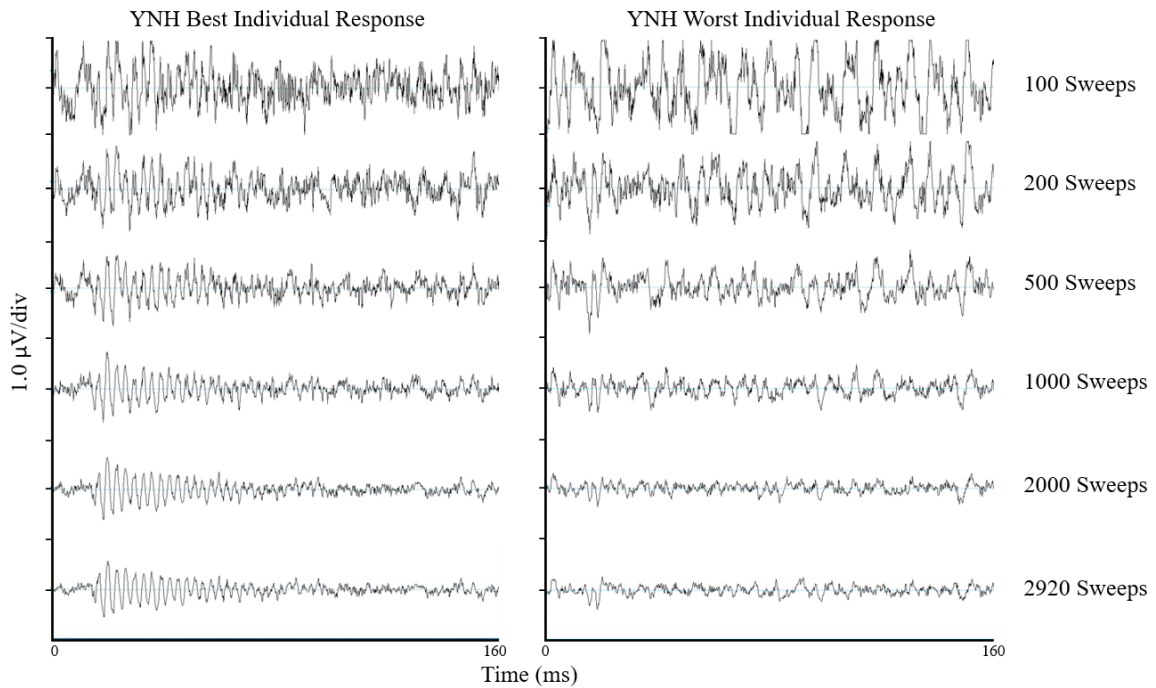


Figure 35. FFR recordings as a function of the number of sweeps included in the averaged waveform ranging from 100 sweeps (top tracing) to 2920 sweeps (bottom tracing) for two YNH participants to showcase good (left) and poor (right) FFR representation. On the x-axis, 0 represents the point in time of stimulus onset.

Predictably, as sweep count increases, the overall amplitude of the recordings decreases because the noise in the recordings decreases as a function of one over the square root of the number of sweeps (Hood, 1998; Özdamar & Delgado, 1996). Generally, this trend is seen for recordings obtained from both the best and poorest individual YNH participants. Theoretically, as sweep count increases, the SNR, and thereby the amplitude of the FFR in relation to the noise, should increase as well. This can be clearly seen for the YNH participant whose waveforms are illustrated in Figure 35 on the left and is characterized by excellent phase-locking during the first half of the

response (from approximately 10-70 ms post-stimulus onset). For the YNH participant on the right, additional recording epochs did not result in greater FFR_{TFS} signal-to-response fidelity and it seems like there is no classic FFR_{TFS} waveform. It should be noted, however, that as the sweep counts increase, two cycles of phase-locking can be seen approximately 10 ms post-stimulus onset, suggesting that some phase-locking is occurring and the response is at least minimally present for a short duration of time. It is unclear whether additional sweep would allow the FFR_{TFS} to become more salient. Similar trends were established in the ONH and OHI groups, where the addition of sweeps resulted in better FFR_{TFS} SNR for some participants in that group but not for others.

Qualitative Individual FFR Spectrogram Analysis as a Function of Sweep Count

Select individual waveforms for the two YNH participants as a function of sweep count were converted from the temporal domain into the frequency domain as spectrograms using MATLAB, as illustrated in Figure 36. As described above, one FFR_{TFS} series from a YNH participant representing the best stimulus-to-response relationship and one FFR_{TFS} series from a YNH participant representing the poorest stimulus-to-response relationship was chosen to illustrate the range of possibly responses elicited by individuals within a given group and the effect of sweep count on the response.

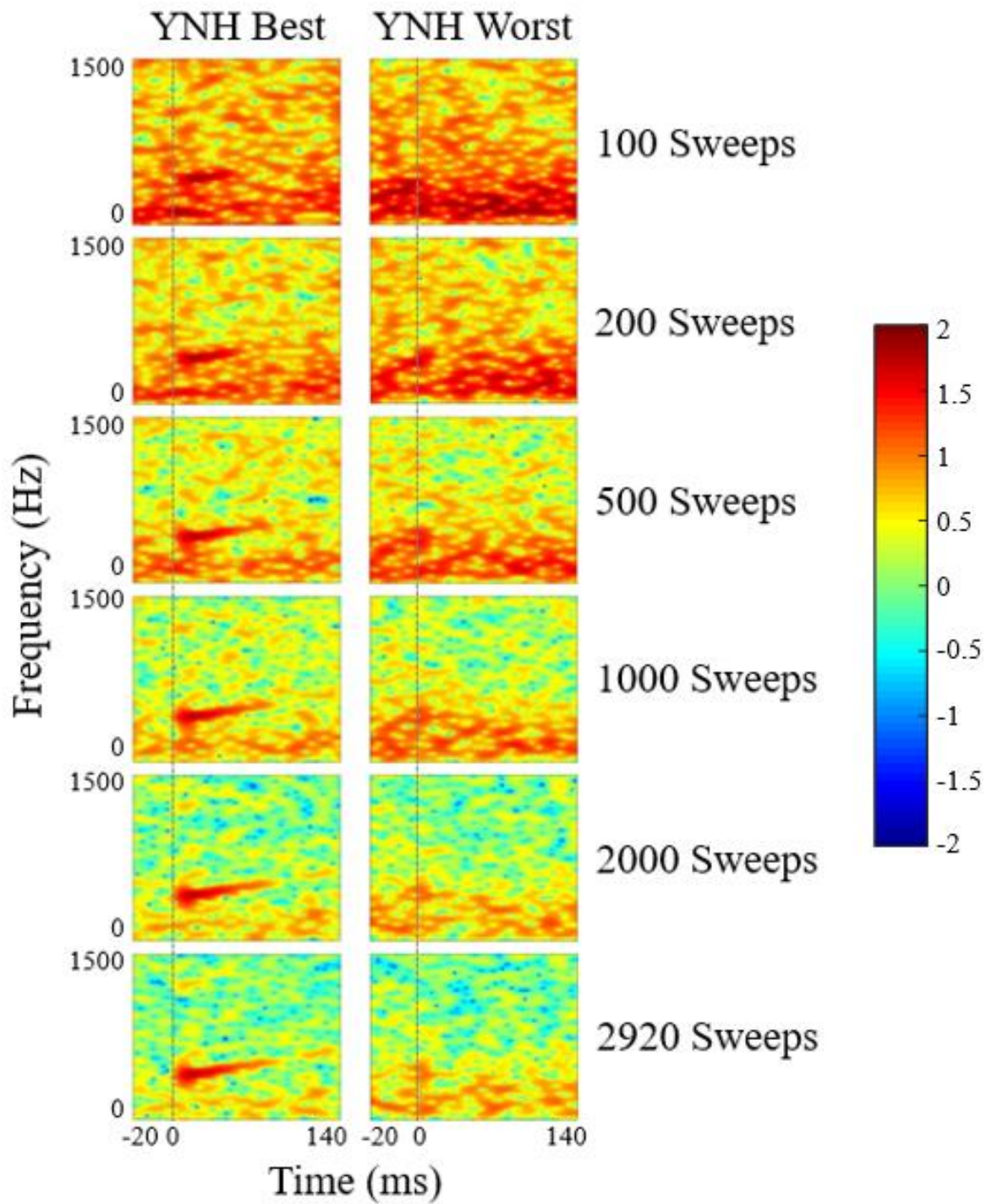


Figure 36. Spectrograms of FFR recordings as a function of the number of sweeps included in the averaged waveform ranging from 100 sweeps (top) to 2920 sweeps (bottom) for two YNH participants to showcase good (left column) and poor (right column) FFR representation. On the x-axis, 0 represents the point in time of stimulus onset.

Inspection of the spectrogram series in Figure 36 corroborates the trend that as the number of sweeps which are included in an averaged response increases, so does the SNR of the response for individuals who already have a clear response at a low sweep count. This can be seen for the YNH participant on the left in Figure 36, who has a response band at 100 sweeps corresponding to the frequency range of the stimulus (398-628 Hz) beginning approximately 10 ms post-stimulus onset. As the number of sweeps included in the averaged response increases, the response band becomes more salient as the noise in the recording is eliminated. For the participant on the right, however, no response band can be seen independent of how many sweeps are included in the averaged response represented in the spectrogram.

Quantitative Analysis of the Effect of Sweep Count on FFR_{TFS}

Figure 37 displays mean cross-correlation coefficients as a function of sweep count by group recorded in response to a dynamic tonal glide 120 ms in length spanning 0.67 octaves, rising from 398 Hz to 629 Hz. An examination of Figure 37 reveals that there is an increase in stimulus-to-response cross-correlation coefficients as a function of sweep count independent of group membership.

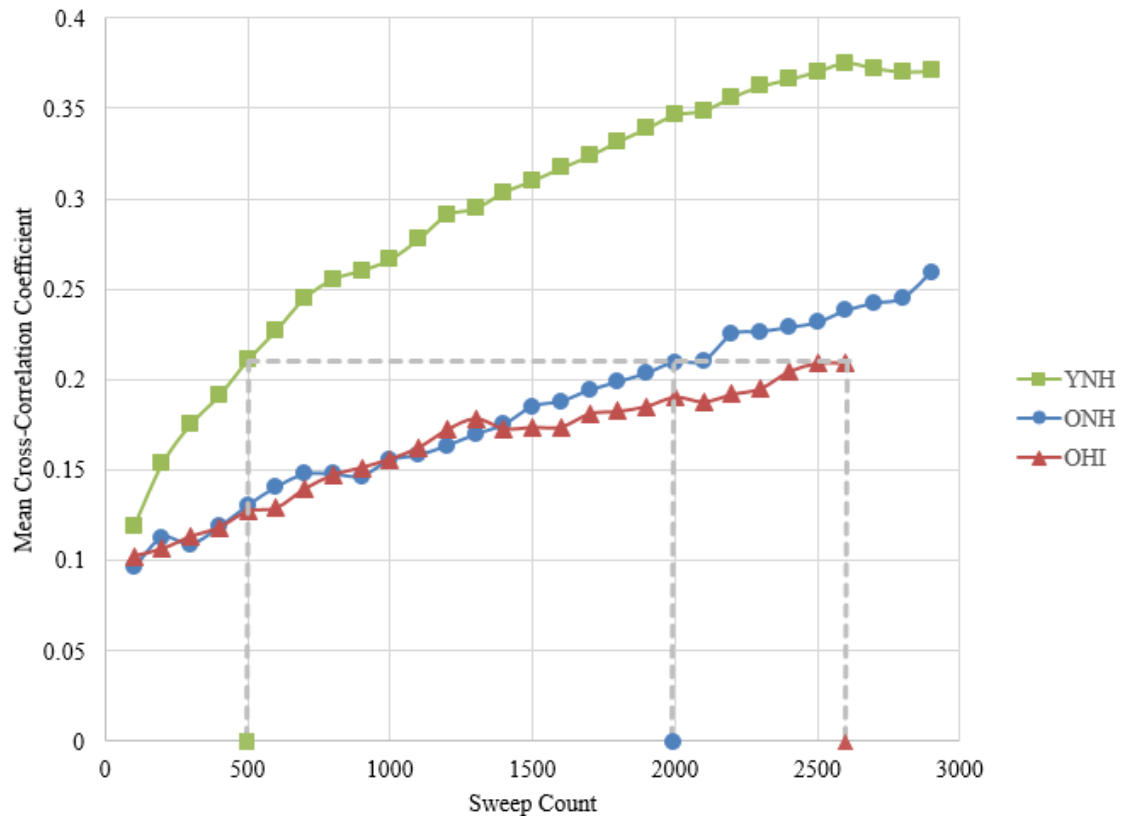


Figure 37. Mean stimulus to frequency-following response cross-correlation coefficients as a function of sweep count by group (YNH vs. ONH vs. OHI) for a dynamic tonal stimulus 120 ms in duration rising over the extent of two-thirds of an octave. Dotted lines super-imposed on graph illustrate that on average, OHI required 2600 sweeps to achieve a maximal cross-correlation coefficient of 0.21, while the ONH group required 2000 sweeps and the YNH group merely required 500 sweeps to achieve similar FFRs. Data points for mean cross-correlation coefficients were eliminated from analysis when more than 2 participants in a given group were unable to complete the full number of sweeps.

Stimulus-to-response agreement is poorest at 100 sweeps and best at sweep counts above 2500 for the YNH, ONH, and OHI groups. In addition, mean cross-correlation coefficients were greatest across all sweep counts for the YNH group. The ONH and OHI groups performed similarly and saw some growth of cross-correlation coefficients as a function of sweep count, but did not achieve as good of stimulus-to-response agreement as the YNH group. Table 6 summarizes mean cross-correlation coefficients and standard deviations by group and sweep count.

Table 6

Mean Cross-Correlation Coefficients by Group and Sweep Count

Sweeps	YNH		ONH		OHI	
	<i>M</i>	<i>SD</i>	<i>M</i>	<i>SD</i>	<i>M</i>	<i>SD</i>
100	0.1188	0.0786	0.0959	0.0420	0.1022	0.0541
200	0.1535	0.0958	0.1127	0.0591	0.1063	0.0691
300	0.1754	0.1054	0.1090	0.0634	0.1131	0.0683
400	0.1913	0.1043	0.1185	0.0846	0.1180	0.0760
500	0.2107	0.1137	0.1304	0.0917	0.1271	0.0942
600	0.2273	0.1184	0.1406	0.1023	0.1289	0.1026
700	0.2451	0.1175	0.1476	0.1094	0.1395	0.1043
800	0.2557	0.1215	0.1477	0.1045	0.1472	0.1084
900	0.2605	0.1354	0.1466	0.1113	0.1513	0.1229
1000	0.2666	0.1408	0.1555	0.1155	0.1560	0.1266
1100	0.2776	0.1451	0.1581	0.1215	0.1623	0.1342
1200	0.2912	0.1503	0.1634	0.1243	0.1722	0.1384
1300	0.2947	0.1535	0.1697	0.1280	0.1784	0.1446
1400	0.3037	0.1541	0.1752	0.1296	0.1729	0.1606
1500	0.3100	0.1567	0.1851	0.1314	0.1736	0.1692
1600	0.3171	0.1578	0.1879	0.1360	0.1738	0.1749
1700	0.3237	0.1632	0.1940	0.1355	0.1811	0.1762
1800	0.3316	0.1649	0.1986	0.1331	0.1824	0.1814
1900	0.3389	0.1681	0.2034	0.1366	0.1852	0.1800
2000	0.3464	0.1688	0.2097	0.1393	0.1903	0.1804
2100	0.3488	0.1717	0.2101	0.1355	0.1877	0.1795
2200	0.3561	0.1685	0.2248	0.1403	0.1918	0.1836
2300	0.3623	0.1683	0.2263	0.1425	0.1950	0.1857
2400	0.3660	0.1682	0.2286	0.1396	0.2045	0.1862
2500	0.3704	0.1698	0.2314	0.1421	0.2090	0.1872
2600	0.3753	0.1696	0.2380	0.1459	0.2091	0.1875
2700	0.3722	0.1741	0.2420	0.1483		
2800	0.3703	0.1801	0.2449	0.1505		
2900	0.3707	0.1802	0.2593	0.1595		
3000						

Note. *M* = mean, *SD* = standard deviation. Data points for mean cross-correlation coefficients were removed when more than 2 participants in a given group did not complete full number of sweeps.

A greater number of sweeps are required for the ONH and OHI groups to achieve cross-correlation coefficients comparable to those achieved by the YNH group, as illustrated in Figure 37. For example, YNH participants on average required 500 sweeps to achieve a cross-correlation coefficient of 0.21, which is the maximal mean cross-correlation coefficient obtained by the OHI. In contrast, ONH participants required 2000 sweeps and OHI participants required 2600 sweeps for similar stimulus-to-response agreement. On average, OHI individuals may require 5.2 times and ONH may require 4.0 times as many sweeps as YNH individuals to achieve FFRs of similar fidelity.

An exploratory data analysis was conducted to determine if cross-correlation coefficients were normally distributed for each of the three groups as using IBM SPSS statistics software version 23. Review of the Lilliefors-corrected Kolmogorov-Smirnova (K-S) test of normality results indicate that cross-correlation coefficients significantly deviated from a normal distribution across all three groups ($D(840) = .162, p < .001$), as well as for each group in the YNH ($D(292) = .108, p < .001$), ONH ($D(283) = .165, p < .001$), and OHI ($D(265) = .224, p < .001$) conditions. To determine homogeneity of variance between the cross-correlation coefficients achieved by YNH, ONH, and OHI participants, Levene's test of equality of variance was conducted. Variances were found to be significantly different between the three groups, $F(2, 837) = 14.557, p < .001$. A natural log transform of the data did not satisfy the assumption of homogeneity of variance required for parametric statistical analysis.

Consequently, Spearman's correlation coefficient was calculated to formalize the relationship between sweep count and mean stimulus-to-response cross-correlation coefficients for YNH, ONH, and OHI groups. Predictably, there was a significant

relationship between sweep count and stimulus-to-response correlation for all study subjects conflated together, $r_s = .331$, $p < .001$, as well as for the YNH, $r_s = .449$, $p < .001$, ONH, $r_s = .373$, $p < .001$, and OHI, $r_s = .192$, $p < .001$, groups, such that as sweep count increased, the signal-to-response fidelity also increased.

To determine if the order in which sweeps were averaged had an effect on FFR_{TFS} growth, response epochs were randomly shuffled and averaged without replacement. In other words, rather than calculating cross-correlation coefficients for the responses in increments of 100 sweeps in the order in which they were collected, cross-correlation coefficients were calculated by randomly selecting a block of sweeps without replacement independent of what order they were collected in during the recording run. For the condition in which sweeps were averaged in the order in which they were collected, responses were averaged at 100, 200, 300, etc. sweeps. For the condition in which the sweeps were shuffled, cross-correlation coefficients were calculated at, say, 400, 1000, 1200, etc. sweeps until all sweeps were accounted for. Randomly shuffling the epochs in which the FFR_{TFS} was collected yielded almost identical cross-correlation coefficient growth as a function of sweep count, as illustrated in Figure 38. This suggests that the sweep order in which the response is analyzed has little to no effect on the sweep-response growth function.

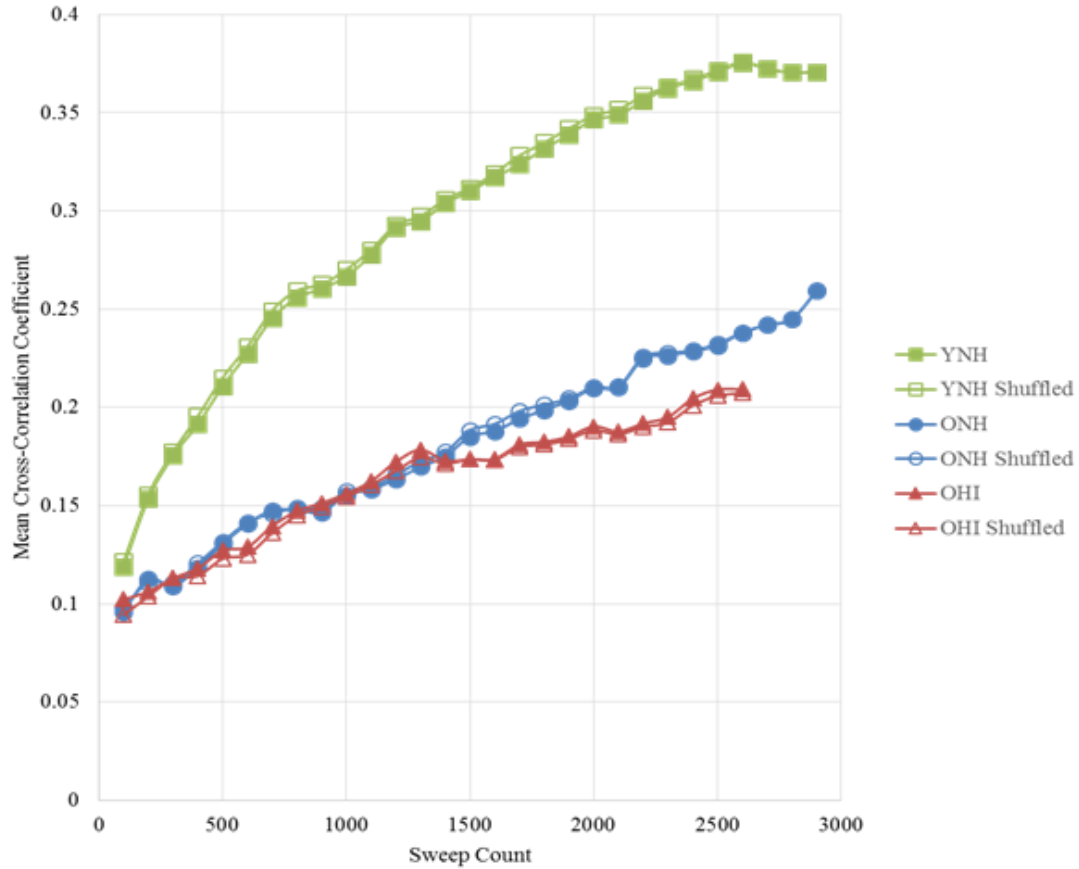


Figure 38. Mean cross-correlation coefficients by group (YNH vs. ONH vs. OHI) and order of epochs (averaged every 100 sweeps as they were collected vs. averaged every 100 sweeps in random epochs without replacement) as a function of sweep count.

Summary of Results

In summary, the present study revealed the following trends and results:

1. Age was a significant predictor of FFR_{TFS} signal-to-response fidelity, such that older individuals achieved lower cross-correlation coefficients than younger individuals. Hearing status did not significantly predict FFR_{TFS} signal-to-response fidelity, with the ONH and OHI groups producing mean responses which were indistinguishable from one another. These results suggest that the neural representation of the FFR_{TFS} is degraded in older subjects independent of hearing loss.

2. There was tremendous qualitative and quantitative inter-subject variability in the FFR_{TFS} of each of the three groups. The YNH, ONH, and OHI groups each contained individuals who produced FFR_{TFS} with good signal-to-response fidelity, as well as individuals whose FFR_{TFS} was markedly degraded, such that it was indistinguishable from the underlying EEG activity of those individuals. This suggests that participant variables besides age and hearing status might affect the fidelity with which the FFR_{TFS} reflects the stimulus.
3. Mean FFR_{TFS} signal-to-response fidelity increased as a function of sweep count as characterized by the cross-correlation coefficient independent of age or hearing status for all three groups. However, the ONH and OHI groups required 4.0 and 5.2 times as many sweeps, respectively, to achieve FFR_{TFS} of comparable fidelity the YNH group. Randomly shuffling the epochs in which the FFR_{TFS} cross-correlation coefficient was calculated had little to no effect on the sweep-response growth function.

CHAPTER 5: DISCUSSION

The goal of the present study was to utilize the FFR to characterize the degree of neural synchrony to synthesized tonal glide stimuli approximating formant transitions in three groups, consisting of YNH, ONH, and OHI individuals. Specifically, the aims were to determine the effect of sweep count and the interaction between sweep count, age and hearing status on FFR recordings and to explore individual FFR differences within and across the three groups that were tested.

On the Effect of Age on the FFR

Neural encoding of the stimulus, as reflected by the FFR, showed a significant decline as a function of increasing age, such that ONH and OHI individuals had poorer FFRs than their YNH counterparts. This decrease in neural encoding was documented as reduced response amplitudes and phase-locking in the temporal FFR waveform, smeared or absent response bands in the spectrogram of the FFR, and lower stimulus-to-response correlations. This purported reduction in neural synchrony in relation to aging is largely consistent with previous studies and has been framed as a reduction in phase-locking ability at the level of the brainstem (Anderson et al., 2012; Clinard & Cotter, 2015; Clinard & Tremblay, 2013; Clinard et al., 2010; Marmel et al., 2013; Presacco et al., 2015). This relationship between age and FFR encoding has been documented to puretone (Clinard & Tremblay, 2013; Clinard et al., 2010; Marmel et al., 2013), tonal glide (Clinard & Cotter, 2015), and synthesized CV syllable (Anderson et al., 2012; Clinard & Tremblay, 2013; Presacco et al., 2015) stimuli. In contrast, results of the present study are inconsistent with findings from Ananthakrishnan et al. (2016), who

suggest that chronological age does not contribute to degraded TFS encoding in individuals with SNHL.

Specifically, Clinard et al. (2010) showed reduced FFR magnitude and phase coherence in response to puretone stimuli as a function of increasing age, but noted that this relationship was contingent on the frequency of the stimulus, such that the age effect was only seen at higher frequencies (925 Hz, 998 Hz, and 1000 Hz) but not for lower frequency stimuli (463 Hz, 498 Hz, 500 Hz). Clinard & Cotter (2015) saw a similar effect of age on the FFR to dynamic tonal stimuli at lower frequencies around 500 Hz. They attributed the differences between aging effects at lower and higher frequencies to the nature of the stimuli and concluded that dynamic stimuli are more prone to aging effects than static stimuli. When elicited in response to a synthesized CV syllable stimulus (/da/), FFRs obtained from older individuals to the sustained portion of the stimulus exhibited poorer phase-locking (Anderson et al., 2012; Presacco et al., 2015), lower spectral response magnitudes (Anderson et al., 2012; Presacco et al., 2015), smaller response amplitudes (Clinard & Tremblay, 2013; Presacco et al., 2015), and had prolonged latency onsets (Clinard & Tremblay, 2013; Presacco et al., 2015).

Several mechanisms contributing to degraded phase-locking in older individuals have been proposed to date; these include theories of age-related auditory deafferentation and subsequent changes in inhibitory neurotransmitter function. Several studies suggest that auditory deafferentation occurs with aging and may be present without a documented audiometric loss (Makary, Shin, Kujawa, Liberman, & Merchant, 2011; Sergeyenko, Lall, Liberman, & Kujawa, 2013). This peripheral deafferentation of the auditory pathway has been shown to trigger a compensatory decrease in inhibitory neurotransmitter function at

the level of the spiral ganglion (Banay-Schwartz, Lajtha, & Palkovits, 1989; Willott, Milbrandt, Bross, & Caspary, 1997), CN (Caspary, Schatterman, & Hughes, 2005), and IC (Caspary, Raza, Armour, Pippin, & Arneric, 1990; Milbrandt, Albin, & Caspary, 1994; Willott et al., 1997) in animal models and is driven by homeostatic plasticity.

Homeostatic plasticity refers to activity-dependent changes, such as those encountered during development or in response to deafferentation, that lead to compensatory responses in neuronal excitation and inhibition which allow a particular neural network or system to retain a certain operating range (Caspary, Ling, Turner, & Hughes, 2008).

The FFR is thought to originate in part from neurons at the level of the CN (Marsh et al., 1970; Smith et al., 1975). While coding of acoustic signals occurs at different sites along the ascending auditory pathway, the dorsal and ventral CN are thought to encode temporally relevant acoustic features of the stimulus (Caspary et al., 2005; Young & Oertel, 2004). In animal models, age-related changes in inhibitory neurotransmitters in the dorsal CN have led to altered temporal and intensity coding. A disruption in neural activity following age-related sensory neural degradation at the level of the CN in humans may therefore provide a likely account for the age-related differences observed in FFR fidelity in the present study.

The age-related findings in the present study are consistent with animal histology and near-field single neuron studies (Caspary et al., 2005; Schatterman, Hughes, & Caspary, 2008; Walton, Frisina, & O'Neill, 1998). To that end, poorer FFR stimulus-to-response cross-correlations may be attributed to age-related peripheral deafferentation of the auditory system which might trigger a decrease in inhibitory neurotransmitter function. This age-related decrement in how sensory information is encoded may help

account for why certain older individuals with normal hearing report difficulty understanding speech in noise and under other adverse listening conditions. Lopez-Poveda and Barrios (2013) suggest that the stochastic nature of how action potentials allow for the encoding of acoustic information might provide an explanation for why deafferentation of auditory neurons results in poorer speech understanding in individuals with nearly normal peripheral hearing sensitivity. Specifically, they contend that single auditory nerve fibers do not fully sample a given waveform; rather, single auditory nerve fibers under-sample a given stimulus. In a normally-functioning system, multiple nerve fibers firing together contribute to high-fidelity encoding of a particular stimulus. In a system that has undergone some degree of deafferentation, say, secondary to a non-descript aging process, the pooled nerve fiber representation of the stimulus does not represent the stimulus with the same degree of fidelity because there are (a) fewer nerve fibers which can be pooled together to reconstruct the stimulus or (b) the individual deafferented nerve fibers which are pooled together are under-sampling even more so than in a healthy system.

It is possible, however, that other age-related changes are affecting the fidelity with which the FFR_{TFS} may be represented, especially given that a seemingly absent response is non-diagnostic. For example, the older participants in the study may have been more restless in the event that they remained awake during the testing session or were perhaps more likely to have fallen asleep. It is difficult to say, however, as these factors were not monitored or documented during the testing session.

While the FFR has been successfully recorded while participants were sleeping (Aiken & Picton, 2008; Dajani et al., 2005; Krishnan et al., 2005), the effect of sleep state

on the FFR has not been studied to date. Evidence from the ABR and ASSR literature suggests, however, that sleep and sleep state might affect the amplitude of the response, intensity-amplitude growth functions, and absolute latencies (minimally) (Linden, Campbell, Hamel, & Picton, 1985; Osterhammel, Shallop, & Terkildsen, 1985). It is unclear whether sleep and sleep state affected the FFR_{TFS} recordings of different individuals in their respective groups and to what degree. While the present study screened participants for any mood altering medications and central nervous suppressants, it is also possible that older participants were more likely to be prescribed multiple medications with potential interactions and side-effects with which the patient is not intuitively familiar as polypharmacy is more common in the elderly (Hajjar, Cafiero & Hanlon, 2007). The effects of central nervous suppressants and mood altering medications on the FFR have not been studied. However, studies evaluating the effects of anesthesia on the ABR and ASSR suggest that amplitudes of the responses may be reduced and latencies might be increased (Plourde & Picton, 1990; Thornton et al., 1983).

On the Effect of Hearing Loss on the FFR

Neural encoding of the stimulus did not show a significant decline as a function of hearing loss; ONH and OHI individuals had FFR_{TFS} which on average were essentially indistinguishable from one another. ONH and OHI individuals exhibited temporal FFR_{TFS} waveforms with similar response amplitudes and phase-locking, spectrograms with similar response bands, and cross-correlation coefficients. This finding is consistent with Marmel et al. (2013), who similarly found no relationship between audiometric thresholds and FFR stimulus-to-response fidelity to various puretones from 620-720 Hz. The lack of an effect on the FFR_{TFS} as a function of hearing loss is consistent with

findings from Anderson, Parbery-Clark, White-Schwoch, Dreihobl, and Kraus (2013), who reported no group differences of TFS encoding to a synthesized CV syllable stimulus /da/ at unequal SL (80.3 dB SPL for both normal-hearing and hearing-impaired groups) and when the stimulus was amplified to account for the hearing loss. Anderson et al. (2013) do suggest, however, that older adults with hearing loss have a *relative* deficit of TFS encoding, such that enhanced envelope encoding is seen in that particular population without a proportional enhancement in TFS encoding.

A lack of difference in FFR encoding between the ONH and OHI groups as a function of hearing loss is inconsistent with previous studies which have explored the effect of hearing loss on the FFR to second formant transitions in synthesized CV syllables /ba/, /da/, /ga/ (Plyler & Ananthanarayan, 2011) and synthesized vowel /u/ (Ananthakrishnan et al., 2016). Specifically, Plyler & Ananthanarayan (2001) reported that hearing-impaired individuals produced FFRs which represented the changing frequency content of the second formant transition with less fidelity than participants with normal hearing. It should be noted, however, that the study did not control for or report on the effects of age. Ananthakrishnan et al. (2016) showed that FFT peak magnitudes of the fundamental frequency and formant-related harmonics in the vowel /u/ was reduced in individuals with hearing loss in comparison to individuals with normal hearing. The effect attributed to hearing loss was reportedly not confounded by age differences between the normal-hearing and hearing-impaired groups.

While PTA was not found to be a statistically significant predictor of FFR_{TFS} encoding, it should be noted that certain differences exist between the ONH and OHI groups. First and foremost, it has previously been suggested that ONH and OHI

individuals require more sweeps than YNH individuals on average to achieve the same signal-to-response fidelity as indexed by the cross-correlation coefficient metric. To that end, ONH individuals required 4.0 times as many sweeps and OHI individuals required 5.2 times as many sweeps. This difference in the number of sweeps required to achieve an equivalent FFR_{TFS} between the two groups indicates that perhaps hearing loss affects the response in a way not otherwise captured by the statistical method employed in the present study.

A subtle effect attributed to hearing loss may furthermore be seen when examining individual responses at the maximal sweep count (i.e., the best possible response obtained by an individual participant) in relation to their underlying EEG activity. In the YNH group, no participants had FFR_{TFS} which were lower than their respective EEG. For the ONH and OHI groups, one individual and four individuals, respectively, had FFR_{TFS} which had poorer cross-correlation coefficients than those of their underlying EEG activity. This furthermore suggests that hearing status might affect FFR_{TFS} fidelity not otherwise captured by the multiple linear regression analysis employed. This lack of statistical difference might be a consequence of the tremendous variability of the FFR_{TFS} in each group and small sample size, leading to a lack of statistical power.

The dearth of statistical difference between the ONH and OHI groups may be accounted for in a number of ways. The FFR in the present study was recorded to a low-frequency stimulus centered around 500 Hz. At 500 Hz, the ONH group saw a mean threshold of 11.5 dB HL, while the OHI group saw a mean threshold of 33.0 dB HL. The lack of statistical difference between ONH and OHI groups may be accounted for in that

hearing losses with thresholds <50-60 dB HL are attributed to OHC degeneration.

Harrison and Evans (1979) evaluated aspects of temporal encoding by single cochlear fibers from regions of cochlear hair cell degeneration to establish if kanamycin-induced OHC degeneration affects phase-locking abilities. They obtained near-field single neuron recordings in guinea pigs whose cochlear OHCs had been destroyed using a kanamycin treatment and found that temporal phase-locking is minimally affected by OHC function or dysfunction. It is therefore possible that greater group differences as a function of hearing loss might be observed in individuals with poorer hearing than that of the present study participants. It should be noted, however, that Ananthakrishnan et al. (2016) and Plyler and Ananthanarayan (2001) observed an effect of hearing loss in individuals with mild to moderately-severe SNHL, which is not unlike the degree and configuration of hearing loss of the OHI individuals who were enrolled for this study.

It is also possible, however, that hearing loss did not predict the variability of the present data in a statistically significant way because TFS encoding has been shown to be minimally affected by peripheral hearing deficits in quiet (Henry & Heinz, 2012; Henry & Heinz, 2013; Kale & Heinz, 2010). Kale and Heinz (2010) obtained single-fiber auditory nerve recordings from nine chinchillas with normal hearing and 11 chinchillas with noise-induced hearing loss to 600 ms long amplitude-modulated tones at the characteristic frequency of the fiber -10 to 40 dB SL (re: the auditory nerve's threshold) at a modulation frequency of 50 Hz. They analyzed envelope and TFS encoding and determined that TFS was not degraded in noise-exposed fibers in that phase-locking to the fine structure of the stimulus was similar between normal and noise-exposed fibers. Surprisingly, phase-locking to the envelope of the stimulus was enhanced in the noise-

exposed fibers relative to the normal auditory nerves. Kale and Heinz (2010) concluded that while no absolute degradation in TFS encoding was documented in Chinchillas with noise-induced SNHL in quiet, enhanced envelope encoding in noise-exposed fibers may lead to a relative deficit in TFS cues.

In a follow-up study, Henry and Heinz (2012) explored temporal coding in anesthetized chinchillas with and without SNHL by recording spike trains to puretone stimuli in quiet and in the presence of background noise at three levels (10, 15, and 20 dB above stimulus) from single auditory nerve fibers. They found that recordings obtained from neurons from hearing-impaired chinchillas had predictably higher thresholds and broader tuning curves than those obtained from healthy chinchillas. Furthermore, Henry and Heinz (2012) determined that SNHL and masking level had a negative impact on phase-locking of the auditory nerve fibers to the stimulus. Remarkably, however, phase-locking was only minimally affected by hearing loss when the stimulus was presented in quiet, but revealed a much greater degradation in noise for chinchillas with hearing loss than for chinchillas without hearing impairment.

Henry and Heinz (2012) suggest that SNHL only reduces the strength of TFS encoding in noise because the broader tuning curves of damaged auditory nerve fibers allow for more noise energy to be processed by the nerve, consequently reducing the number of neural spikes synchronized to the intended stimulus and increasing the number of neural spikes elicited by the noise. Following the findings from Henry and Heinz (2012), it is possible that a lack of an effect of hearing loss on the FFR_{TFS} in the present study is due to the experiment having been conducted in quiet. Perhaps a greater

degradation of phase-locking could have been documented in hearing-impaired individuals if the experiment had been conducted in the presence of background noise.

On Within and Across Group Variability of the FFR

The present study saw tremendous qualitative and quantitative inter-subject variability in the FFR_{TFS} of each of the three groups. The YNH, ONH, and OHI groups each contained individuals who produced FFR_{TFS} with good signal-to-response fidelity, as well as individuals whose FFR_{TFS} was markedly degraded, such that it was indistinguishable from the underlying EEG activity of those individuals. This response variability in neural encoding was documented as a spectrum of response amplitudes and phase-locking in the temporal FFR_{TFS} waveform, robustness of response bands in the spectrogram of the FFR_{TFS}, and maximal stimulus-to-response cross-correlation coefficients ranging from 0.052-0.6187 (on a scale from 0 to 1) across all 3 groups.

It is critical to acknowledge that factors other than aging and hearing status might have affected the FFR_{TFS} recordings in the present study, especially since R^2 values suggest that age does not account for the majority of the variance in the FFR_{TFS} data and PTA does not statistically predict the current findings. Other variables, such as recording parameters, response analysis methods, and individual participant differences, which were not controlled for in this study, might help illuminate some of the individual variability and poor FFR_{TFS} recordings in general.

Recording factors, such as the sampling rate at which the response is collected are also known to affect the precision with which a response is represented. Specifically, a higher sampling rate is more sensitive to small temporal variations within a given response waveform (Krishnan, 2007; Skoe & Kraus, 2010). The present study utilized a

sampling rate of 20 kHz, which is easily considered to be more than sufficient, but higher sampling rates have been reported in the literature (Galbraith & Brown, 1990).

It is also possible that the metric chosen to quantify the FFR is not the best measure to use. It is possible that there is an underlying response but that that response is not being detected by the current signal processing strategies used for this study. For example, the cross-correlation coefficient analysis takes into account the entire waveform with respect to latency and amplitude and compares this to the stimulus waveform. Even if the latencies of the respective stimulus and response waveforms align perfectly, a mismatch in amplitude would result in a lowered (less than 1) cross-correlation coefficient. The inclusion of amplitude in the analysis might be of particular importance in accounting for some of the variability seen in the data as it is an inherently variable metric. Amplitude has been shown to be sensitive to effects relating to electrode placement (ACNS, 2006; Beattie & Taggart, 1989; Terkildsen & Osterhammel, 1981), impedance (Picton, 2011), gender (Don, Ponton, Eggermont, & Masuda, 1994), head diameter (Trune, Mitchell, & Phillips, 1988) and age (Burkard & Sims, 2001) in other auditory evoked potential measures. A more suitable analysis metric, perhaps, might have been the phase coherence (PC) (Clinard et al. 2010; Krishnan & Parkinson, 2010), which compares the stimulus to the response in terms of the degree of phase-locking that is occurring only and does not consider the amplitude component of the response waveform.

Individual factors which were not controlled for in this study, such as experience-related plasticity secondary to hearing aid use, musical training or auditory training, language experience and attention might have contributed to the inter-subject variability

seen within each group. Neural plasticity refers to the reorganization of neuronal structures either in response to intrinsic factors, such as those relating to development, aging and hearing loss, or extrinsic factors, such as language experience or musical training. For example, reduced auditory input secondary to peripheral hearing loss has been documented to alter subcortical neuronal circuits through a subsequent reduction in inhibitory neurotransmitter function (Casparly et al., 2005; Willott, 1996). It stands to reason, then, that an increase in auditory input following the use of amplification would also lead to subcortical neural reorganization. Unfortunately, the OHI participants in the present study were not queried about the onset and progression of their hearing loss or whether they made use of hearing aids and to what extent. It is possible that differences in the duration spent with hearing loss and the use of amplification (or lack thereof) between individual OHI participants might further contribute an account of the variability of FFR_{TFS} documented in that group.

Subcortical neural encoding of pitch has also been documented to be strongly affected by experience-dependent factors such as musical training (Bidelman & Krishnan, 2010; Krishnan, Gandour, & Bidelman, 2012; Musacchia et al., 2007; Wong et al., 2007) and language experience (Krishnan et al., 2005; Krishnan, Gandour, Bidelman, & Swaminathan, 2009). Extended musical training has been shown to enhance the magnitude and precision with which the FFR represent a particular stimulus (Bidelman & Krishnan, 2010; Bidelman et al., 2011; Krishnan et al., 2012; Musacchia et al., 2007; Wong et al., 2007). It is therefore possible that a history of musical training may have further contributed to some of the variability seen across study participants. For example, the YNH, ONH, and OHI groups each saw one or two participants who exhibited

excellent FFR_{TFS}. Perhaps long-term music exposure contributed to those participants having enhanced FFR_{TFS} relative to their peers. Since musical experience was not documented, however, the relationship between FFR_{TFS} fidelity and musical experience cannot be determined.

Language experience has been shown to have a similar effect on the encoding of pitch contours which occur in Mandarin. Specifically, Mandarin speakers more robustly encode pitch patterns which approximate the pitch contours found in Mandarin than English speakers (Krishnan et al., 2005; Krishnan et al., 2009; Xu, Krishnan, & Gandour, 2006). This effect, however, was not documented for non-linguistically relevant pitch patterns. It is therefore unlikely that language experience contributed to the response variability documented in the present study.

In addition to the variables described above, the aging process in and of itself might help account for the variability described for the ONH and OHI groups. Age-related decrements in neural synchrony have been attributed to a number of peripheral and central structural and functional changes in the auditory system, such as alterations of cochlear metabolic activity (Mills et al., 2006), changes in synaptic function (Stamatakis, Francis, Lehar, & Ryugo, 2006), deafferentation of auditory nerve fibers (Frisina & Walton, 2006; add source from aging section above), subsequent adaptive decreases in inhibitory neurotransmitters (Caspary et al., 2005), prolonged neural recovery time (Walton et al., 1998), and changes in neural adaptation (Javel, 1996).

The role of neural adaptation and its effect on the FFR to 1000 Hz toneburst stimuli has been discussed in greater detail by Clinard and Tremblay (2013). They suggest that following repeated repetition of a stimulus, neuronal responses may adapt in

that they become less robust as stimulus presentation frequency increases. Specifically, this neural adaptation process is thought to be degraded in older individuals. Clinard and Tremblay (2013) saw an increase in the heterogeneity of the FFR (as indexed by phase coherence between the stimulus and the response) at higher sweep counts than at lower sweep counts. This increase in the heterogeneity of the FFR was most notable for older participants (61-80 years), followed by the middle-aged participants (41-60 years), and least marked for the youngest participants (21-40 years). Clinard and Tremblay (2013) account for this increased variability among the oldest participants in that aging is an individualized process affected by many intrinsic and extrinsic factors, which may lead to differences in biologic age even when chronological age is held constant.

The present study is consistent with some of the findings reported by Clinard and Tremblay (2013). Specifically, a similar trend of an increase in the variability of the FFR_{TFS} was documented for the YNH, ONH, and OHI groups as the number of stimulus presentations increased (Figure 34), supporting the notion of individual differences in the neural adaptation processes. The greatest variability in the response seen at the maximal stimulus presentations, however, was documented for the OHI group, followed by the YNH group, and was least evident for the ONH group. In contrast, Clinard and Tremblay (2013) report that variability was seen across the age span, but that this response variability was reduced at the extreme ends of the age continuum of their participant cohort. It is possible that the smaller variance in FFR_{TFS} documented for the ONH group relative to the other two groups in the present study is secondary to the homogenous nature of that group. In other words, older individuals *without* hearing loss comprise a very particular subset of the aging population. As such, the intrinsic and extrinsic factors

governing their hearing status might also influence their aging processes and vice versa. On the other hand, older individuals *with* hearing loss and younger individuals *without* hearing loss are representative of more heterogeneous populations, as the relative hearing status for each population is the norm, rather than the exception. This selection bias might therefor contribute to the ONH individuals being more similar to one another than the OHI and YNH individuals.

On the Effect of Sweep Count on the FFR

In general, mean FFR_{TFS} signal-to-response fidelity increased as a function of sweep count as characterized by the cross-correlation coefficient independent of age or hearing status for all three groups. However, the ONH and OHI groups required 4.0 and 5.2 times as many sweeps, respectively, to achieve FFR_{TFS} of comparable fidelity to the YNH group. When examining the effect of sweep count on responses obtained from individual participants, the addition of sweeps allowed the FFR_{TFS} waveform to be distinguished from the underlying EEG activity for some participants, but not for others. This response growth as a function of sweep count seen for some participants was documented as an increase of amplitudes and phase-locking in the temporal FFR_{TFS} waveform, an increase in the robustness of the response bands in the spectrogram of the FFR_{TFS} , and an increase in the stimulus-to-response cross-correlation coefficients. For other participants, additional sweep counts had little to no effect on the amplitudes or phase-locking of the temporal FFR_{TFS} , the response bands in the spectrograms of the FFR_{TFS} , or the cross-correlation coefficients. Of particular interest is that the ONH group saw one and the OHI group saw four individuals for whom the addition of added sweeps did not allow for their FFR_{TFS} to be distinguished from their underlying EEG, meaning

that the maximal cross-correlation coefficient achieved by those individuals was lower than the maximal cross-correlation coefficient observed in the artifact condition. In contrast, the YNH group was comprised entirely of individuals for whom the addition of sweep counts produced cross-correlation coefficients which were at least marginally greater than their underlying EEG activity.

It was hypothesized that the signal-to-response fidelity of the FFR would improve with increasing sweep count following the square root of the sample size principle, in which averaged noise levels decrease as a function of 1 over the square root of the number of sweeps utilized to record a particular response (Elberling & Don, 1984; Hood, 1998; Özdamar & Delgado, 1996), allowing the small amplitude FFR to be detected in the underlying noise. In order to satisfy this description of SNR growth, however, the following assumptions must be met: (1) the FFR is a deterministic signal, meaning that there are no variations in the response between each trial, (2) the underlying noise is an ergodic random process, meaning that every potential iteration of the noise is likely to occur, and (3) the FFR and noise are independent of each other (Elberling & Don, 1984). These assumptions, however, were not strictly fulfilled in the present study with respect to the requisite ergodicity of the noise in the recording.

It is possible that the OHI group saw a greater number of individual participants whose FFR_{TFS} was below their EEG because the OHI group saw a baseline EEG which had a higher cross-correlation coefficient on average ($M = 0.0754$, $SD = 0.0176$) than the ONH ($M = 0.0646$, $SD = 0.0174$) and YNH ($M = 0.0554$, $SD = 0.0132$) groups. This suggests that the OHI individuals may have greater levels of noise in their recordings, which might obscure the targeted response signal. As a reminder, cross-correlation

coefficients for each individual's underlying EEG were approximated by comparing the response waveform obtained during the artifact condition with the stimulus. During this condition, the insert transducer was clamped, the participants wore earplugs, and the transducers were removed from the participants' ears to ensure that the stimulus could not be heard. Furthermore, a higher cross-correlation coefficient might suggest that the covariance of the noise between individual sweeps is not zero.

Following Özdamar & Delgado (1996), the SNR estimation formula for other brainstem-evoked potentials, such as the ABR, relies on a noise covariance of zero between sweeps, such that the noise components of individual sweeps are not correlated. Given that the cross-correlation coefficient of the YNH, ONH, and OHI groups is not zero, it is likely that the noise component of the individual response signals are to some degree mildly correlated, with the OHI group seeing the greatest amount of correlation. This may be of particular significance for brainstem-evoked potentials, such as the ABR and FFR, since the signal of interest is embedded in the noise and only becomes apparent after multiple sweeps have been acquired. It is unlikely, however, that noise alone accounts for response variability; it is likely that there is a confounding effect of response differences from trial to trial (Coppola, Tabor, & Buchsbaum, 1978).

Another possible account for why some individuals saw a growth in the FFR_{TFS} fidelity as a function of sweep count and others did not relates back to differences in neural adaptation (Javel, 1996) previously discussed with respect to the variability seen in the FFR_{TFS} across individual participants. Clinard and Tremblay (2013) suggested that neural adaptation is more variable in older individuals and can be most robustly seen at higher sweep counts because biological aging is a heterogeneous process modulated by

many extrinsic and intrinsic factors which do not always correspond to chronological age. It is unclear, however, to what degree a degradation in neural adaptation contributes to the variability seen among the YNH individuals, as the assumption is that young individuals would have an intact neural system.

While neural adaptation provides a possible explanation of the variability seen as a function of sweep count, it is rather unlikely that neural adaptation processes or degradation thereof is impacting the growth in SNR of the FFR_{TFS} as scrambling the order of sweeps in which the FFR_{TFS} is averaged has little to no impact on the cross-correlation coefficient, as previously illustrated in Figure 36. If short-term neural plasticity effects were to have an impact on the FFR_{TFS} , the sweep-response growth functions would be different if sweeps were averaged in the order in which they were collected and if sweeps were averaged randomly without replacement.

It should be noted, however, that small variations in the sweep-response growth function occur when sweep count is shuffled and when the response is analyzed in the order in which it was collected. Furthermore, independent of the sweep order in which the response is analyzed, the sweep-response growth function is not perfectly smooth, meaning that the addition of sweeps does not always result in a higher cross-correlation coefficient at the next highest sweep count. Referring back to Figure 35, the OHI group on average saw an increase of 0.0027 in cross-correlation coefficient from 1200 to 1300 sweeps and a decrease of 0.0020 in cross-correlation coefficient with the addition of a subsequent 100 sweeps from 1300 to 1400 sweeps. These small variations in the sweep-response growth curve may be accounted for by oscillations in the correlation of the noise in the response, such that the noise is sometimes positively and sometimes negatively

correlated between sweeps (Özdamar & Delgado, 1996). Positively correlated noise between sweeps will result in an overestimation of the SNR and negatively correlated noise between sweeps will result in the underestimation of the SNR (Özdamar & Delgado, 1996).

Clinical Implications

A number of clinical implications emerge from the present study. First and foremost, the FFR might be used to differentiate individuals whose TFS representation is degraded without the presence of classic hearing loss. While the ONH individuals in this study did not have a peripheral hearing deficit, their poorer FFR recordings suggest a potential TFS encoding deficit. Documenting the presence of an age-related temporal processing deficit may be used to guide and pursue rehabilitative options for individuals who report difficulties hearing in the absence of clinically significant hearing loss. These strategies would extend beyond the traditional strategies of extending audibility with hearing aids to auditory training strategies which might improve synchronous firing of auditory neurons. Musical or other auditory-training schemes might also be suggested to these individuals in an effort to improve TFS encoding and FFR pre- and post-training measures might be utilized to track auditory training benefit.

Although the FFR is not currently utilized clinically, establishing the relationship between the number of sweeps which are collected and the fidelity with which the stimulus is encoded may help drive clinical protocols in the future. For example, clinicians might anticipate needing more clinical time when collecting FFRs from older individuals than they might from younger individuals. More importantly, however, given the tremendous variability observed in the FFR in the present study, the usability of the

FFR as a clinical measure as it currently stands is questionable. More research is needed to determine the sources of variability prior to deploying the FFR as a clinically-useful measure.

Study Limitations

The present study was met with several limitations related to study design and data analysis. First, one of the goals of the study was to explore group differences as a function of age and hearing loss on the FFR. In order to evaluate these variables, three groups of individuals were assembled. A group comprised of younger individuals with normal hearing was compared to two older groups, one with normal hearing and one with hearing loss, matched in age to one another. Notably, a younger group with hearing loss was not included in the study as it is difficult to recruit younger individuals with hearing losses that are likely to be audiometrically similar and have a common etiology. The inclusion of a younger group with hearing loss might have strengthened the findings related to the effect of hearing loss on the FFR and could potentially serve to tease out the relative effects of age and hearing loss on subcortical neural encoding.

While the present study did not see any mean effect of hearing loss on the FFR, the response was collected at a set intensity of 85 dB SPL, meaning that the sensation level of the stimulus varied between participants with hearing loss and those with normal hearing. While no group effect was documented as a function of hearing loss, individual response variability in the OHI group might be partially accounted for by differences in audibility.

The statistical method used to analyze group differences in the present study was a standard multiple linear regression, in which the dependent variable was the cross-

correlation coefficient and the independent predictor variables were age, degree of hearing loss (PTA), and sweep count. Since data was collected at discrete points in a time-dependent manner, a time series multiple linear regression would have provided a more accurate model of the data. The multiple linear regression approach that was used is likely to underestimate the error in the model and cannot be used to forecast.

A significant finding of the present study relates to the great variability documented in the FFR within each group. It remains unclear, however, why some YNH individuals exhibited excellent subcortical neural encoding of the stimulus while others had seemingly undetected FFRs. A similar trend was seen in the ONH and OHI group and remains hitherto unexplained. It is possible that musical training or language experience, both variables which have been documented to affect the FFR, may help account for the variability inherent to each group. The present study, however, did not query the study participants about factors relating to musical training or other language proficiencies, making it difficult to explain some of the variability found in the response across participants.

Another major goal of the present study was to explore the effect of sweep count on the FFR. As predicted, as sweep count increased, so did the fidelity with which the stimulus was represented in the FFR waveform on average. However, not all individual FFRs saw the same growth in fidelity as a function of sweep count. Because FFR collection was stopped at 3000 sweeps, it is unclear whether the fidelity with which the FFR waveform represented the stimulus was maximally obtained. It is possible that continuing FFR data collection at higher sweep counts might have improved the fidelity of the response further, especially for individuals whose FFRs were indistinguishable

from their underlying EEG activity. Furthermore, it would have been a point of interest to document at what point in the averaging process the response quality begins to deteriorate to more succinctly identify an “ideal” number of sweep counts for clinical purposes.

Future Directions

Perhaps of greatest interest is whether the FFR may provide an objective clinical measure of listening difficulty and effort. To further evaluate this, future studies might consider evaluating whether individuals with poorer FFRs have a greater likelihood of reporting difficulty understanding speech in quiet and speech in adverse listening environments. This rests on the following assumption: (1) phase-locking is indexed by the FFR, (2) phase-locking is thought to support TFS encoding, and (3) TFS is critical for speech-in-noise understanding.

REFERENCES

- Abel, S. M., Krever, E. M., & Alberti, P. W. (1990). Auditory detection, discrimination and speech processing in ageing, noise-sensitive and hearing-impaired listeners. *Scandinavian Audiology*, 19(1), 43-54.
- Abrams, D. A., & Kraus, N. (2009) Auditory pathway representations of speech sounds in humans. In J. Katz (Ed.), *Handbook of Clinical Audiology* (pp. 611–676). Philadelphia, PA: Lippincott Williams & Wilkins.
- Aiken, S. J., & Picton, T. W. (2006). Envelope following responses to natural vowels. *Audiology and Neurotology*, 11(4), 213-232. doi: 10.1159/000092589
- Aiken, S. J., & Picton, T. W. (2008). Envelope and spectral frequency-following responses to vowel sounds. *Hearing Research*, 245(1), 35-47.
- Akhoun, I., Gallégo, S., Moulin, A., Ménard, M., Veuillet, E., Berger-Vachon, C., ... & Thai-Van, H. (2008). The temporal relationship between speech auditory brainstem responses and the acoustic pattern of the phoneme /ba/ in normal-hearing adults. *Clinical Neurophysiology*, 119(4), 922-933.
- American Clinical Neurophysiology Society. (2006). Guideline 9C: Guidelines for standard electrode position nomenclature. *American Journal of Electroneurodiagnostic Technology*, 46(3), 275-86.
- Ananthakrishnan, S., Krishnan, A., & Bartlett, E. (2016). Human Frequency Following Response: Neural Representation of Envelope and Temporal Fine Structure in Listeners with Normal Hearing and Sensorineural Hearing Loss. *Ear and Hearing*, 37(2), e91-e103.

- Anderson, S., Parbery-Clark, A., White-Schwoch, T., & Kraus, N. (2012). Aging affects neural precision of speech encoding. *The Journal of Neuroscience*, 32(41), 14156-14164.
- Anderson, S., Parbery-Clark, A., White-Schwoch, T., Dreihobl, S., & Kraus, N. (2013). Effects of hearing loss on the subcortical representation of speech cues. *The Journal of the Acoustical Society of America*, 133(5), 3030-3038.
- Banai, K., Hornickel, J., Skoe, E., Nicol, T., Zecker, S., & Kraus, N. (2009). Reading and subcortical auditory function. *Cerebral Cortex*, 19(11), 2699-2707.
- Banay-Schwartz, M., Lajtha, A., & Palkovits, M. (1989). Changes with aging in the levels of amino acids in rat CNS structural elements I. Glutamate and related amino acids. *Neurochemical Research*, 14(6), 555-562.
- Batra, R., Kuwada, S., & Maher, V. L. (1986). The frequency-following response to continuous tones in humans. *Hearing Research*, 21(2), 167-177.
- Beattie, R. C., & Taggart, L. A. (1989). Electrode Placement and Mode of Recording (Differential vs. Single-Ended) Effects on the Early Auditory-Evoked Response: Original Papers. *International Journal of Audiology*, 28(1), 1-18.
- Bidelman, G. M., Gandour, J. T., & Krishnan, A. (2011). Musicians and tone-language speakers share enhanced brainstem encoding but not perceptual benefits for musical pitch. *Brain and Cognition*, 77(1), 1-10.
- Bidelman, G. M., & Krishnan, A. (2009). Neural correlates of consonance, dissonance, and the hierarchy of musical pitch in the human brainstem. *The Journal of Neuroscience*, 29(42), 13165-13171.

- Bidelman, G. M., & Krishnan, A. (2010). Effects of reverberation on brainstem representation of speech in musicians and non-musicians. *Brain Research, 1355*, 112-125.
- Burkard, R. F., & Sims, D. (2001). The Human Auditory Brainstem Response to High Click Rates: Aging Effects. *American Journal of Audiology, 10*(2), 53-61.
- Carcagno, S., & Plack, C. J. (2011). Subcortical plasticity following perceptual learning in a pitch discrimination task. *Journal of the Association for Research in Otolaryngology, 12*(1), 89-100.
- Casparly, D. M., Ling, L., Turner, J. G., & Hughes, L. F. (2008). Inhibitory neurotransmission, plasticity and aging in the mammalian central auditory system. *Journal of Experimental Biology, 211*(11), 1781-1791.
- Casparly, D. M., Raza, A., Armour, B. L., Pippin, J., & Arneric, S. P. (1990). Immunocytochemical and neurochemical evidence for age-related loss of GABA in the inferior colliculus: implications for neural presbycusis. *The Journal of Neuroscience, 10*(7), 2363-2372.
- Casparly, D. M., Schatteman, T. A., & Hughes, L. F. (2005). Age-related changes in the inhibitory response properties of dorsal cochlear nucleus output neurons: role of inhibitory inputs. *The Journal of Neuroscience, 25*(47), 10952-10959.
- Chandrasekaran, B., Hornickel, J., Skoe, E., Nicol, T., & Kraus, N. (2009). Context-dependent encoding in the human auditory brainstem relates to hearing speech in noise: implications for developmental dyslexia. *Neuron, 64*(3), 311-319.
- Chiappa, K. H. (1997). *Evoked potentials in clinical medicine*. Lippincott-Raven.
Retrieved from <http://books.google.com/books?id=h5mOjnTimT8C>

- Clinard, C. G., & Cotter, C. M. (2015). Neural representation of dynamic frequency is degraded in older adults. *Hearing Research*, 323, 91-98. doi: 10.1016/j.heares.2015.02.002
- Clinard, C. G., & Tremblay, K. L. (2013). Aging degrades the neural encoding of simple and complex sounds in the human brainstem. *Journal of the American Academy of Audiology*, 24(7), 590-599.
- Clinard, C. G., Tremblay, K. L., & Krishnan, A. R. (2010). Aging alters the perception and physiological representation of frequency: evidence from human frequency-following response recordings. *Hearing Research*, 264(1), 48-55. doi:10.1016/j.heares.2009.11.010
- Coppola, R., Tabor, R., & Buchsbaum, M. S. (1978). Signal to noise ratio and response variability measurements in single trial evoked potentials. *Electroencephalography and Clinical Neurophysiology*, 44(2), 214-222.
- Cunningham, J., Nicol, T., Zecker, S. G., Bradlow, A., & Kraus, N. (2001). Neurobiologic responses to speech in noise in children with learning problems: deficits and strategies for improvement. *Clinical Neurophysiology*, 112(5), 758-767.
- Dajani, H. R., Purcell, D., Wong, W., Kunov, H., & Picton, T. W. (2005). Recording human evoked potentials that follow the pitch contour of a natural vowel. *IEEE Transactions on Biomedical Engineering*, 52(9), 1614-1618.
- Davis, H., & Hirsh, S. K. (1976). The audiometric utility of brain stem responses to low-frequency sounds. *International Journal of Audiology*, 15(3), 181-195.
- Don, M., Ponton, C. W., Eggermont, J. J., & Masuda, A. (1994). Auditory brainstem response (ABR) peak amplitude variability reflects individual differences in

- cochlear response times. *The Journal of the Acoustical Society of America*, 96(6), 3476-3491.
- Elberling, C., & Don, M. (1984). Quality estimation of averaged auditory brainstem responses. *Scandinavian Audiology*, 13(3), 187-197.
- Fitzgibbons, P. J., & Gordon-Salant, S. (1995). Age effects on duration discrimination with simple and complex stimuli. *The Journal of the Acoustical Society of America*, 98(6), 3140-3145.
- Frisina, R. D., & Walton, J. P. (2006). Age-related structural and functional changes in the cochlear nucleus. *Hearing Research*, 216, 216-223.
- Galbraith, G. C. (1994). Two-channel brain-stem frequency-following responses to pure tone and missing fundamental stimuli. *Electroencephalography and Clinical Neurophysiology/Evoked Potentials Section*, 92(4), 321-330.
- Galbraith, G. C., & Arroyo, C. (1993). Selective attention and brainstem frequency-following responses. *Biological Psychology*, 37(1), 3-22.
- Galbraith, G. C., Bhuta, S. M., Choate, A. K., Kitahara, J. M., & Mullen Jr, T. A. (1998). Brain stem frequency-following response to dichotic vowels during attention. *Neuroreport*, 9(8), 1889-1893.
- Galbraith, G. C., & Brown, W. S. (1990). Cross-correlation and latency compensation analysis of click-evoked and frequency-following brain-stem responses in man. *Electroencephalography and Clinical Neurophysiology*, 77(4), 295-308.
- Galbraith, G. C., & Doan, B. Q. (1995). Brainstem frequency-following and behavioral responses during selective attention to pure tone and missing fundamental stimuli. *International Journal of Psychophysiology*, 19(3), 203-214.

- Galbraith, G. C., & Kane, J. M. (1993). Brainstem frequency-following responses and cortical event-related potentials during attention. *Perceptual and Motor Skills*, 76(3c), 1231-1241. doi: 10.2466/pms.1993.76.3c.1231
- Galbraith, G. C., Olfman, D. M., & Huffman, T. M. (2003). Selective attention affects human brain stem frequency-following response. *Neuroreport*, 14(5), 735-738.
- Gardi, J., Merzenich, M., & McKean, C. (1979). Origins of the scalp-recorded frequency-following response in the cat. *International Journal of Audiology*, 18(5), 353-380.
- Gelfand, S. A. (2004). *Hearing: An Introduction to Psychological and Physiological Acoustics*. CRC Press.
- Gerken, G. M., Moushegian, G., Stillman, R. D., & Rupert, A. L. (1975). Human frequency-following responses to monaural and binaural stimuli. *Electroencephalography and Clinical Neurophysiology*, 38(4), 379-386.
- Glaser, E. M., Suter, C. M., Dasheiff, R., & Goldberg, A. (1976). The human frequency-following response: its behavior during continuous tone and tone burst stimulation. *Electroencephalography and Clinical Neurophysiology*, 40(1), 25-32.
- Greenberg, S., Marsh, J. T., Brown, W. S., & Smith, J. C. (1987). Neural temporal coding of low pitch. I. Human frequency-following responses to complex tones. *Hearing Research*, 25(2), 91-114.
- Hajjar, E. R., Cafiero, A. C., & Hanlon, J. T. (2007). Polypharmacy in elderly patients. *The American Journal of Geriatric Pharmacotherapy*, 5(4), 345-351.
- Hall, J. W. (2007). *New handbook of auditory evoked responses*. Pearson.

- Harrison, R. V., & Evans, E. F. (1979). Some aspects of temporal coding by single cochlear fibres from regions of cochlear hair cell degeneration in the guinea pig. *Archives of Otorhinolaryngology*, 224(1), 71-78.
- Henry, K. S., & Heinz, M. G. (2012). Diminished temporal coding with sensorineural hearing loss emerges in background noise. *Nature Neuroscience*, 15(10), 1362-1364.
- Henry, K. S., & Heinz, M. G. (2013). Effects of sensorineural hearing loss on temporal coding of narrowband and broadband signals in the auditory periphery. *Hearing Research*, 303, 39-47.
- Hood, L. J. (1998). *Clinical applications of the auditory brainstem response*. Singular.
- Hoormann, J., Falkenstein, M., & Hohnsbein, J. (1994). Effect of selective attention on the latency of human frequency-following potentials. *Neuroreport*, 5(13), 1609-1612.
- Hoormann, J., Falkenstein, M., Hohnsbein, J., & Blanke, L. (1992). The human frequency-following response (FFR): normal variability and relation to the click-evoked brainstem response. *Hearing Research*, 59(2), 179-188.
- Javel, E. (1996). Long-term adaptation in cat auditory-nerve fiber responses. *The Journal of the Acoustical Society of America*, 99(2), 1040-1052.
- Kale, S., & Heinz, M. G. (2010). Envelope coding in auditory nerve fibers following noise-induced hearing loss. *Journal of the Association for Research in Otolaryngology*, 11(4), 657-673.

- King, C., Warrier, C. M., Hayes, E., & Kraus, N. (2002). Deficits in auditory brainstem pathway encoding of speech sounds in children with learning problems. *Neuroscience Letters*, 319(2), 111-115.
- Krishnan, A. (1999). Human frequency-following responses to two-tone approximations of steady-state vowels. *Audiology and Neurotology*, 4(2), 95-103.
- Krishnan, A. (2002). Human frequency-following responses: representation of steady-state synthetic vowels. *Hearing Research*, 166(1), 192-201.
- Krishnan, A. (2007). Frequency-following response. In R. F. Burkard, M. Don, & J.J. Eggermont (Eds.), *Auditory evoked potentials: Basic principles and clinical applications* (pp. 313-333). Baltimore, MD: Lippincott Williams & Wilkins.
- Krishnan, A., Bidelman, G. M., & Gandour, J. T. (2010). Neural representation of pitch salience in the human brainstem revealed by psychophysical and electrophysiological indices. *Hearing Research*, 268(1), 60-66.
- Krishnan, A., Bidelman, G. M., Smalt, C. J., Ananthakrishnan, S., & Gandour, J. T. (2012). Relationship between brainstem, cortical and behavioral measures relevant to pitch salience in humans. *Neuropsychologia*, 50(12), 2849-2859.
- Krishnan, A., Gandour, J. T., & Bidelman, G. M. (2012). Experience-dependent plasticity in pitch encoding: from brainstem to auditory cortex. *Neuroreport*, 23(8), 498.
- Krishnan, A., Gandour, J. T., Bidelman, G. M., & Swaminathan, J. (2009). Experience dependent neural representation of dynamic pitch in the brainstem. *Neuroreport*, 20(4), 408-413.
- Krishnan, A., & Parkinson, J. (2000). Human frequency-following response: representation of tonal sweeps. *Audiology and Neurotology*, 5(6), 312-321.

- Krishnan, A., Xu, Y., Gandour, J. T., & Cariani, P. A. (2004). Human frequency-following response: representation of pitch contours in Chinese tones. *Hearing Research*, 189(1), 1-12.
- Krishnan, A., Xu, Y., Gandour, J., & Cariani, P. (2005). Encoding of pitch in the human brainstem is sensitive to language experience. *Cognitive Brain Research*, 25(1), 161-168.
- Ladefoged, P. (1996). *Elements of acoustic phonetics*. University of Chicago Press.
- Lee, K. M., Skoe, E., Kraus, N., & Ashley, R. (2009). Selective subcortical enhancement of musical intervals in musicians. *The Journal of Neuroscience*, 29(18), 5832-5840.
- Liederman, J., Frye, R., Fisher, J. M., Greenwood, K., & Alexander, R. (2005). A temporally dynamic context effect that disrupts voice onset time discrimination of rapidly successive stimuli. *Psychonomic Bulletin & Review*, 12(2), 380-386.
- Linden, R. D., Campbell, K. B., Hamel, G., & Picton, T. W. (1985). Human auditory steady state evoked potentials during sleep. *Ear and Hearing*, 6(3), 167-174.
- Lister, J. J., & Roberts, R. A. (2005). Effects of age and hearing loss on gap detection and the precedence effect: narrow-band stimuli. *Journal of Speech, Language, and Hearing Research*, 48(2), 482-493.
- Lister, J., & Tarver, K. (2004). Effect of age on silent gap discrimination in synthetic speech stimuli. *Journal of Speech, Language, and Hearing Research*, 47(2), 257-268.

- Lopez-Poveda, E. A., & Barrios, P. (2013). Perception of stochastically undersampled sound waveforms: a model of auditory deafferentation. *Frontiers in Neuroscience*, 7(124), 10-3389.
- Lorenzi, C., Gilbert, G., Carn, H., Garnier, S., & Moore, B. C. (2006). Speech perception problems of the hearing impaired reflect inability to use temporal fine structure. *Proceedings of the National Academy of Sciences*, 103(49), 18866-18869.
- Makary, C. A., Shin, J., Kujawa, S. G., Liberman, M. C., & Merchant, S. N. (2011). Age-related primary cochlear neuronal degeneration in human temporal bones. *Journal of the Association for Research in Otolaryngology*, 12(6), 711-717.
- Marmel, F., Linley, D., Carlyon, R. P., Gockel, H. E., Hopkins, K., & Plack, C. J. (2013). Subcortical neural synchrony and absolute thresholds predict frequency discrimination independently. *Journal of the Association for Research in Otolaryngology*, 14(5), 757-766.
- Marsh, J. T., Brown, W. S., & Smith, J. C. (1974). Differential brainstem pathways for the conduction of auditory frequency-following responses. *Electroencephalography and Clinical Neurophysiology*, 36, 415-424.
- Marsh, J. T., Brown, W. S., & Smith, J. C. (1975). Far-field recorded frequency-following responses: Correlates of low pitch auditory perception in humans. *Electroencephalography and Clinical Neurophysiology*, 38(2), 113-119.
- Marsh, J. T., Worden, F. G., & Smith, J. C. (1970). Auditory frequency-following response: neural or artifact? *Science*, 169(3951), 1222-1223.

- Milbrandt, J. C., Albin, R. L., & Caspary, D. M. (1994). Age-related decrease in GABA B receptor binding in the Fischer 344 rat inferior colliculus. *Neurobiology of Aging*, 15(6), 699-703.
- Mills, J. H., Schmiedt, R. A., Schulte, B. A., & Dubno, J. R. (2006). Age-related hearing loss: A loss of voltage, not hair cells. *Seminars in Hearing*, 27(4), 228-236.
- Moore, B. C. (2008). The role of temporal fine structure processing in pitch perception, masking, and speech perception for normal-hearing and hearing-impaired people. *Journal of the Association for Research in Otolaryngology*, 9(4), 399-406.
- Moushegian, G., Rupert, A. L., & Stillman, R. D. (1973). Scalp-recorded early responses in man to frequencies in the speech range. *Electroencephalography and Clinical Neurophysiology*, 35(6), 665-667.
- Musacchia, G., Sams, M., Skoe, E., & Kraus, N. (2007). Musicians have enhanced subcortical auditory and audiovisual processing of speech and music. *Proceedings of the National Academy of Sciences*, 104(40), 15894-15898.
doi: 10.1073/pnas.0701498104
- Musacchia, G., Strait, D., & Kraus, N. (2008). Relationships between behavior, brainstem and cortical encoding of seen and heard speech in musicians and non-musicians. *Hearing Research*, 241(1), 34-42.
- Özdamar, Ö., & Delgado, R. E. (1996). Measurement of signal and noise characteristics in ongoing auditory brainstem response averaging. *Annals of Biomedical Engineering*, 24(6), 702-715.

- Osterhammel, P. A., Shallop, J. K., & Terkildsen, K. (1985). The effect of sleep on the auditory brainstem response (ABR) and the middle latency response (MLR). *Scandinavian Audiology*, 14(1), 47-50.
- Parbery-Clark, A., Skoe, E., & Kraus, N. (2009). Musical experience limits the degradative effects of background noise on the neural processing of sound. *The Journal of Neuroscience*, 29(45), 14100-14107.
- Picton, T. W. (2011). *Human auditory evoked potentials*. Plural Pub Incorporated.
- Plourde, G., & Picton, T. W. (1990). Human auditory steady-state response during general anesthesia. *Anesthesia & Analgesia*, 71(5), 460-468.
- Plyler, P. N., & Ananthanarayan, A. K. (2001). Human frequency-following responses: representation of second formant transitions in normal-hearing and hearing-impaired listeners. *Journal of the American Academy of Audiology*, 12(10), 523-533.
- Presacco, A., Jenkins, K., Lieberman, R., & Anderson, S. (2015). Effects of Aging on the Encoding of Dynamic and Static Components of Speech. *Ear and Hearing*, 36(6), 352-363.
- Russo, N., Nicol, T., Musacchia, G., & Kraus, N. (2004). Brainstem responses to speech syllables. *Clinical Neurophysiology*, 115(9), 2021-2030.
- Russo, N., Nicol, T., Trommer, B., Zecker, S., & Kraus, N. (2009). Brainstem transcription of speech is disrupted in children with autism spectrum disorders. *Developmental Science*, 12(4), 557-567.

- Russo, N. M., Skoe, E., Trommer, B., Nicol, T., Zecker, S., Bradlow, A., & Kraus, N. (2008). Deficient brainstem encoding of pitch in children with autism spectrum disorders. *Clinical Neurophysiology*, 119(8), 1720-1731.
- Sayles, M., & Winter, I. M. (2008). Ambiguous pitch and the temporal representation of inharmonic iterated rippled noise in the ventral cochlear nucleus. *The Journal of Schattelman, T. A., Hughes, L. F., & Caspary, D. M. (2008). Aged-related loss of temporal processing: altered responses to amplitude modulated tones in rat dorsal cochlear nucleus. Neuroscience*, 154(1), 329-337.
- Sergeyenko, Y., Lall, K., Liberman, M. C., & Kujawa, S. G. (2013). Age-related cochlear synaptopathy: an early-onset contributor to auditory functional decline. *The Journal of Neuroscience*, 33(34), 13686-13694.
- Sharbrough, F., Chatrian, G. E., Lesser, R. P., Lüders, H., Nuwer, M., & Picton, T. W. (1991). American Electroencephalographic Society guidelines for standard electrode position nomenclature. *Journal of Clinical Neurophysiology*, 8(2), 200-202.
- Skoe, E., & Kraus, N. (2010). Auditory brainstem response to complex sounds: a tutorial. *Ear and Hearing*, 31(3), 302.
- Smith, J. C., Marsh, J. T., & Brown, W. S. (1975). Far-field recorded frequency-following responses: evidence for the locus of brainstem sources. *Electroencephalography and Clinical Neurophysiology*, 39(5), 465-472.
- Stamatakis, S., Francis, H. W., Lehar, M., May, B. J., & Ryugo, D. K. (2006). Synaptic alterations at inner hair cells precede spiral ganglion cell loss in aging C57BL/6J mice. *Hearing Research*, 221(1), 104-118.

- Starr, A., & Hellerstein, D. (1971). Distribution of frequency following responses in cat cochlear nucleus to sinusoidal acoustic signals. *Brain Research*, 33(2), 367-377.
- Stillman, R. D., Crow, G., & Moushegian, G. (1978). Components of the frequency-following potential in man. *Electroencephalography and Clinical Neurophysiology*, 44(4), 438-446.
- Stillman, R. D., Moushegian, G., & Rupert, A. L. (1976). Early tone-evoked responses in normal and hearing-impaired subjects. *Audiology*, 15, 10-22.
- Strouse, A., Ashmead, D. H., Ohde, R. N., & Grantham, D. W. (1998). Temporal processing in the aging auditory system. *The Journal of the Acoustical Society of America*, 104(4), 2385-2399.
- Swaminathan, J., Krishnan, A., & Gandour, J. T. (2008). Pitch encoding in speech and nonspeech contexts in the human auditory brainstem. *Neuroreport*, 19(11), 1163. doi: 10.1097/WNR.0b013e3283088d31
- Terkildsen, K., & Osterhammel, P. (1981). The influence of reference electrode position on recordings of the auditory brainstem responses. *Ear and Hearing*, 2(1), 9-14.
- Thornton, C., Catley, D. M., Jordan, C., Lehane, J. R., Royston, D., & Jones, J. G. (1983). Enflurane anaesthesia causes graded changes in the brainstem and early cortical auditory evoked response in man. *British Journal of Anaesthesia*, 55(6), 479-486.
- Tremblay, K. L., Piskosz, M., & Souza, P. (2003). Effects of age and age-related hearing loss on the neural representation of speech cues. *Clinical Neurophysiology*, 114(7), 1332-1343.

- Trune, D. R., Mitchell, C., & Phillips, D. S. (1988). The relative importance of head size, gender and age on the auditory brainstem response. *Hearing Research*, 32(2), 165-174.
- Walsh, P., Kane, N., & Butler, S. (2005). The clinical role of evoked potentials. *Journal of Neurology, Neurosurgery & Psychiatry*, 76(2), ii16-ii22.
- Walton, J. P., Frisina, R. D., & O'Neill, W. E. (1998). Age-related alteration in processing of temporal sound features in the auditory midbrain of the CBA mouse. *The Journal of Neuroscience*, 18(7), 2764-2776.
- Wever, E., & Bray, C. (1930). Auditory nerve impulses. *Science*, 71(1834), 215.
- Wible, B., Nicol, T., & Kraus, N. (2004). Atypical brainstem representation of onset and formant structure of speech sounds in children with language-based learning problems. *Biological Psychology*, 67(3), 299-317.
- Willott, J. F. (1996). Anatomic and physiologic aging: a behavioral neuroscience perspective. *Journal of the American Academy of Audiology*, 7, 141-151.
- Willott, J. F., Milbrandt, J. C., Bross, L. S., & Caspary, D. M. (1997). Glycine immunoreactivity and receptor binding in the cochlear nucleus of C57BL/6J and CBA/CaJ mice: effects of cochlear impairment and aging. *Journal of Comparative Neurology*, 385(3), 405-414.
- Wong, P. C., Skoe, E., Russo, N. M., Dees, T., & Kraus, N. (2007). Musical experience shapes human brainstem encoding of linguistic pitch patterns. *Nature Neuroscience*, 10(4), 420-422.

- Worden, F. G., & Marsh, J. T. (1968). Frequency-following (microphonic-like) neural responses evoked by sound. *Electroencephalography and Clinical Neurophysiology*, 25(1), 42-52.
- Xu, Y., Krishnan, A., & Gandour, J. T. (2006). Specificity of experience-dependent pitch representation in the brainstem. *Neuroreport*, 17(15), 1601-1605.
- Xu, Q., & Ye, D. (2014), Stimulus polarity effects on individual components of speech-evoked frequency following response. *Proceedings of the 2014 7th International Conference on Biomedical Engineering and Informatics*, 383-387.
- Young, E. D. & Oertel, D. (2004). Cochlear nucleus. In G. M. Shepherd (Ed.), *The Synaptic Organization of the Brain* (pp. 125-163). New York, NY: Oxford University Press.

CURRICULUM VITA

NAME: Jane Grabowski

PERMANENT ADDRESS: 5720 Fishers Lane; Rockville, MD 20852

PROGRAM OF STUDY: Audiology

DEGREE AND DATE TO BE CONFERRED: Doctor of Audiology; May, 2017

Secondary education: North High School; Phoenix, AZ; May 2003

Collegiate Institutions Attended	Dates	Degree	Date of Degree
Phoenix Community College	2005-2007	A.S. in Chemistry	August 2007
Arizona State University	2007-2009	B.A. in German and Biochemistry	January 2009
Arizona State University	2009-2011	M.A. in Germanic Linguistics	May 2011
University of Texas at Austin	2011-2012	Ph.D. in Germanic Linguistics	Not conferred
Towson University	2013-2017	Au.D. in Audiology	May 2017

Professional positions held:

- DC VA Medical Center: *Audiology Extern*
- The River School: *Audiology Student Clinician*
- National Institutes of Health/National Institute on Deafness and Other Communication Disorders: *Audiology Student Clinician*
- Johns Hopkins Bayview Medical Center: *Audiology Student Clinician*
- Towson University Hearing and Balance Center: *Graduate Student Clinician*

